NOLTR 62-155

ENERGY PARTITION OF WATER-CASED EXPLOSIONS IN AN IDEALIZED MODEL REACTOR VESSEL

NOL

1 JUNE 1960

UNITED STATES NAVAL ORDNANCE LABORATORY, WHITE OAK, MARYLAND

NOLTR 62-155

ENERGY PARTITION OF WATER-CASED EXPLOSIONS IN AN IDEALIZED MODEL REACTOR VESSEL

Prepared by:
James F. Proctor

ABSTRACT: The broad purpose of the energy-partition work currently being conducted by the Naval Ordnance Laboratory is to determine the response of a model shield plug to simulated excursion-type loadings generated within an idealized model reactor plant. This purpose is being achieved through an investigation of the partition of mechanical and non-mechanical energies resulting from the detonation of a water-cased explosive surrounded by air in a closed piston-fitted vessel. Of eight postulated governing parameters, this report presents an investigation of the effects of only three of the more important parameters, charge weight, mass-per-frontal area, and water-to-air ratio, on energy partition.

Analytic equations have been established that express energy partition in terms of model-plug response to simulated excursion-type loading. These equations require for their solutions only a knowledge of the displacement-time history of the model plug. Eleven energy-partition experiments have been conducted in a test apparatus that simulates the Enrico Fermi Atomic Power Plant. Experimental displacement-time data have been graphically and analytically treated to obtain various plug-response functions and the subject energy partition. Comprehensive analyses of the plug-response data are presented in considerable detail in tabular and graphical forms.

For the subject experiments only, it is concluded from this investigation that increasing water-to-air ratios have a marked decreasing effect on energy partition (ratio of mechanical to non-mechanical energy), that increasing mass-per-frontal-area ratios have only a slight decreasing effect on energy partition, and that increasing charge weights have a slight increasing effect on energy partition. No statement, qualitative or quantitative, based on these results alone can be made concerning a full-scale reactor plant. Only through an extensive investigation of all the governing parameters in an improved test apparatus can the general solution be obtained. Such a general solution is being pursued and will be reported at a later date.

PUBLISHED APRIL 1963

Air-Ground Explosions Division
EXPLOSIONS RESEARCH DEPARTMENT
U.S. NAVAL ORDNANCE LABORATORY
WHITE OAK, MARYLAND

NOLTR 62-155 1 June 1960

Energy Partition of Water-Cased Explosions in an Idealized Model Reactor Vessel

The work described in this report was performed under Task V of NOL Task-285, NOL Reactor-Vessel Containment Program. The objective of Task V is to determine the partition of mechanical and non-mechanical energy resulting from the detonation of water-cased and sodium-cased explosives surrounded by air and confined within a piston-fitted vessel. This report presents the results of preliminary work designed to establish the governing parameters and to show the method of solution to be sound. Experimental facilities and the results of eleven tests are described in considerable detail. This material was submitted in fulfillment of the thesis requirements for the M.S. degree in Mechanical Engineering at the University of Maryland.

W. D. COLEMAN
Captain, USN
Commander

C. J. Aronson

C. J. ARONSON
By direction

CONTENTS

LIST OF FIGURES

LIST OF FIGURES (Cont'd)

LIST OF TABLES

NOMENCLATURE

A . . . . . . frontal area of model plug, in^2, ft^2

a . . . . . . acceleration of model plug, ft/sec^2

a_c . . . . . calculated acceleration, ft/sec^2

a_g . . . . . graphically obtained acceleration, ft/sec^2

d . . . . . . diameter of reactor-vessel simulant, in

EP . . . . . energy partition, $\frac{ME}{NonME}$

E_r . . . . . total explosive energy, ft-lb, cal

F . . . . . . friction force acting on model plug, lb

g . . . . . . acceleration due to gravity, ft/sec^2

H . . . . . . maximum height attained by model plug, ft

h . . . . . . height of reactor-vessel simulant, in

ME . . . . . mechanical energy absorbed by plug, ft-lb

m . . . . . . mass of model plug, slugs

NonME . . . . non-mechanical energy absorbed by surroundings, ft-lb

PE . . . . . maximum potential energy of model plug, ft-lb

p . . . . . . transient pressure acting on frontal area, psig, psia, psfa

p_{eo} . . . . . maximum effective pressure corresponding to initial chamber volume, psig, psia, psfa

s . . . . . . displacement of model plug, ft

s_e . . . . . experimentally obtained displacement, ft

s_f . . . . . length of power stroke, ft

NOMENCLATURE (Continued)

s_g . . . . . . graphically obtained displacement, ft

t . . . . . . time, msec, sec

v . . . . . . velocity of model plug, ft/sec

v_c . . . . . . calculated velocity of plug, ft/sec

v_f . . . . . . velocity of plug at end of power stroke, ft/sec

v_g . . . . . . graphically obtained velocity of plug, ft/sec

v_p . . . . . . mean particle velocity of water casing, ft/sec

INTRODUCTION

All nuclear reactor power facilities are subject to the remote possibility of an accidental power excursion. Although numerous safety devices are employed to prevent accidental excursions, it is essential that the plant housing and equipment be designed to contain all radioactive products in the unlikely event of such an accident. Otherwise, violation of the plant containment integrity would possibly allow radioactive products to contaminate the immediate atmosphere and underground water supply.

Of particular public interest in regard to reactor safety is the Enrico Fermi Atomic Power Plant currently being constructed at Lagoona Beach, Michigan. The Fermi installation, described in detail in reference (a), utilizes a sodium-cooled, fast-breeder reactor that provides energy for a 100,000-kw, steam-electric power plant. Of the plant's various facilities, our ultimate concern here is with the containment building that houses the reactor proper. Figure 1 is a simplified sketch showing a cross-sectional view of the containment building and components of importance to containment.

The containment building is an air-tight steel structure with a diameter of 72 feet, an overall height of 120 feet, and a wall thickness of 1 1/8 inches. The configuration of this structure is that of a right-circular cylinder with a

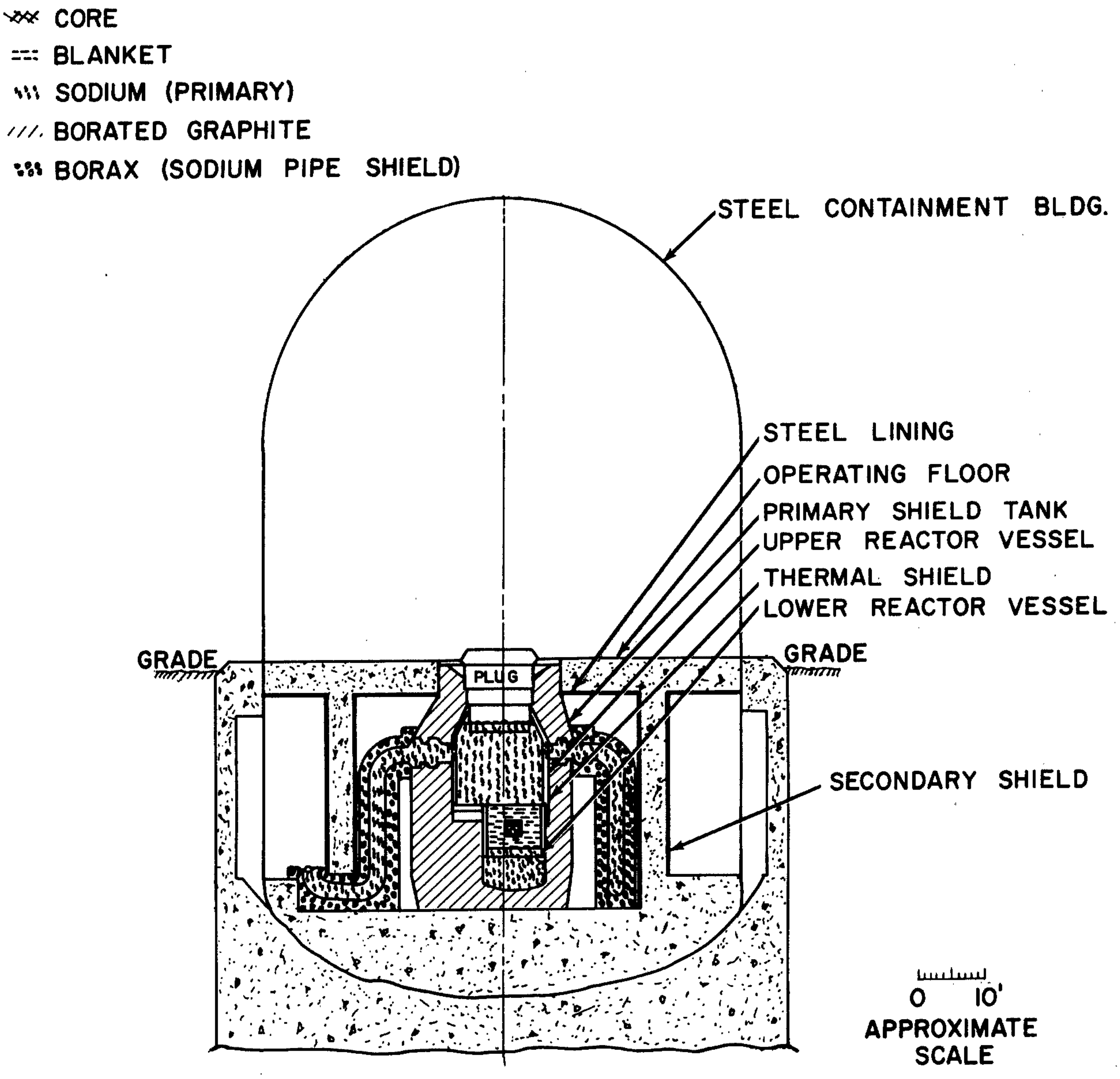

FIG. 1 CROSS-SECTIONAL VIEW OF FERMI-PLANT CONTAINMENT BUILDING

hemispherical top and an ellipsoidal bottom that is embedded in concrete. The lower half of this building is below ground level and contains the reactor core and associated equipment. The reactor core and breeder blanket together constitute a right-circular cylinder about 80 inches in diameter and 70 inches in height; the core of uranium fuel elements alone approximates a right-circular cylinder 30 inches in diameter and 30 inches in height. Primary sodium coolant enters the core and blanket at 550°F, leaves at 800°F, and is circulated at the rate of 13.2 X 10^6 lb/hr. The core and blanket are housed in the lower reactor vessel which is cylindrical in shape. The diameter of this vessel is 9 1/2 feet, its height is 13 feet, and it is constructed of 2-inch stainless-steel plate. The upper reactor vessel, also constructed of 2-inch stainless steel plate, is essentially a right-circular cylinder 14 feet in diameter and 22 feet in height. The combined weight of sodium maintained in these two compartments is approximately 44.5 tons. Fitted into the top of the upper reactor vessel is the reactor shield plug. This nearly solid steel plug is 9 1/3 feet in diameter and 12 feet in overall height and weighs approximately 143 tons. Its mass-per-frontal-area ratio (mass of plug divided by the frontal area) is 0.902 slugs/in^2. The primary purposes of the plug are to allow the introduction of control rods and fuel elements into the core while the plant is in operation and to provide access to the core for maintenance.

Immediately surrounding the reactor vessel is a thick layer of graphite housed in a cylindrical steel tank that is 24 feet in diameter and 38 feet in height and is constructed of 5/8-inch steel plate. The tank and graphite layer constitute the primary thermal and radiation shield for the reactor. Enclosing the primary-shield tank are the secondary-shield wall and operating floor. The secondary shield is constructed with 3-foot concrete walls lined with 1/2-inch steel plate on the internal surface, and the operating floor is a 5-foot thick concrete platform lined with 4-inch steel plate. Aside from enclosing the primary-shield tank, these joint structures envelop an air space of approximately 10,000 cubic feet. This air, which has been made nearly inert by removing 75 per cent of the oxygen, greatly reduces the possibility of a chemical reaction resulting from an accidental sodium leak. The normal operating temperature of the steel lining and air space is approximately 180°F. The ratio of the volume of sodium at 800°F in the reactor vessel to the volume of enclosed air is 0.165.

In mid-1957 the Atomic Energy Commission requested that the U. S. Naval Ordnance Laboratory conduct a containment study of the Enrico Fermi plant. The purpose of the study was to determine the damage to the containment building that might result from an accidental nuclear excursion equivalent in violence to the detonation of 1,000 pounds of TNT at the reactor core. This study, which was conducted by E. M. Fisher and W. R. Wise, Jr., reference (b), established an upper bound on possible explosive damage to the plant. Among the various findings of the study, it was concluded that the detonation of 1,000 pounds of TNT occurring at the reactor-core position would not develop shock waves in the sodium and air of sufficient strength to threaten the integrity of the outer containment building. If the shock waves ruptured the reactor vessel and the primary-shield tank, the secondary shield and operating floor would contain the blast and all resulting fragments. The shield plug is free to move vertically upward to relieve any excess-pressure build-up, and it would rise no more than 2 feet when subjected to the shock wave. Whereas the maximum damage resulting from the shock wave alone was based on known information, the evaluation of the static equilibrium pressure (internal blast pressure) that follows the shock wave for the conditions of a liquid-cased explosion was largely unknown.

For the case where the reactor vessel and primary-shield tank ruptured, maximum equilibrium pressure would result if the total explosive energy were transferred to the 10,000 cubic feet of air enclosed by the secondary shield. In this case, a pressure of the order of 300 psi could occur within the secondary shield; the shield plug would respond much as a projectile in a gun and would move vertically upward to a height of the order of 130 feet above its initial position. If this did occur, then the plug, while acting as a missile, would penetrate the outer walls of the containment building. It should be emphasized that the Fisher-Wise study does not postulate that the total explosive energy <u>must</u> go into pressure build-up, but only that if it did, the plug-missile hazard would exist. The exact amount of energy that would be available for a pressure rise in the event of an accidental excursion is unknown at this time. Therefore, it is important to investigate the nature of the loading resulting from an upper-bound energy release, e.g., the previously discussed detonation of 1,000 pounds of TNT. It follows that the response of the shield plug to such loading must be determined in order to assess the hazard factor of the plug as a possible missile.

PURPOSE AND OBJECTIVES

The purpose of this study is to determine model shield plug response to simulated excursion-type loadings by investigating the resultant partition of mechanical and non-mechanical energy. Mechanical energy is defined as the energy absorbed by the shield plug by virtue of its motion, and the non-mechanical energy is defined as the energy absorbed by the surroundings. A partial solution to this problem can be achieved by investigating the response of a model shield plug to simulated excursion loading generated by the detonation of a water-cased explosive surrounded by air in a closed, piston-fitted, secondary-shield simulant. The efficiency of converting explosive energy to mechanical energy, as determined by plug response, is a function of various parameters. It is postulated that the governing parameters are charge composition and weight, mass-per-frontal area of the shield plug, water-to-air volume ratio in the confining vessel, length of the power stroke of the plug, temperature of the water, temperature of air and secondary-shield wall, and size and configuration of the secondary-shield simulant. This list is not necessarily a complete statement of the governing parameters; however, it includes the parameters that have been observed and contemplated to date. The general solution to this problem, including the consideration of scaling laws, would require a lengthy, time-consuming investigation. Some basic principles and concepts, however, can be established by investigating three of the more important parameters which are charge weight, mass-per-frontal area of the plug, and water-to-air volume ratio. The scope of this report is limited to a study of these parameters.

The technical approach used to achieve the objectives of this study is:

1. to vary simulated excursion loadings in a model, secondary-shield container as functions of charge weight, mass-per-frontal area of the model plug, and water-to-air volume ratio.

2. to investigate the effects of these three parameters upon model-plug response, and hence upon energy partition, in terms of displacement, velocity, acceleration, and loading pressure.

3. to establish and qualitatively analyze possible mechanisms by which the water casing surrounding the charge absorbs explosive energy.

ENERGY-PARTITION ANALYSIS

To implement the technical approach previously stated, appropriate analytic equations were required to relate the partition of mechanical and non-mechanical energy to model-plug response resulting from explosive loading. These governing equations were formulated and expressed in a manner such that their solutions required only a knowledge of the plug motion as a function of time.

Energy-Partition Ratio. Energy partition is defined here as the ratio of mechanical energy to non-mechanical energy resulting from simulated excursion-type loading. Expressed analytically, this definition appears as

$$EP = \frac{ME}{NonME} \tag{1}$$

where

EP .... is the subject energy partition

ME .... is mechanical energy absorbed by plug, ft-lb

NonME .... is non-mechanical energy absorbed by surroundings, ft-lb

Mechanical Energy. Mechanical energy is more specifically defined as the pressure-force work done on the model plug as it moves upward through the power stroke. The full power stroke is the predetermined displacement of the plug, measured from its initial position, through which the transient pressure acts on the frontal area. Instantaneous pressure release to the atmosphere is assumed to occur after the plug has traversed the power stroke. From the above definition, mechanical energy can be expressed as

$$ME = A \int_{s=0}^{s=s_f} p \, ds \quad , \quad p = p\,(s) \tag{2}$$

where

A .... is frontal area of plug, in^2

p .... is transient pressure acting on frontal area, psig

s .... is displacement of plug measured from initial position s=0, ft

s_f ... is length of power stroke, ft

In order to assess the mechanical energy, it is necessary to determine the equation of dynamic equilibrium for the plug. Assuming the system of forces acting upon the plug as shown in the free-body diagram of figure 2 and assuming wind losses to be negligible, we find the equilibrium equation to be

$$pA = mv\,\frac{dv}{ds} + mg + F \tag{3}$$

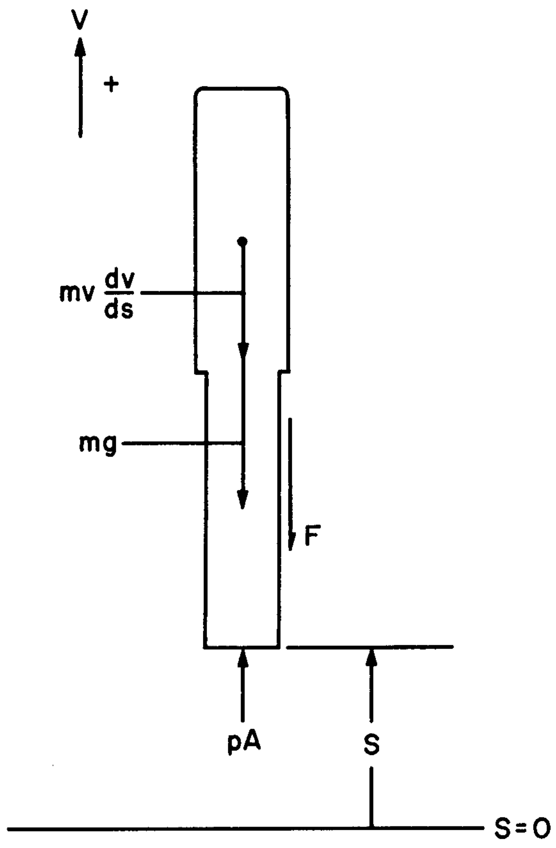

FIG. 2 FREE-BODY DIAGRAM OF MODEL PLUG SHOWING FORCE SYSTEM

where the constants are

A ... frontal area of plug, in^2

m ... mass of plug, slugs

g ... acceleration due to gravity, ft/sec^2

F ... friction force, lb

and the variables are

p ... transient pressure acting on frontal area, psig

v ... velocity of plug, ft/sec

s ... displacement of plug, ft

The friction force F was measured at a slow constant velocity and was found to be approximately 2 pounds. Although this force is sufficiently small to be neglected, we elect to retain it as a constant of 2 pounds acting in opposition to the motion. Rearranging equation (3) and integrating, we can write

$$A \int_{s=0}^{s=s_f} p \, ds = m \int_{v=0}^{v=v_f} v \, dv + (mg+F) \int_{s=0}^{s=s_f} ds \qquad (4)$$

where v_f is the velocity of the plug at the end of the power stroke, ft/sec. Performing the indicated integration and substituting into equation (2), we obtain

$$ME = A \int_{s=0}^{s=s_f} p \; ds = \frac{m}{2} v_f^2 + mgs_f + F \; s_f \tag{5}$$

This equation states that the pressure-force work done on the plug is manifested in the form of kinetic energy ($\frac{m}{2} v_f^2$), potential energy (mgs_f), and heat lost to friction ($F \; s_f$). The complete numerical solution of the equation can be achieved with a knowledge of the displacement as a function of time

$$s = s \; (t)$$

alone, since first and second derivatives of this displacement function with respect to time in combination with the equilibrium equation (3) yield

$$v = v \; (t)$$
$$a = a \; (t)$$
$$p = p \; (s)$$

where "a" is the acceleration of the plug, ft/sec^2.

To complement this analysis, one can utilize the maximum height attained by the plug to determine its maximum increase of potential energy. From the conservation of energy, we can write

$$PE = mg\,H = \frac{m}{2} v_f^2 + mgs_f \qquad (6)$$

where

PE ... is maximum potential energy of plug, ft-lb

H .... is maximum height of plug travel, ft

This equation can be used to check the validity of the assumptions concerning the friction force and windage loss.

<u>Non-Mechanical Energy</u>. Non-mechanical energy has been defined as the energy absorbed by the surroundings. In other words, this quantity is the sum of all energy released by the explosive that does not appear as mechanical energy. Analytically expressed,

$$NonME = E_r - ME \qquad (7)$$

where E_r is the total energy released from the explosive (explosive energy), ft-lb. A typical example of the method used to determine the total explosive energy is found in Appendix A.

Substituting the results obtained from equations (5) and (7) into equation (1) will yield the energy-partition ratio for a particular set of parameters.

EXPERIMENTAL FACILITIES AND PROCEDURE

Investigation of the subject energy partition required the use of a test mechanism in which model experiments could be performed. Since the previously discussed hypothetical Fermi plant explosion would be contained within the secondary shield, it was considered necessary here to simulate only the shield and its internals. We wished to subject the plug simulant to the type of loading that would be experienced by the Fermi plant in event of the hypothetical excursion previously described. This was achieved most conveniently by scaling down the physical dimensions of the Fermi plant to those of a model plant in accord with Hopkinson's (cube-root) scaling law commonly used in explosive work. A scale factor of about 1/30 was chosen.

Figure 3 shows a cross-sectional view of the secondary-shield simulant. The scaled simulant, a cylindrical chamber 10 inches in diameter and 9.2 inches in height, was constructed from an existing cylinder fitted at the ends with rigid closures. A steel filler was used to achieve the desired chamber volume and to provide a bore for the model shield plug.

In the hypothetical Fermi plant explosion, we considered only the case where the reactor vessel and the primary-shield tank were assumed to offer little resistance to the resultant shock wave. For simplicity in the model tests, these two vessels were simulated by one thin-wall cylindrical container, denoted

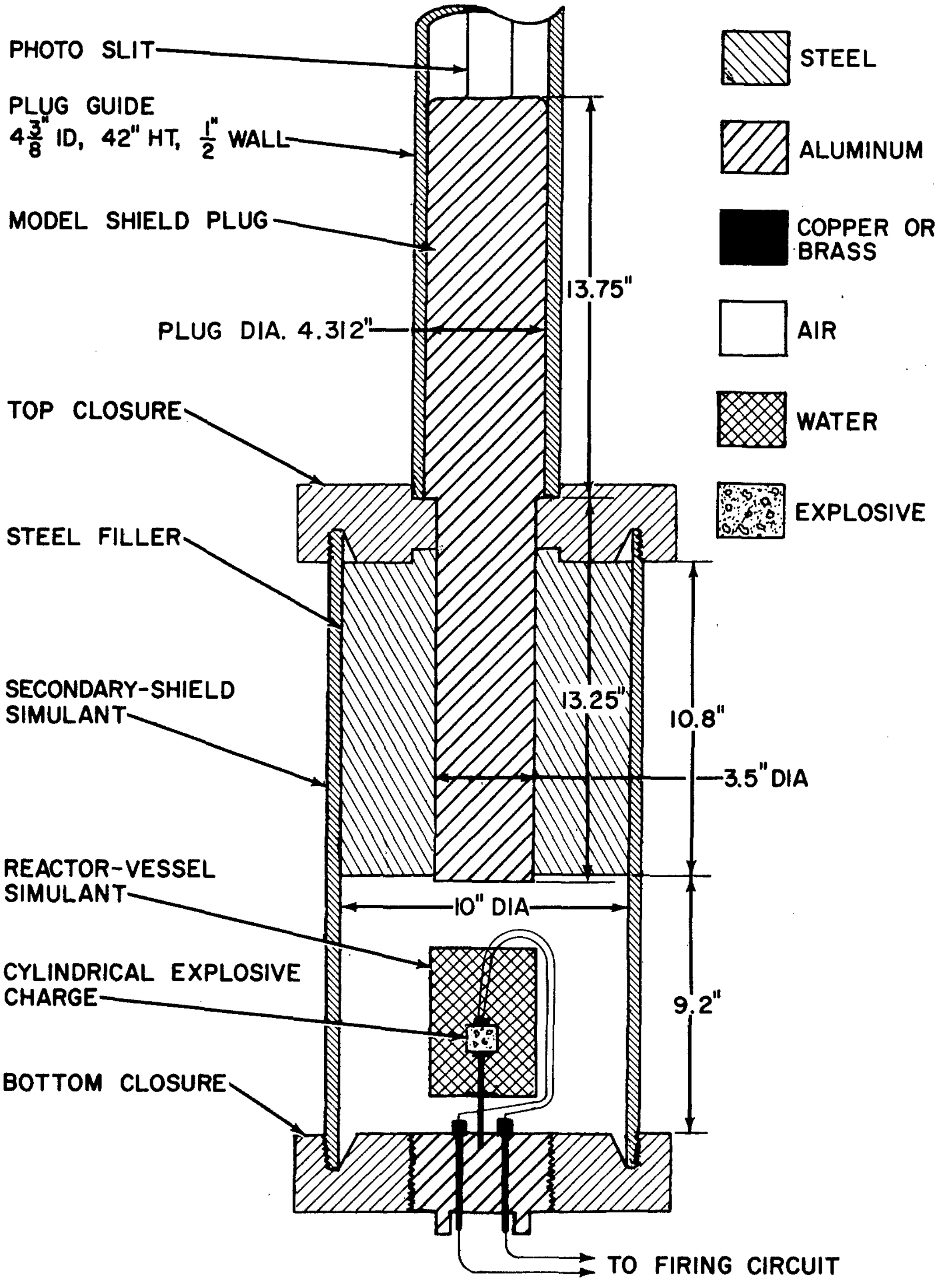

FIG. 3 CROSS-SECTIONAL VIEW OF SECONDARY-SHIELD SIMULANT WITH MODEL PLUG

as the reactor-vessel simulant. Since many problems arise with the handling and use of molten sodium, water was chosen as a convenient substitute. This choice was based on the similarity of water and sodium densities. The diameter and height of the container, which was constructed from 1/64-inch brass shim stock, varied from 2 to 3.5 inches and 2.5 to 9.2 inches, respectively, depending upon the desired quantity of water. A cylindrically shaped pentolite charge, fitted with detonator, was supported on a brass pedestal and was completely encased by water. In all cases, where practicable, the centroid of the charge coincided with the centroid of the water casing. The firing leads from the detonator passed through the bottom closure by means of high-pressure, sealed, electrical connectors. Introduction of the water-cased charge into the secondary-shield simulant was accomplished by means of a screw-plug located in the bottom closure.

In order to satisfy particular apparatus design criteria, weight and dimensions of the model shield plug, with the exception of the frontal diameter, were not scaled. In accord with cube-root scaling, the frontal diameter of the model plug was chosen to be 3.5 inches. The power stroke (length of the lower portion of the plug) was taken to be 13.25 inches. The upper portion of the plug was 4.312 inches in diameter and 13.75 inches in length. To vary the mass-per-frontal area of the plug without changing any physical dimensions, plugs of different densities were used. One plug was made of aluminum weighing

31.7 pounds, and another of steel weighing 91.9 pounds. It is noted here that the mass-per-frontal-area ratios of these two model plugs were 0.102 and 0.297 slugs/in^2, respectively, as compared to 0.902 slugs/in^2 for the full-scale plug; and the power stroke of the model plug was 13.25 inches as compared to 12 feet for the full-scale case. The model shield plug was guided during its first 40 inches of displacement by a cylindrical steel tube (plug guide) whose internal diameter corresponds to the outside diameter of the upper portion of the model plug. Two slits, two inches wide and 30 inches long, were machined in the guide 180° apart to allow observation of the plug motion during the power stroke. The need for these slits will become more apparent later when the photographic system is described. At the lower portion of the plug guide an array of 1/2-inch diameter holes were machined through the walls to act as gas vents. These vents permitted the chamber gases to escape and produce a nearly step-function release of pressure in the chamber when the model plug reached the end of the power stroke.

The entire test mechanism was rigidly constrained in a steel stand as illustrated in figure 4. Shown in this photograph is the fully assembled test apparatus. The entire apparatus was inclined 5° to prevent the model plug from falling back upon the mechanism after the plug traveled out of the guide. Upon close observation, the model plug can be seen in its initial position through the front photo slit.

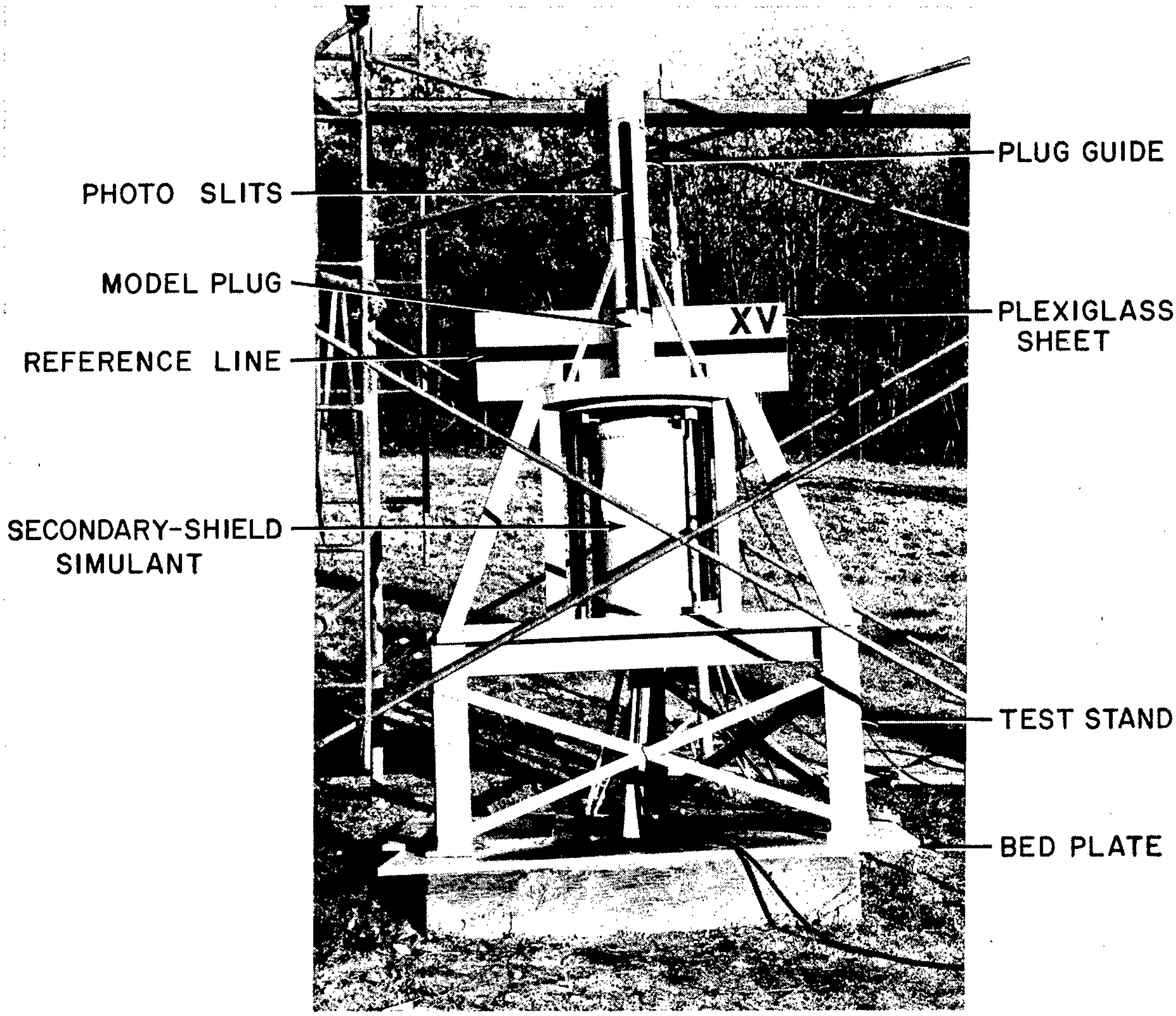

FIG.4 FULLY ASSEMBLED TEST APPARATUS

The displacement-time function of the model plug during the power stroke was determined by high-speed photography. Motion of the model plug was photographed through the photo slit by an Eastman High-Speed 16-millimeter camera operating at about 3,000 frames per second. The position of the camera with respect to the apparatus is shown in figure 5. The camera was electronically synchronized with the event in a manner that allowed the camera to initiate the detonator when nearly full speed was attained. Accurate time calibration was placed on the camera film by a small neon bulb powered by a pulse generator controlled by a 1,000-cps vacuum-tube-fork frequency standard.

To eliminate problems arising from daylight lighting conditions, silhouette-type lighting was used to photograph the plug motion. This was accomplished by focusing photo lights on the back side of a sand-blasted strip of plexiglass that covered the photo slit directly behind the plug. To provide a fixed reference line in the field of view of the camera, a large sheet of sand-blasted plexiglass with a black horizontal line was mounted on the test stand as shown in figure 4. Again, compatible silhouette lighting was used to photograph the reference line. A better concept of the lighting system is given pictorially in figure 6. With this type of photography, the model plug and reference line appeared black against a brilliant white background, and a sharp profile contrast was obtained.

EASTMAN HIGH-SPEED CAMERA

TEST APPARATUS

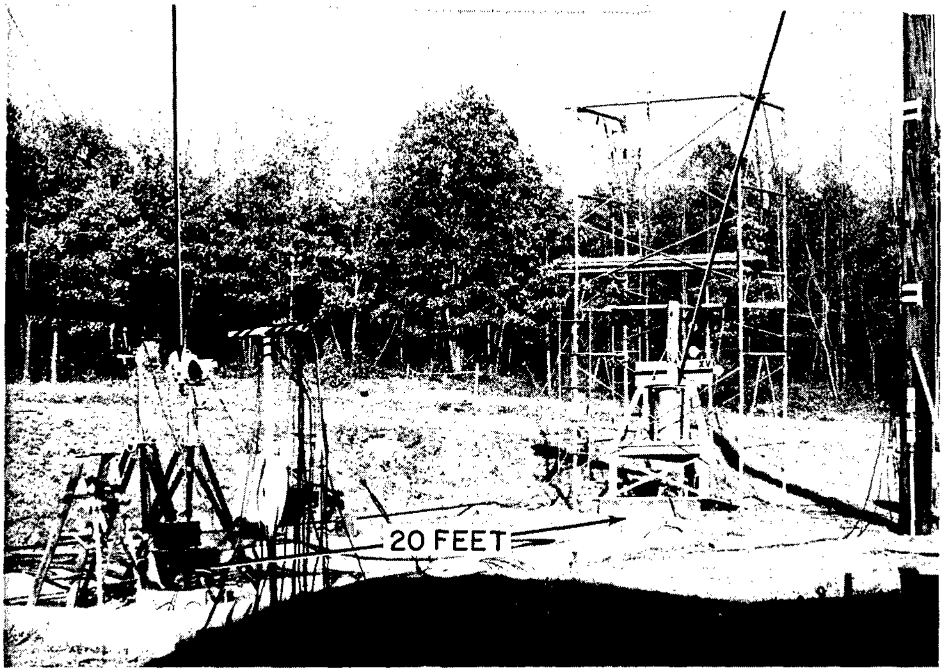

FIG. 5 LOCATION OF EASTMAN HIGH-SPEED CAMERA

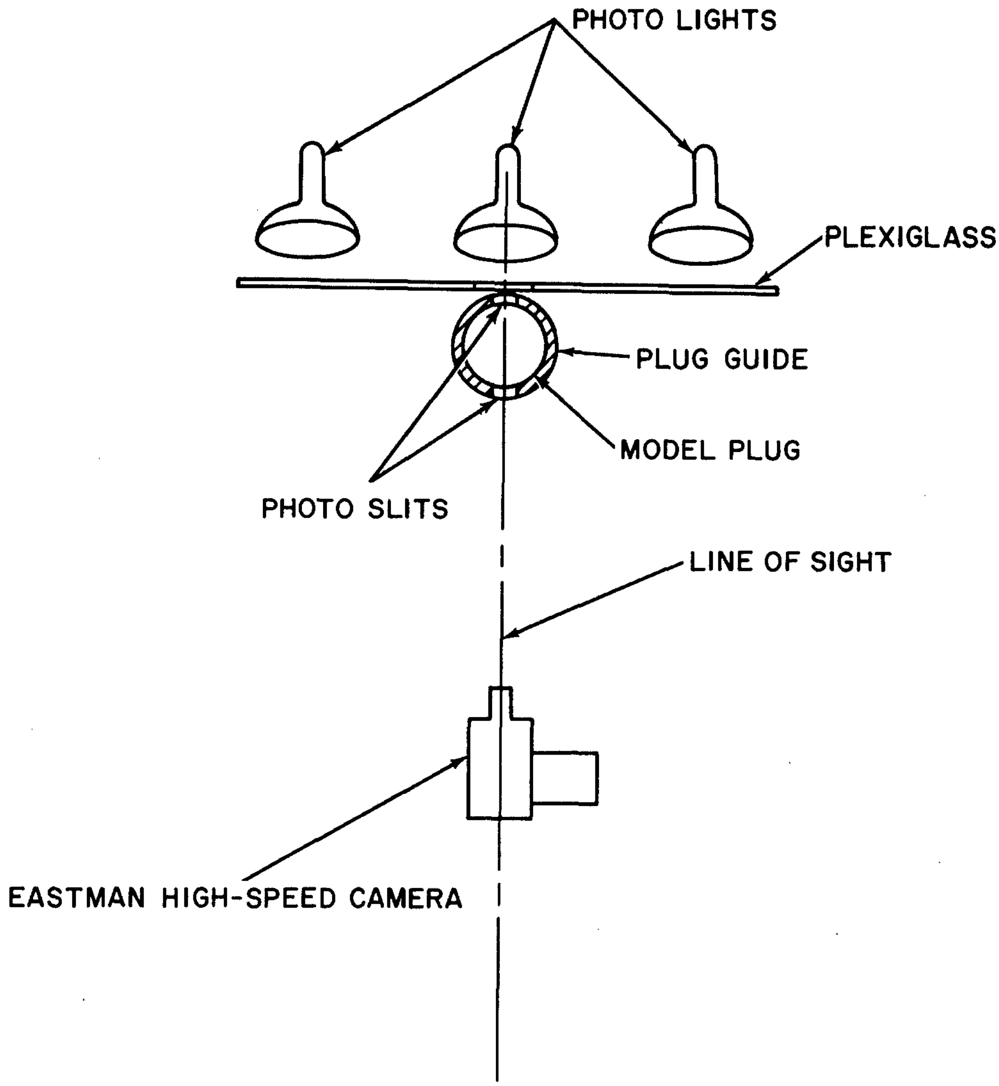

FIG. 6 TOP VIEW OF TEST APPARATUS SHOWING PHOTO-LIGHT ARRANGEMENT

The maximum height attained by the model plug after leaving the plug guide was recorded by a Kodak Ciné-Special camera operating at 64 frames per second. This camera was located approximately 120 feet from the test apparatus atop a 30-foot tower as shown in figure 7. Since only a record of the maximum height of plug travel was required from this camera, no timing or synchronization was necessary in its operation.

FIG. 7 LOCATION OF KODAK CINE-SPECIAL CAMERA

EXPERIMENTAL RESULTS

Eleven energy-partition experiments were conducted utilizing the test apparatus and photographic system described in the previous section. Since the conduct of each test required approximately 16-man hours, effort was limited to experiments with judiciously chosen values of the three governing parameters, previously selected in the section Purpose and Objectives. The results from eleven tests were used to establish the effect on energy partition of varying the water-to-air ratio, from four tests to indicate the effect of varying charge weight, and from four tests to indicate the effect of varying mass-per-frontal area. Detailed specifications of these tests and an index for data comparisons are given in table 1. Pentolite-charge weights were nominally 15 and 30 grams, mass-per-frontal area values were 0.102 and 0.297 slugs/in^2 (plug weights of 31.7 and 91.9 lb), and water-to-air-ratio values ranged from 0 to 0.171.

The films obtained from the high-speed camera for the subject eleven tests were analyzed on a high-magnification Telereadex 29A film reader. Sequential-motion views of the model plug during the power stroke (Test No. 8) are shown in figure 8. For each test, experimental displacement-time data describing the motion of the model plug during the power stroke are given in the Experimental Data sections of tables B-1 through

VARIABLE PARAMETERS

TEST NUMBER (ENERGY PARTITION)*		1 (0.0013)	2 (0.0007)	3 (0.0018)	4 (0.0173)	5 (0.0139)	6 (0.0191)	7 (0.0039)	8 (0.0029)	9 (0.0020)	10 (0.0016)	11 (0.0017)
WATER-TO-AIR RATIO (VOL/VOL)	0				X	X	X					
	0.003							X				
	0.007								X			
	0.019									X		
	0.028										X	
	0.038											X
	0.171	X	X	X								
CHARGE WEIGHT (GM)	13.9	X	X		X	X						
	16.2							X	X	X	X	X
	30.0			X								
MASS-PER-FRONTAL AREA (SLUGS/IN²)	0.102	X		X	X		X	X	X	X	X	X
	0.297		X			X						
VOLUME OF AIR (CC)		10255	10255	10255	12011	12011	12011	11965	11906	11778	11662	11546
VOLUME OF WATER (CC)		1744	1744	1744	0	0	0	32	88	221	323	442
DIAMETER OF REACTOR-VESSEL SIMULANT (IN)		3.80	3.80	3.80	-	-	-	1.50	2.00	3.00	3.00	3.00
HEIGHT OF REACTOR-VESSEL SIMULANT (IN)		9.20	9.20	9.20	-	-	-	2.00	2.50	2.50	3.50	4.50

* ENERGY PARTITION RESULTS ARE GIVEN HERE FOR CONVENIENT REFERENCE; DETAILED DEVELOPMENT IS GIVEN IN TABLE 6.

FIXED PARAMETERS

1. FRONTAL AREA OF PLUG . . . . 9.62 IN^2
2. TEMPERATURE OF WATER . . . . 55°F
3. TEMPERATURE OF AIR . . . . 50°F
4. TEMPERATURE OF SECONDARY-SHIELD SIMULANT . . . . 50°F
5. COMPOSITION OF EXPLOSIVE CHARGE . . . . PENTOLITE

TEST COMPARISONS

EFFECT OF MASS-PER-FRONTAL AREA	EFFECT OF CHARGE WEIGHT**	EFFECT OF WATER-TO-AIR RATIO**
1 vs 2	1 vs 3	2 vs 5
4 vs 5	4 vs 6	3 vs 6
		1 vs 4,7,8,9,10,11

** FOR THE PURPOSE OF COMPARISONS, ENERGY-PARTITION RESULTS FROM 13.9- AND 16.2-GRAM CHARGES CAN BE CONSIDERED EQUIVALENT TO THOSE EXPECTED FROM A CHARGE WEIGHING NOMINALLY 15 GRAMS WITHOUT SIGNIFICANT ERROR.

TABLE 1 TEST SPECIFICATIONS

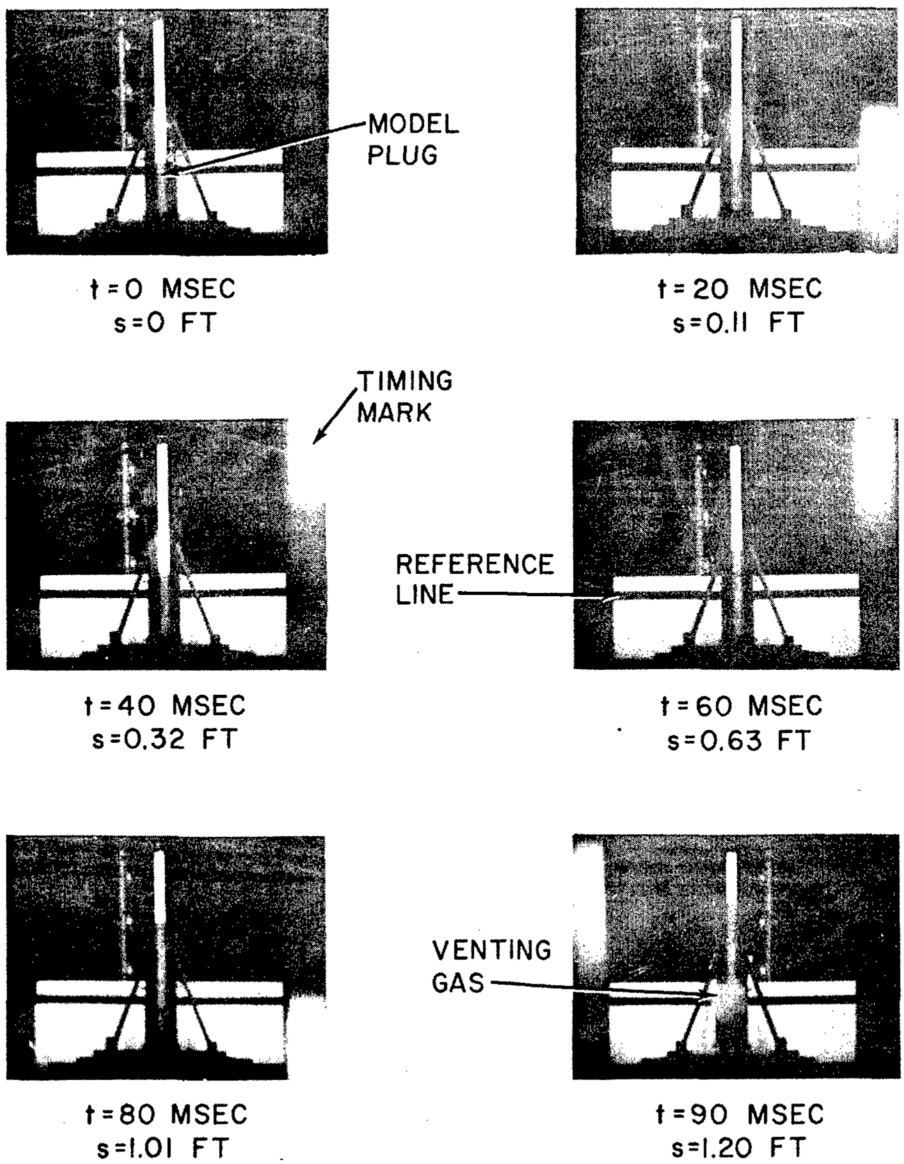

FIG. 8 SEQUENCE OF PHOTOGRAPHS SHOWING MODEL-PLUG MOTION FOR TEST NO. 8

B-11 found in Appendix B. (Data from Test No. 1 are found in table B-1, Test No. 2 in table B-2, etc.) To identify experimentally obtained displacement data, the notation s_e is used. Graphical representations of the displacement-time data for each test are shown as the "displacement curves" in figures B-1 through B-11 found in Appendix B.

Since a vacuum-tube-fork frequency standard was used for time calibration, it is reasonable to expect that the time data were not in error by more than $\pm$ 1 per cent. Film resolution will not produce an error of more than $\pm$ 0.005 foot in the experimental displacement data, but an error in film reading could appreciably alter this deviation. Although nothing more can be said at this time concerning displacement-data accuracy, a more meaningful statement will be made in the subsequent section after certain numerical treatments of the data have been performed.

The films obtained from the Kodak Ciné-Special camera were also analyzed with the Telereadex film reader to obtain values of maximum height of plug travel for each test. These data are presented in table 2. The accuracy of these data is likewise subject to reading error, but it is reasonable to expect a deviation of no more than $\pm$ 5 per cent.

TEST NUMBER	MAX. HEIGHT
	H
	(FT)
1	3.25
2	0.59
3	7.44
4	42.11
5	12.58
6	77.56
7	11.95
8	7.64
9	5.61
10	4.38
11	4.45

TABLE 2 MAXIMUM HEIGHTS ATTAINED BY MODEL PLUG

CALCULATED AND GRAPHICAL RESULTS

<u>Plug-Response Results.</u> In accord with the governing equations established in the section Energy-Partition Analysis, we express the first and second derivatives of the displacement function

$$s = s\ (t)$$

as the velocity and acceleration functions

$$v = v\ (t)$$

$$a = a\ (t)$$

Substitution of these plug-response functions into the equilibrium equation (3) yields the pressure-displacement function

$$p = p\ (s)$$

To obtain first and second derivatives of a function expressed as experimental data, extreme care must be exercised if a reasonable degree of accuracy is to be achieved.

The following is the step-by-step procedure used to determine the plug-response functions for each test.

1. Experimentally obtained displacement-time data,

$$s_e = s_e\ (t)$$

given in tables B-1 through B-11 in Appendix B, were plotted to greatly expanded scales to form graphs with nominal dimensions of 8 X 8 feet. A smooth curve drawn through these points became a more accurate representation of the actual displacement function, since random reading errors were attenuated. New displacement data were obtained from this smooth curve for equal intervals of time and are presented in the Calculated Data sections of tables B-1 through B-11 with the notation s_g, where the subscript g denotes graphical data. It is noted that the time intervals have been varied to permit a more careful delineation in regions of rapidly changing slope. In any given region, however, the time intervals are constant.

2. To obtain additional smoothing of the displacement data, the Gram least-square approximation, given in reference (c), was used. From the resultant displacement data, the first derivative with respect to time was taken. A modification to the Gram method was made that allowed the data smoothing and first-derivative calculations to be made in one step. For a least-square fit of a polynominal of degree two over a discrete range of five equally spaced points, the Gram approximation becomes

$$y(z) = \sum_{r=0}^{2} b_r \, G_r(z) \qquad (8)$$

where

$$b_r = \frac{\sum_{z=-2}^{2} f(z) \quad G_r(z)}{\sum_{z=-2}^{2} G_r^2(z)}$$

$$G_{r=0}(z) = 1$$

$$G_{r=1}(z) = z/2$$

$$G_{r=2}(z) = 1/2 \ (z^2 -2)$$

Terms that require additional explanation are as follows:

z ...... Gram method coordinate

$f(z)$ ... graphically smoothed function

$y(z)$ ... resultant smoothed function.

The transformation of the known time coordinate t to the coordinate z is

$$t = c + ez$$

where

c ... is constant equal to t at $z = 0$

e ... is equal time interval between five points

and z takes on interger values of -2, -1, 0, 1, and 2 for the five points. Taking the derivative of this equation with respect to z and rearranging, we can write

$$dz = \frac{dt}{e}$$

From this relationship, the derivative of equation (8) with respect to time t is

$$e \frac{dy}{dt} = 1/2\ b_{r=1} + b_{r=2}\ z$$

If we elect to determine the derivative at z = 0, this equation becomes

$$\frac{dy}{dt} = \frac{b_{r=1}}{2e}$$

Substituting the value of $b_{r=1}$, we can write

$$\frac{dy}{dt} = \frac{2f(z=2) + f(z=1) - f(z=-1) - 2f(z=-2)}{10e} \qquad (9)$$

If the operations of equation (9) are performed on the displacement-time data s_g, calculated values of velocity may be determined. Such velocity-time data are given in tables B-1 through B-11 in the column denoted by v_c, where the subscript c represents calculated data.

3. The calculated velocity-time data

$$v_c = v_c(t)$$

were also plotted to greatly expanded scales. Again a smooth curve was drawn through the points to obtain greater accuracy. From the smoothed curve, new velocity-time data were obtained, and these data are presented in tables B-1 through B-11 in the column denoted v_g. The operations of equation (9) were performed on these velocity data to obtain calculated acceleration-time data given in tables B-1 through B-11 in the column denoted a_c.

4. The calculated acceleration-time data

$$a_c = a_c(t)$$

were also plotted to expanded scales. A smooth curve was drawn through the points, and more accurate acceleration values were obtained. These data are presented in tables B-1 through B-11 in the column denoted a_g. The graphically obtained acceleration data were substituted into the equilibrium equation (3) to obtain the pressure-displacement function

$$p = p(s)$$

The values of this function are presented in tables B-1 through B-11 in the column denoted p.

Smoothed curves for the graphically obtained displacement-, velocity-, and acceleration-time data are shown for each test in figures B-1 through B-11 found in Appendix B. Little can be said concerning the accuracy of the first portion of these curves, for the plug was responding to shock loading. It is noted in the figures that, with respect to the shock region, the values of the various parameters should be taken as qualitative only. Although the response of the recording system was not adequate to permit accurate monitoring of the shock phenomena, it is believed that accuracy of the response data is good for the equilibrium conditions following the shock wave. For the equilibrium region, it is believed that the displacement data are within the limit of ± 1 per cent error, the velocity data within ± 3 per cent error, and the acceleration data within ± 5 per cent error.

Graphical representations of the pressure-displacement data are given in figures B-12 through B-18 found in Appendix B. Here, the grouping of tests was chosen to give the following comparisons.

1. Figure B-12 gives a comparison of Tests No. 7, 8, 9, 10, and 11 to show the effects of water-to-air ratio on pressure for a charge weight of 16 gm. and a mass-per-frontal area of 0.102 slugs/in^2.

2. Figure B-13 gives a comparison of Tests No. 2 and 5 to show the effects of water-to-air ratio on pressure for a charge weight of 14 gm. and a mass-per-frontal area of 0.297 slugs/in^2.

3. Figure B-14 gives a comparison of Tests No. 3 and 6 to show the effects of water-to-air ratio on pressure for a charge weight of 30 gm. and a mass-per-frontal area of 0.102 slugs/in^2.

4. Figure B-15 gives a comparison of Tests No. 4 and 6 to show the effects of charge weight on pressure for a water-to-air ratio of 0 and a mass-per-frontal area of 0.102 slugs/in^2.

5. Figure B-16 gives a comparison of Tests No. 1 and 3 to show the effects of charge weight on pressure for a water-to-air ratio of 0.171 and a mass-per-frontal area of 0.102 slugs/in^2.

6. Figure B-17 gives a comparison of Tests No. 4 and 5 to show the effects of mass-per-frontal area on pressure for a water-to-air ratio of 0 and a charge weight of 14 grams.

7. Figure B-18 gives a comparison of Tests No. 1 and 2 to show the effects of mass-per-frontal area on pressure for a water-to-air ratio of 0.171 and a charge weight of 14 grams.

It is believed that the pressure data represented by these curves are not in error by more than $\pm$ 5 per cent for the near equilibrium conditions following the shock phenomena.

From an observation of the pressure curves for all tests, we note that a more significant decay of pressure existed for high-pressure levels than for low levels and that a residual pressure continued to act on the plug after it had completed the power stroke. The pressure decay can be explained as excessive gas leakage around the plug for high pressures, and the residual pressure as the dynamic pressure resulting from the jet of gas being released from the chamber subsequent to completion of the power stroke. Appendix C gives an evaluation of the gas-jet effect. Since pressure leakage prevented any meaningful conclusions being drawn from the high-pressure tests, any trends or indications had to be obtained from the low-pressure tests. Aside from the obvious effects of water-to-air ratio on pressure, these tests indicated that maximum equilibrium pressure was approximately proportional to charge weight and that mass-per-frontal area had only a small, if any, effect on pressure.

Mechanical-Energy Results. The most accurate method of calculating mechanical energy is given by equation (5), which states

$$ME = \frac{m}{2} v_f^2 + mgs_f + F\ s_f$$

where s_f is a known quantity equal to 13.25 inches or 1.104 feet, and v_f corresponding to s_f can be obtained from the velocity curves given in figures B-1 through B-11. Test No. 2 does not lend itself to this analysis as the plug did not reach s_f; therefore, the values of s and v to be used here are the maximum displacement s = 0.5891 feet and v = 0. For each test, table 3 presents the displacement s_f, velocity v_f, kinetic energy of plug $\frac{m}{2} v_f^2$, potential energy of plug mgs_f, heat lost to friction Fs_f, and total mechanical energy absorbed by plug ME. A comparison of mechanical energy and maximum potential energy, which is determined from equation (6) and the maximum height data in table 2, is given in table 4. It is noted from this comparison

TEST NUMBER	DISPLACEMENT	VELOCITY	KINETIC ENERGY OF PLUG	POTENTIAL ENERGY OF PLUG	HEAT LOSS TO FRICTION	MECHANICAL ENERGY
	s_f	v_f				ME
	(FT)	(FT/SEC)	(FT-LB)	(FT-LB)	(FT-LB)	(FT-LB)
1	1.1042	11.61	66.3	35.0	2.2	103.5
2	0.5891	0	0	54.1	1.2	55.3
3	1.1042	18.84	174.6	35.0	2.2	211.8
4	1.1042	53.03	1383.6	35.0	2.2	1420.8
5	1.1042	27.03	1042.6	101.5	2.2	1146.3
6	1.1042	69.26	2360.1	35.0	2.2	2397.3
7	1.1042	25.18	311.9	35.0	2.2	349.1
8	1.1042	21.26	222.4	35.0	2.2	259.6
9	1.1042	16.86	139.9	35.0	2.2	177.1
10	1.1042	14.57	104.4	35.0	2.2	141.6
11	1.1042	14.92	109.5	35.0	2.2	146.7

TABLE 3 MECHANICAL ENERGY ABSORBED BY MODEL PLUG

TEST NUMBER	MAX. HEIGHT	WEIGHT OF PLUG	POTENTIAL ENERGY		MECHANICAL ENERGY
	H	mg	PE		ME
	(FT)	(LB)	(FT-LB)		(FT-LB)
1	3.25	31.7	103.0		103.5
2	0.59	91.9	54.2		55.3
3	7.44	31.7	235.8		211.8
4	42.11	31.7	1334.9		1420.8
5	12.58	91.9	1156.1		1146.3
6	77.56	31.7	2458.7		2397.3
7	11.95	31.7	378.8		349.1
8	7.64	31.7	242.2		259.6
9	5.61	31.7	177.8		177.1
10	4.38	31.7	138.8		141.6
11	4.45	31.7	141.1		146.7

TABLE 4 COMPARISON OF MECHANICAL ENERGY AND MAXIMUM POTENTIAL ENERGY

that assumptions concerning friction and wind losses stated in the Energy-Partition Analysis section are valid, for their effects are included in the average ± 5 per cent variation between mechanical energy and maximum potential energy seen in table 4. Also the contribution to mechanical energy provided by the gas jet previously described must be negligible for it too is included in this average ± 5 per cent variation.

Explosive-Energy Results. The procedure outlined in Appendix A was used to determine the explosive energy for the charge weight and environmental conditions peculiar to each test. Charge weight, air weight, products of combustion, and explosive energy for each test are given in table 5. The accuracy of these results is dependent upon the predictions of chemical reactions under transient and unstable conditions of extremely high pressure and temperatures. There exists, however, good agreement (deviations of the order of 10 per cent) between the explosive energy determined by this type of prediction and the explosive energy obtained experimentally from bomb-calorimeter-type tests.

Energy-Partition Results. The energy partition for each test was determined by substituting into equations (7) and (1) corresponding values of mechanical energy and explosive energy given previously in tables 3 and 5. These energy-partition results are given in table 6 along with the corresponding values of mechanical energy and explosive energy. Accuracy of the

TEST NUMBER	CHARGE WEIGHT	AIR WEIGHT	MOLES H_2O	MOLES CO	MOLES CO_2	MOLES N_2	EXPLOSIVE ENERGY
							E_r
	(GM)	(GM)	(G-MOL)	(G-MOL)	(G-MOL)	(G-MOL)	(CAL)
1	13.9	12.79	0.1645	0.1793	0.1450	0.4402	24870
2	13.9	12.79	0.1645	0.1793	0.1450	0.4402	24870
3	30.0	12.79	0.3551	0.6026	0.0973	0.5444	39170
4	13.9	14.98	0.1645	0.1474	0.1769	0.5002	27020
5	13.9	14.98	0.1645	0.1474	0.1769	0.5002	27020
6	30.0	14.98	0.3551	0.5707	0.1292	0.6043	41320
7	16.2	14.92	0.1917	0.2087	0.1693	0.5136	29010
8	16.2	14.85	0.1917	0.2098	0.1682	0.5115	28940
9	16.2	14.69	0.1917	0.2121	0.1659	0.5071	28780
10	16.2	14.54	0.1917	0.2142	0.1638	0.5032	28640
11	16.2	14.40	0.1917	0.2163	0.1617	0.4992	28500

TABLE 5 EXPLOSIVE ENERGY

TEST NUMBER	MECHANICAL ENERGY	EXPLOSIVE ENERGY	ENERGY PARTITION
	ME (FT-LB)	E_r (FT-LB)	EP
1	103.5	76800	0.0013
2	55.3	76800	0.0007
3	211.8	120900	0.0018
4	1420.8	83400	0.0173
5	1146.3	83400	0.0139
6	2397.3	127600	0.0191
7	349.1	89600	0.0039
8	259.6	89300	0.0029
9	177.1	88800	0.0020
10	141.6	88400	0.0016
11	146.7	88000	0.0017

TABLE 6 ENERGY PARTITION

energy-partition results is largely dependent upon the possible 10 per cent error of the explosive energy results. With the values of energy partition available, an evaluation of the effects of the three governing parameters on energy partition can be made.

Graphical representations given in figure 9 show the variation of energy partition with water-to-air ratio for the tests utilizing a charge weight of approximately 16 grams and mass-per-frontal-area ratios of 0.102 and 0.297 slugs/in^2. It is noted that values of energy partition for the lighter plug are greater than those for the heavier plug. This effect of varying the mass-per-frontal area is to be expected if we consider the consequence of the heavier plug requiring more time to traverse the power stroke than the lighter plug for similar loading conditions. Here, a larger pressure decay results for the longer time duration from leakage around the unsealed plug, and more heat is lost to the surrounding walls. This larger pressure decay would appear as a decrease in mechanical energy that would in turn decrease the energy partition.

Graphical representations given in figure 10 show the variation of energy partition with water-to-air ratio for the tests utilizing a mass-per-frontal area of 0.102 slugs/in^2 and charge weights of approximately 16 and 30 grams. It is observed that the values of energy partition for the larger charge were

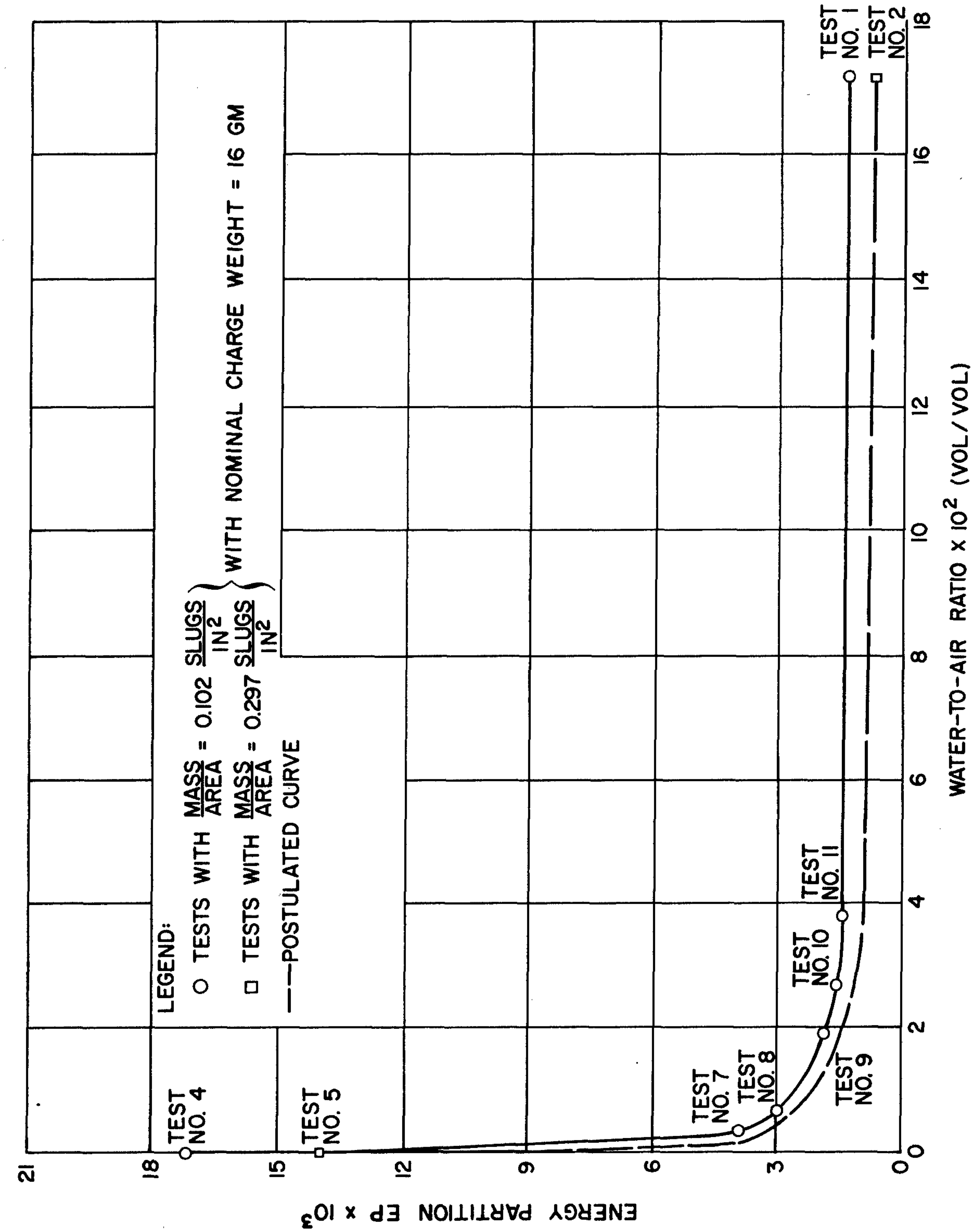

FIG. 9 VARIATION OF ENERGY PARTITION WITH WATER-TO-AIR RATIO FOR TWO VALUES OF MASS-PER-FRONTAL AREA

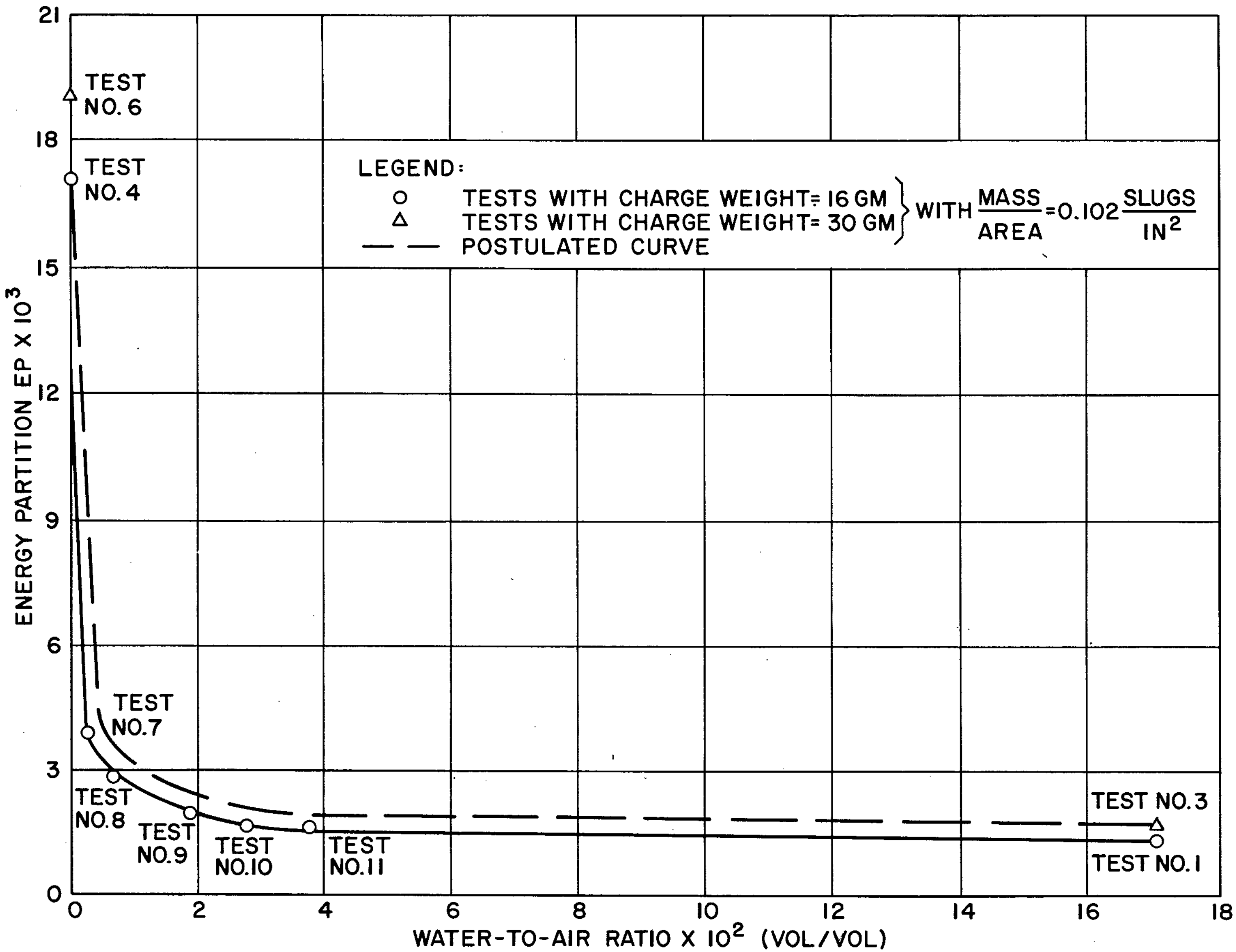

FIG. 10 VARIATION OF ENERGY PARTITION WITH WATER-TO-AIR RATIO FOR TWO VALUES OF CHARGE WEIGHT

greater than those for the smaller charge. Since the pressure loading for the small charge was lower than that for the large charge, the test duration was longer for the small-charge test. Although gas pressure and temperature were higher for the large-charge case than for the small-charge case, it is believed that gas leakage and heat transfer to the simulant walls for the longer duration test were the overriding factors responsible for the decrease in energy partition.

From figures 9 and 10 it is observed that water-to-air ratio had a marked effect on energy partition. Energy-partition ratios for the extreme values of water-to-air ratio, 0 and 0.171, differed by a factor of approximately 12. It is noted that the addition of only 32 cc of water reduced energy partition from 0.0173 (Test No. 4) to 0.0039 (Test No. 7), a factor greater than four. Also for water-to-air ratios greater than 0.03, energy partition appeared nearly constant.

Energy-Absorption Mechanisms. For all the experiments, the mechanical energy absorbed by the plug represented only a small portion of the total explosive energy. The remainder was absorbed by the surroundings in some manner. It is postulated here that the total explosive energy was manifested largely in the forms of kinetic energy of the water; strain energy and kinetic energy of the reactor-vessel simulant; heat added to the enclosed gas; and heat transferred to the water, reactor-vessel simulant, and secondary-shield simulant by conduction, convection, and/or radiation. The following paragraph consists of brief statements concerning the significance and possible method of calculation of each of the above energy absorbers.

The initial shock wave emitted from the explosion gave motion to the water casing. This motion was the result of the particle velocity of water following a shock wave. Reference (d) gives values of particle velocity as a function of pressure for the case of an infinite water medium. Since pressure at the shock front decreased with distance from the charge and since pressure behind the shock front decreased exponentially with time, particle velocity varied through the water casing. If we consider the entire water casing traveling at a mean particle velocity, then the total kinetic energy of the casing was

$$\frac{1}{2} m_w v_p^2$$

where

m_w ... is mass of water casing, slugs

v_p ... is mean particle velocity, ft/sec

The shock wave imparted energy to the reactor-vessel simulant by means of fracture and motion. It is assumed that the fragments of the simulant resulting from fracture moved with the mean particle velocity of the water. Methods of approximating both the kinetic energy and strain energy of the simulant are given in Appendix D. Following the shock phenomena there exists a static equilibrium pressure in the chamber that causes the model plug to move subsequent to whatever motion has been imparted by the shock wave. This pressure is the result of mixing the hot, expanding explosive gas products with the initial chamber gas. We elect to define that portion of the explosive energy that remains in this final gas mixture as the heat added to the enclosed gas (explosive products plus initial gas). A method of estimating the heat added is given in Appendix D. Since the heat transfer to the previously listed surroundings is largely unknown for the turbulent and transient conditions found within the secondary-shield simulant, the various heat-transfer absorptions are lumped together and denoted as energy losses. The magnitude of these losses is determined by subtracting the summation of the previously described absorptions from the total explosive energy.

In the section Sample Calculations of Appendix D, estimates of the various energy absorptions are given for the conditions of Test No. 8. It was found that the kinetic energy of the water casing was 9,370 calories, the kinetic energy of the reactor-vessel simulant was 4,410 calories, the strain energy of the simulant was 130 calories, the heat added to the gas was 740 calories, and the energy losses were 14,290 calories. From these estimates we see that kinetic energy of the water casing and the simulant may account for nearly 50 per cent of the total 28,940 calories released by the charge. Although the values of these energy absorptions are only estimates, motion given to the water casing and the reactor-vessel simulant appears to be an effective energy-absorption mechanism.

SUMMARY AND CONCLUSIONS

Summary. The governing parameters of energy partition resulting from the detonation of a water-cased explosive surrounded by air in a closed piston-fitted vessel have been postulated to be

1. charge weight and composition.
2. water-to-air ratio.
3. mass-per-frontal area.
4. length of power stroke.
5. temperature of water.
6. temperature of secondary-shield-simulant walls.
7. temperature of enclosed air.
8. size and configuration of secondary-shield simulant.

Analytic equations expressing the energy partition resulting from model-plug response to simulated excursion-type loadings have been established. A test apparatus for the conduct of energy-partition experiments has been constructed, and eleven experiments have been conducted. These experiments were designed to investigate the effects of the three parameters, water-to-air ratio, charge weight, and mass-per-frontal area, on energy partition. Methods of reducing experimentally obtained data to forms required for use in the analytic equations have been formulated. Possible energy-absorption mechanisms have been examined and qualitatively analyzed to

determine their relative effectiveness. All experimental, calculated, and graphical results pertinent to the technical objectives have been presented in tabular and graphical forms in considerable detail.

Conclusions. The experimental, calculated, and graphical data and results presented in this report constitute the sole basis for the following conclusions.

1. The parameter water-to-air ratio has a marked effect on energy partition. Comparing values of energy partition from table 6 for Tests No. 4 and 1, we see that for the extreme water-to-air ratio of 0.171 the energy partition was reduced by a factor greater than 12. From the consistency and symmetry of the data that constitute the plot shown in figure 9, it is concluded that for increasing values of water-to-air ratio within the region of 0 to 0.171, energy partition will decrease.

2. Effects of charge weight and mass-per-frontal area on energy partition are small for the subject experiments. Decreasing the charge weight and increasing the mass-per-frontal area resulted in slight decreases of energy partition. Excessive gas leakage prevented a precise evaluation of these two parameters.

3. From qualitative analyses of the postulated energy absorptions for the conditions of Test No. 8, motion given to the water casing and reactor-vessel simulant appears as a probable and significant energy-absorption mechanism.

It is to be emphasized that these conclusions are valid only for the subject model experiments, and no statement, qualitative or quantitative, can be made at this time that would apply to a full-scale reactor plant. However, the following meaningful statements can be made concerning applicability of the solution of the subject energy-partition problem to the Enrico Fermi and other nuclear power facilities.

1. If additional experiments designed to investigate all the governing parameters are conducted in an improved mechanism incorporating a sealed model plug, if the effectiveness of water as a simulant for sodium is determined, and if the effect of the governing parameters on energy partition are investigated through scaled-up model experiments, then a general solution applicable to the Fermi plant can be achieved.

2. Not only would the results from these additional experiments be directly applicable to the Fermi plant, but they would also serve as valuable design data for future nuclear power plants utilizing the basic concepts of the Fermi plant design.

FUTURE WORK

An extensive experimental program is currently being planned to investigate the eight governing parameters given in the previous section. Where appropriate, several parameters will be modified to include molten sodium as the explosive casing and oxygen-depleted air as the gas enclosed within the secondary-shield simulant. Experiments will be conducted using sodium casings at temperatures up to 850°F, enclosed gas at temperatures up to 200°F or more, and secondary-shield-simulant walls at temperatures up to 200°F or more. The need for oxygen-depleted air within the simulant is to eliminate any chemical reactions with the molten sodium that could release energy.

An improved test apparatus is being designed with secondary-shield-simulant dimensions identical to those of the apparatus described herein. Aside from design considerations that will facilitate conduct of the new experiments, improved features such as a sealed model plug and a greatly extended power stroke, 6 feet in length, will be incorporated into the new mechanism. Still another test mechanism is being designed with secondary-shield simulant dimensions twice those of the simulant described herein. Experiments in this double-scale apparatus will indicate the effects of scaling on energy partition.

To complete the experimental program, a large number of tests will be required. If the energy partition and the pressure-displacement function were determined for this large number of tests in accord with the procedure outlined in the section Calculated and Graphical Results, an inordinately large effort would be expended in analyzing film and reducing data. It is desirable, then, to correlate these parameters with a knowledge of the maximum height of plug travel which is easily and simply obtained. A possible method of correlation for the new experiments is given in Appendix E.

For all of the experiments reported herein, it was assumed that the reactor vessel will rupture non-marginally for the 1000-pound TNT accident. Fundamental containment studies on model reactor vessels conducted by NOL and reported in reference (e) indicate that this assumption may not be valid, particularly for slower energy releases. If containment of the Fermi vessel did occur, a greater plug-jump would necessarily result. Therefore, it is imperative that the containment potential of the Fermi vessel be established if a meaningful missile-hazard analysis is to be achieved.

It is believed that the experimental program briefly described in this section will determine the general character of the subject energy partition and, hence, achieve the solution to the missile-hazard problem created by response of the shield plug in the Fermi plant to possible excursion loading.

The author acknowledges a special debt of gratitude to his immediate supervisor, Dr. Walter R. Wise, Jr., Structural Research Engineer, for his advice and guidance in the direction of the subject program and for his careful technical review of this presentation. Also the author is indebted to members of the Air-Ground Explosions Division, particularly Mr. Lloyd P. Walker, Jr. and Mr. William S. Filler for their assistance in the design of the test apparatus and in the conduct of the experiments. Commendation is given to the Publications and Photographic Divisions for their help in the preparation of the various tables and figures.

REFERENCES

(a) Atomic Power Development Associates, Inc., Enrico Fermi Atomic Power Plant, APDA-124, Jan 1959

(b) Fisher, E. M. and Wise, W. R., Jr., Containment Study of the Enrico Fermi Fast Breeder Reactor Plant, NAVORD Report 5747, 7 Oct 1957, Unclassified

(c) Hildebrand, F. B., Introduction to Numerical Analysis, New York, McGraw-Hill, 1956

(d) Cole, Robert H., Underwater Explosions, New Jersey, Princeton University Press, 1948

(e) Wise, Walter R. Jr., An Investigation of Strain-Energy Absorption Potential as the Criterion for Determining Optimum Reactor-Vessel Containment Design, NAVORD 5748, 30 Jun 1958, Unclassified

APPENDIX A

Method of Calculating Energy Released by Explosive

Combustion products resulting from the detonation of the pentolite charge and from the afterburning of explosive gas with the surrounding air must be determined. The chemical composition of pentolite is 50 per cent PETN and 50 per cent TNT by weight. The chemical formulas for these two explosive compounds are

$$\text{PETN} \ldots C_5H_8N_4O_{12}$$

$$\text{TNT} \ldots C_7H_5N_3O_6$$

An arbitrary chemical equation representing the reaction is

$$\frac{\text{charge weight (gm)}}{632} \left(C_5H_8N_4O_{12} + \frac{316}{227} C_7H_5N_3O_6 \right)$$

$$+ \frac{\text{air weight (gm)}}{28.84} (0.79\ N_2 + 0.21\ O_2) \longrightarrow$$

$$(a)\ H_2O + (b)\ CO + (c)\ CO_2 + (d)\ N_2$$

where

a, b, c, d ... are constants.

The number of moles of each product (H_2O, CO, and CO_2) is multiplied by the respective heat of formation of each product for the conditions of one atmosphere pressure and 25°C temperature. A summation of these heats of formation less the heat of formation of the explosive compound is the energy released for the conditions of one atmosphere and 25°C. However, a correction must be made to account for a constant volume process. Analytically expressed, the corrected explosive energy is

$$E_r = E_p - E_e + \Delta nRT$$

where

E_r ... is explosive energy (taken positive), cal

E_p ... is summation of heats of formation of gas products (taken positive), cal

E_e ... is heat of formation of explosive charge (taken positive), cal

Δn ... is the change of moles of gas products, g-mol

R .... is universal gas constant, cal/g-mol °K

T .... is temperature at standard conditions, °K

We take the respective heats of formation of PETN and TNT to be 125,000 cal/g-mol and 17,800 cal/g-mol.

Values of the combustion products and explosive energy for each experiment are presented in the text in table 5.

APPENDIX B

Tables and Graphs of Model-Plug Response Data

The following is a list of tables and graphs given in this appendix in order of presentation.

1. Tables B-1 through B-11 give model-plug response data for each of the eleven tests.

2. Figures B-1 through B-11 give graphical representations of model-plug response data for each of the eleven tests.

3. Figures B-12 through B-18 give graphical representations of pressure-displacement functions for the various tests.

The notations used to identify the various parameters are as follows.

t .... time, msec

s_e ... experimentally obtained displacement, ft

s_g ... graphically obtained displacement, ft

v_c ... calculated velocity, ft/sec

v_g ... graphically obtained velocity, ft/sec

a_c ... calculated acceleration, ft/sec^2

a_g ... graphically obtained acceleration, ft/sec^2

p .... calculated pressure, psig

TABLE B-I MODEL-PLUG RESPONSE DATA FOR TEST NO. I

EXPERIMENTAL DATA		CALCULATED DATA						
TIME	DISPLACE-MENT	TIME	DISPLACE-MENT	VELOCITY	VELOCITY	ACCEL-ERATION	ACCEL-ERATION	PRESSURE
t	s_e	t	s_g	v_c	v_g	a_c	a_g	p
(MSEC)	(FT)	(MSEC)	(FT)	(FT/SEC)	(FT/SEC)	(FT/SEC^2)	(FT/SEC^2)	(PSIG)
0	0	0	0	0	0	0	0	0
0.41	0.0031	0.05	-	-	-	19500	19500	1992.5
0.82	0.0043	0.10	-	-	1.95	-	7100	727.7
1.22	0.0000	0.20	-	-	2.26	2600	2400	248.3
1.63	0.0031	0.30	-	-	2.47	1600	1600	166.7
2.04	0.0098	0.40	-	-	2.58	1050	1180	123.9
2.44	0.0067	0.50	0.0013	2.80	2.69	950	970	102.4
2.85	0.0080	0.60	-	-	2.77	850	845	89.7
3.26	0.0117	0.70	-	-	2.85	750	771	82.1
3.67	0.0098	0.80	-	-	2.92	650	712	76.1
4.07	0.0129	0.90	-	-	2.98	-	674	72.2
4.48	0.0166	1.00	0.0028	3.06	3.05	-	637	68.5
4.89	0.0178	1.50	0.0044	3.30	3.31	534	535	58.1
5.29	0.0190	2.00	0.0061	3.50	3.56	464	489	53.4
5.70	0.0239	2.50	0.0079	3.70	3.77	432	458	50.2
6.11	0.0227	3.00	0.0098	3.90	3.98	406	424	46.7
6.51	0.0282	3.50	0.0118	4.14	4.18	394	392	43.5
6.92	0.0301	4.00	0.0139	4.36	4.37	372	361	40.3
7.33	0.0331	4.50	0.0162	4.52	4.56	354	331	37.2
7.73	0.0350	5.00	0.0185	4.72	4.72	330	302	34.3
8.14	0.0344	5.50	0.0208	4.86	4.89	314	277	31.8
8.55	0.0393	6.00	0.0234	5.06	5.03	284	249	28.9
8.95	0.0417	6.50	0.0259	5.24	5.19	250	224	26.3
9.26	0.0460	7.00	0.0286	5.32	5.28	200	201	24.0
9.76	0.0442	7.50	0.0313	5.44	5.39	158	179	21.7
10.17	0.0479	8.00	0.0340	5.50	5.43	140	160	19.8
10.58	0.0515	8.50	0.0368	5.56	5.51	120	141	17.9
10.98	0.0540	9.00	0.0396	5.64	5.57	118	126	16.4
11.39	0.0552	9.50	0.0424	5.70	5.62	100	112	14.9
11.79	0.0589	10.00	0.0453	5.72	5.67	94	101	13.8

TABLE B-1 CONTINUED

12.20	0.0595	10.5	0.0482	-	5.71	90	-	-
12.60	0.0614	11.0	0.0510	5.80	5.76	86	86.0	12.2
13.01	0.0614	12	0.0569	5.86	5.84	75	75.4	11.2
13.41	0.0663	13	0.0628	5.92	5.91	69	70.8	10.7
13.82	0.0663	14	0.0687	5.97	5.97	65	67.7	10.4
14.22	0.0693	15	0.0747	6.03	6.04	63	66.0	10.2
14.53	0.0724	16	0.0808	6.12	6.10	64	65.1	10.1
15.03	0.0730	17	0.0869	6.10	6.16	63	64.7	10.1
15.44	0.0749	18	0.0932	6.11	6.23	65	64.7	10.1
15.84	0.0773	19	0.0990	-	6.29	65	64.7	10.1
16.25	0.0822	20	0.1053	6.21	6.36	63	64.6	10.1
16.65	0.0847	21	-	-	6.42	-	-	-
17.87	0.0920	22	0.1173	6.35	6.48	65	64.6	10.1
19.08	0.1000	24	0.1308	6.57	6.62	66	64.6	10.1
20.26	0.1074	26	0.1440	6.71	6.75	65	64.5	10.1
21.50	0.1154	28	0.1576	6.72	6.88	64	64.5	10.1
22.71	0.1215	30	0.1710	6.79	7.00	64	64.5	10.1
23.92	0.1301	32	0.1845	6.90	7.13	63	64.4	10.1
25.13	0.1393	34	0.1984	7.08	7.26	65	64.4	10.1
26.34	0.1497	36	0.2129	7.28	7.38	65	64.4	10.1
27.55	0.1528	38	0.2276	7.37	7.52	65	64.3	10.1
28.76	0.1632	40	0.2427	7.48	7.65	65	64.2	10.0
30.77	0.1736	42	0.2572	7.58	7.77	65	63.9	10.0
32.78	0.1896	44	0.2729	7.72	7.90	66	63.5	10.0
34.79	0.2043	46	0.2883	7.93	8.04	66	63.0	9.9
36.79	0.2197	48	0.3043	8.05	8.17	65	62.3	9.9
38.79	0.2332	50	0.3208	8.21	8.29	63	61.5	9.8
41.80	0.2503	52	0.3371	8.35	8.42	63	60.7	9.7
42.80	0.2700	54	0.3540	8.49	8.54	62	60.0	9.6
45.99	0.2890	56	0.3712	8.66	8.67	61	59.3	9.5
47.99	0.3025	58	0.3886	8.88	8.78	60	58.6	9.5
49.98	0.3166	60	0.4064	9.10	8.91	58	57.8	9.4
51.97	0.3375	62	0.4252	9.32	9.02	56	57.2	9.3
53.96	0.3522	64	0.4439	9.44	9.13	54	56.5	9.3
55.95	0.3731	66	0.4630	9.50	9.23	54	55.8	9.2
57.93	0.3878	68	0.4819	9.60	9.34	53	55.0	9.1

TABLE B-I CONTINUED

59.92	0.4019	70	0.5012	9.70	9.45	53	54.3	9.0
61.90	0.4234	72	0.5208	9.77	9.55	51	53.6	9.0
63.88	0.4442	74	0.5405	9.79	9.65	50	52.9	8.9
65.86	0.4633	76	0.5599	9.77	9.75	50	52.2	8.8
67.83	0.4798	78	0.5795	9.79	9.85	50	51.4	8.7
69.81	0.4964	80	0.5990	9.81	9.95	50	50.7	8.7
71.78	0.5197	82	0.6188	9.84	10.05	50	50.0	8.6
73.75	0.5387	84	0.6383	9.97	10.15	49	49.3	8.5
75.72	0.5590	86	0.6582	10.06	10.25	48	48.6	8.5
77.68	0.5786	88	0.6790	10.21	10.34	46	47.9	8.4
79.65	0.5989	90	0.6990	10.35	10.43	45	47.2	8.3
81.61	0.6142	92	0.7200	10.42	10.52	45	46.5	8.2
83.18	0.6289	94	0.7412	10.54	10.61	45	45.8	8.2
85.14	0.6486	96	0.7621	10.57	10.70	45	45.1	8.1
87.49	0.6762	98	0.7833	10.64	10.79	45	44.3	8.0
89.44	0.6958	100	0.8046	10.81	10.88	44	43.6	7.9
91.40	0.7185	102	0.8263	10.97	10.97	43	42.8	7.9
93.37	0.7357	104	0.8487	11.08	11.05	42	42.2	7.8
95.30	0.7541	106	0.8709	11.12	11.13	42	41.5	7.7
97.25	0.7780	108	0.8931	11.13	11.22	41	40.8	7.7
99.19	0.7995	110	0.9153	11.21	11.30	40	40.1	7.6
101.14	0.8247	112	0.9378	11.33	11.37	39	39.3	7.5
103.08	0.8400	114	0.9606	11.42	11.45	38	38.2	7.4
105.02	0.8584	116	0.9837	11.50	11.53	38	35.9	7.2
106.96	0.8824	118	1.0065	11.56	11.60	31	30.8	6.6
108.90	0.9063	120	1.0298	11.65	11.67	20	19.2	5.5
110.83	0.9253	122	1.0531	11.71	11.69	6	9.4	4.5
112.76	0.9437	124	1.0769	11.69	11.68	− 8	− 8.8	2.2
114.69	0.9646	126	1.1000	11.63	11.65	− 17	−15.4	1.5
116.62	0.9873	128	1.1232	11.58	11.61	− 21	−19.0	1.2
118.53	1.0094	130	1.1462	11.57	11.56	− 23	−21.0	0.9
120.48	1.0351	132	1.1696	11.50	11.52	− 24	−22.2	0.8
122.40	1.0566	134	1.1925	11.43	11.47	− 23	−23.1	0.7
124.32	1.0787	136	1.2150	11.31	11.42	− 23	−23.8	0.7
126.24	1.1020	138	1.2378	11.28	11.38	− 22	−24.5	0.6
128.16	1.1253	140	1.2600	11.27	11.34	− 23	−25.3	0.5

TABLE B-1 CONCLUDED

130.08	1.1480	142	1.2828	11.25	11.29	−25	−25.9	0.4
132.00	1.1646	144	1.3052	11.27	11.24	−27	−26.6	0.4
133.90	1.1898	146	1.3277	11.17	11.18	−27	−27.3	0.3
135.81	1.2119	148	1.3502	11.09	11.13	−27	−28.0	0.2
137.72	1.2333	150	1.3720	10.99	11.08	−28	−28.6	0.2
139.63	1.2579	152	1.3939	10.92	11.02	−29	−29.3	0.1
141.53	1.2818	154	1.4157	10.90	10.96	−30	−29.9	0.0
143.44	1.2990	156	1.4375	10.88	10.90	−30	−30.5	0.4
145.34	1.3205	158	1.4592	10.88	10.84	−30	−31.0	0.4
147.24	1.3383	160	1.4809	10.83	10.78	−31	−31.5	0.3
149.13	1.3653	162	1.5028	10.75	10.72	−33	−32.0	0.3
151.03	1.3831	164	1.5240	10.68	10.65	−33	−32.4	0.3
152.92	1.4039	166	1.5451	10.57	10.58	−34	−32.8	0.2
154.81	1.4236	168	1.5665	10.52	10.52	−34	−33.2	0.2
156.33	1.4395	170	1.5872	10.47	10.45	−33	−33.4	0.2
158.59	1.4677	172	1.6081	10.38	10.38	−34	−33.5	0.1
162.36	1.5064	174	1.6290	10.33	10.32	−34	−33.5	0.1
166.12	1.5500	176	1.6494	10.24	10.25	−33	−33.5	0.1
169.88	1.5855	178	1.6698	10.20	10.18	-	-	-
173.25	1.6217	180	1.6901	10.13	10.12	-	-	-
177.37	1.6622	182	1.7106	10.11	-	-	-	-
181.10	1.6978	184	1.7303	10.10	-	-	-	-
184.83	1.7420	186	1.7508	10.08	-	-	-	-
188.54	1.7721	188	1.7710	10.06	-	-	-	-
191.25	1.8120	190	1.7910	9.89	-	-	-	-
195.96	1.8506	192	1.8108	9.72	-	-	-	-
199.65	1.8801	194	1.8298	9.39	-	-	-	-
203.34	1.9077	196	1.8488	8.88	-	-	-	-
207.02	1.9242	198	1.8659	8.14	-	-	-	-
		200	1.8815	7.17	-	-	-	-

TABLE B-2 MODEL-PLUG RESPONSE DATA FOR TEST NO. 2

EXPERIMENTAL DATA		CALCULATED DATA						
TIME	DISPLACE-MENT	TIME	DISPLACE-MENT	VELOCITY	VELOCITY	ACCEL-ERATION	ACCEL-ERATION	PRESSURE
t	s_e	t	s_g	v_c	v_g	a_c	a_g	p
(MSEC)	(FT)	(MSEC)	(FT)	(FT/SEC)	(FT/SEC)	(FT/SEC^2)	(FT/SEC^2)	(PSIG)
0	0	0	0	0	0	0	0	0
0.41	0.0023	0.05	-	-	-	10000	10000	2969.8
0.82	0.0008	0.1	-	-	1.000	-	5700	1697.0
1.24	0.0000	0.2	-	-	1.103	2440	600	187.4
1.65	0.0015	0.3	-	-	1.136	377	230	77.8
20.6	0.0060	0.4	-	-	1.152	164	140	51.2
2.47	0.0030	0.5	0.0006	1.20	1.164	105	110	42.3
2.88	0.0053	0.6	-	-	1.171	75	90	36.4
3.30	0.0015	0.7	-	-	1.179	55	70	30.5
3.71	0.0030	0.8	-	-	1.182	51	58	26.9
4.12	0.0060	0.9	-	-	1.186	-	48	24.0
4.53	0.0068	1.0	0.0012	1.20	1.193	-	41	21.9
4.94	0.0053	1.5	0.0018	1.20	-	-	-	-
5.35	0.0075	2.0	0.0024	1.16	1.241	-	35	20.1
5.77	0.0053	2.5	0.0030	1.18	-	-	-	-
6.18	0.0121	3.0	0.0035	1.20	1.282	40.4	33	19.5
6.59	0.0075	3.5	0.0042	1.26	-	-	-	-
7.00	0.0098	4.0	0.0048	1.34	1.321	37.1	32	19.2
7.41	0.0113	4.5	0.0055	1.32	-	-	-	-
7.82	0.0098	5.0	0.0062	1.34	1.355	34.9	30	18.6
8.24	0.0113	5.5	0.0068	1.34	-	-	-	-
8.65	0.0106	6.0	0.0075	1.36	1.390	32.3	30	18.6
9.06	0.0121	6.5	0.0082	1.40	-	-	-	-
9.47	0.0106	7.0	0.0089	1.40	1.422	29.5	29	18.3
9.88	0.0121	7.5	0.0096	1.44	-	-	-	-
10.29	0.0128	8.0	0.0103	1.46	1.449	25.9	28	18.0
10.71	0.0136	8.5	0.0111	-	-	-	-	-
11.12	0.0113	9.0	0.0118	1.35	1.473	-	25	17.2
11.53	0.0136	10	0.0130	1.19	1.494	21.95	24	16.9
11.94	0.0151	11	0.0143	1.28	-	-	-	-
12.35	0.0181	12	0.0150	1.43	1.534	18.05	18.1	15.1

TABLE B-2 CONTINUED

12.76	0.0204	13	0.0172	1.55	-	-	-	-
13.17	0.0204	14	0.0187	1.66	1.567	15.25	15.2	14.3
13.59	0.0173	15	0.0202	1.51	-	-	-	-
14.00	0.0181	16	0.0218	1.46	1.593	12.70	13.2	13.7
14.41	0.0211	17	0.0232	-	-	-	-	-
14.82	0.0204	18	0.0245	1.53	1.617	11.05	11.7	13.2
15.23	0.0211	20	0.0279	1.56	1.636	9.85	10.4	12.8
15.64	0.0241	22	0.0309	1.65	1.656	8.90	9.4	12.5
16.05	0.0219	24	0.0342	1.69	1.672	9.00	8.5	12.3
16.46	0.0219	25	-	-	1.680	-	-	-
16.88	0.0226	26	0.0378	1.69	1.688	8.00	7.7	12.0
17.29	0.0287	28	0.0413	1.70	1.710	-	7.0	11.8
17.70	0.0219	30	0.0442	1.72	1.717	6.44	6.4	11.7
18.11	0.0279	32	0.0480	1.73	-	-	-	-
19.34	0.0234	34	0.0516	1.79	-	-	-	-
20.58	0.0294	35	-	-	1.744	5.04	5.2	11.3
21.81	0.0324	36	0.0549	1.78	-	-	-	-
23.04	0.0362	38	0.0586	1.79	-	-	-	-
24.27	0.0312	40	0.0623	1.79	1.765	4.16	4.4	11.1
25.51	0.0392	42	0.0658	1.77	-	-	-	-
26.74	0.0445	44	0.0692	1.77	-	-	-	-
30.43	0.0498	45	0.0713	-	1.782	3.78	3.9	10.9
34.54	0.0528	46	0.0728	1.79	-	-	-	-
38.64	0.0588	48	0.0765	-	-	-	-	-
42.74	0.0694	50	0.0800	1.802	1.802	3.68	3.7	10.9
52.99	0.0875	55	0.0892	1.812	1.820	3.60	3.6	10.8
63.22	0.1018	60	0.0984	1.836	1.838	3.44	3.5	10.8
73.44	0.1252	65	0.1074	1.848	1.854	3.34	3.3	10.7
83.65	0.1440	70	0.1168	1.876	1.871	3.14	3.2	10.7
93.84	0.1629	75	0.1262	1.898	1.887	2.98	3.0	10.6
104.02	0.1825	80	0.1359	1.902	1.900	2.82	2.8	10.6
114.20	0.1848	85	0.1453	1.918	1.914	2.64	2.7	10.6
124.36	0.2247	90	0.1548	1.928	1.928	2.50	2.6	10.5
134.50	0.2473	95	0.1647	1.948	1.939	2.32	2.4	10.5
144.64	0.2677	100	0.1744	1.958	1.950	2.12	2.2	10.4
154.76	0.2850	105	0.1842	1.964	1.961	1.92	1.8	10.3

TABLE B-2 CONTINUED

164.87	0.3031	110	0.1940	1.980	1.970	1.68	1.7	10.3
174.97	0.3243	115	0.2040	1.988	1.977	1.40	1.5	10.2
185.06	0.3393	120	0.2140	1.990	1.984	1.20	1.2	10.1
195.14	0.3650	125	0.2239	1.988	1.989	1.00	1.0	10.0
205.20	0.3800	130	0.2338	1.982	1.994	0.76	0.8	10.0
215.65	0.3967	135	0.2438	1.968	1.997	0.46	0.4	9.9
225.29	0.4148	140	0.2536	1.952	1.999	0.06	0	9.8
235.32	0.4306	145	0.2632	1.950	1.998	− 0.36	−0.5	9.6
245.33	0.4472	150	0.2729	1.970	1.995	− 0.84	−0.9	9.5
255.34	0.4585	155	0.2829	1.994	1.990	− 1.22	−1.3	9.4
265.33	0.4789	160	0.2930	2.006	1.982	− 1.64	−1.7	9.3
275.31	0.4864	165	0.3030	1.996	1.974	− 2.08	−2.1	9.1
285.28	0.5105	170	0.3130	1.972	1.962	− 2.52	− 2.6	9.0
295.21	0.5158	175	0.3228	1.948	1.948	− 3.00	− 2.9	8.9
305.18	0.5249	180	0.3324	1.928	1.932	− 3.36	− 3.4	8.8
315.11	0.5354	185	0.3428	1.904	1.914	− 3.70	− 3.7	8.7
325.03	0.5452	190	0.3516	1.888	1.895	− 4.00	− 4.1	8.5
334.94	0.5588	195	0.3608	1.864	1.874	-	− 4.5	8.4
344.83	0.5656	200	0.3702	1.834	1.852	− 4.41	− 4.9	8.3
354.71	0.5731	210	0.3882	1.780	1.806	− 4.82	− 5.6	8.1
364.59	0.5761	220	0.4059	1.752	1.756	− 5.22	− 6.2	7.9
374.45	0.5784	230	0.4232	1.714	1.702	− 5.69	− 6.8	7.8
384.29	0.5859	240	0.4401	1.656	1.643	− 6.26	− 7.3	7.6
394.13	0.5852	250	0.4563	1.602	1.578	− 6.90	− 7.7	7.5
403.95	0.5890	260	0.4720	1.496	1.505	− 7.56	− 8.2	7.3
413.76	0.5890	270	0.4863	1.396	1.426	− 8.20	− 8.6	7.2
423.56	0.5859	280	0.4999	1.278	1.341	− 8.86	− 9.0	7.1
443.13	0.5784	290	0.5120	1.194	1.250	− 9.47	− 9.4	7.0
462.64	0.5663	300	0.5238	1.126	1.150	− 9.98	− 9.7	6.9
482.11	0.5460	310	0.5345	1.056	1.048	− 10.35	− 10.0	6.8
520.90	0.5000	320	0.5448	0.980	0.943	− 10.60	− 10.3	6.7
559.50	0.4321	340	0.5630	0.858	0.726	− 11.00	− 10.9	6.5
598.29	0.3416	360	0.5779	0.544	0.503	− 11.46	− 11.3	6.4
599.44	0.3348	380	0.5858	0.282	0.268	− 11.69	− 11.7	6.3
636.12	0.2300	400	0.5885	0.070	0.035	− 11.81	− 12.1	6.2
		420	0.5880	-0.194	-0.204	− 12.13	− 12.4	5.7

TABLE B-2 CONCLUDED

		440	0.5807	-0.558	-0.450	− 12.39	−12.7	5.6
		460	0.5668	-0.748	-0.700	− 12.70	−13.0	5.5
		480	0.5500	-1.000	-0.958	− 13.09	−13.2	5.4
		500	0.5272	-1.212	-1.224	− 13.42	−13.4	5.4
		520	0.5009	-1.442	-1.494	− 13.85	−13.7	5.3
		540	0.4698	-1.716	-1.779	− 15.16	−13.9	5.3
		560	0.4312	-2.116	-2.102	− 16.27	−14.0	5.2
		580	0.3860	-2.434	-2.426	− 15.65	−14.2	5.1
		600	0.3347	-2.738	-2.728	− 14.36	−14.4	5.1
		620	0.2770	-2.960	-3.000	-	-	-

TABLE B-3 MODEL-PLUG RESPONSE DATA FOR TEST NO.3

EXPERIMENTAL DATA		CALCULATED DATA								
TIME	DISPLACE-MENT	TIME	DISPLACE-MENT	VELOCITY	VELOCITY	ACCEL-ERATION	ACCEL-ERATION	PRESSURE
t	s_e	t	s_g	v_c	v_g	a_c	a_g	p
(MSEC)	(FT)	(MSEC)	(FT)	(FT/SEC)	(FT/SEC)	(FT/SEC^2)	(FT/SEC^2)	(PSIG)
0	0	0	0	0	0	0	0	0
0.41	0.0053	0.1	-	-	2.75	-	-	-
0.82	0.0008	0.2	-	-	3.50	9840	9840	1007.2
1.23	0.0030	0.3	-	-	3.95	4560	4740	487.0
1.64	0.0083	0.4	-	-	4.32	3370	3440	354.4
2.05	0.0098	0.5	0.0025	5.20	4.62	2710	2710	279.9
2.46	0.0083	0.6	-	-	4.85	2220	2220	229.9
2.87	0.0150	0.7	-	-	5.04	1830	1860	193.2
3.28	0.0180	0.8	-	-	5.22	1550	1600	166.7
3.69	0.0211	0.9	-	-	5.35	-	1420	148.3
4.10	0.0211	1.0	0.0052	5.56	5.47	-	1290	135.1
4.51	0.0271	1.5	0.0081	5.90	5.93	978	900	95.3
4.92	0.0308	2.0	0.0111	6.24	6.32	740	720	76.9
5.33	0.0323	2.5	0.0143	6.60	6.65	656	630	67.8
5.74	0.0361	3.0	0.0177	6.96	6.96	600	560	60.6
6.17	0.0414	3.5	0.0213	7.26	7.25	564	510	55.5
6.56	0.0451	4.0	0.0250	7.50	7.52	538	480	52.5
6.97	0.0489	4.5	0.0288	7.74	7.78	516	440	48.4
7.38	0.0504	5.0	0.0327	8.00	8.04	484	430	47.4
7.79	0.0534	5.5	0.0368	8.26	8.28	444	410	45.3
8.19	0.0587	6.0	0.0410	8.54	8.48	398	380	42.3
8.60	0.0662	6.5	0.0453	8.76	8.67	360	360	40.2
9.02	0.0647	7.0	0.0498	8.96	8.84	330	340	38.2
9.42	0.0729	7.5	0.0543	8.94	9.00	304	320	36.1
9.83	0.0729	8.0	0.0589	9.16	9.14	288	310	35.1
10.24	0.0782	8.5	0.0631	9.18	9.28	272	280	32.1
10.65	0.0827	9.0	0.0683	9.54	9.42	260	260	30.0
11.05	0.0895	9.5	0.0730	9.70	9.54	240	240	28.0
11.46	0.0887	10.0	0.0778	9.60	9.66	220	220	25.9
11.87	0.0940	10.5	0.0826	9.70	9.76	204	207	24.6
12.28	0.0948	11.0	0.0875	9.80	9.86	194	194	23.3
12.69	0.1023	11.5	0.0924	9.86	9.95	186	182	22.1

TABLE B-3 CONTINUED

13.09	0.1053		12.0		0.0974		9.94	10.05		172	171		20.9
13.50	0.1090		12.5		0.1023		10.04	10.13		162	160		19.8
13.91	0.1128		13.0		0.1074		10.08	10.20		150	155		19.3
14.32	0.1218		13.5		0.1125		10.14	10.28		142	152		19.0
14.72	0.1226		14.0		0.1175		10.10	10.35		134	150		18.8
15.13	0.1241		14.5		0.1226		-	10.41		124	149		18.7
15.54	0.1286		15.0		0.1276		10.31	10.47		124	149		18.6
15.94	0.1339		15.5		-		-	10.53		-	149		18.6
16.35	0.1369		16.0		0.1380		10.55	10.60		143	149		18.7
16.76	0.1421		17		0.1487		10.75	10.76		152	152		19.0
17.16	0.1504		18		0.1597		10.88	10.92		159	156		19.4
18.38	0.1609		19		0.1705		10.94	11.07		160	158		19.6
19.60	0.1745		20		0.1815		11.00	11.24		161	159		19.7
20.82	0.1857		21		0.1925		11.24	11.40		162	159		19.7
22.04	0.2008		22		0.2037		11.23	11.56		160	158		19.6
23.25	0.2181		23		0.2156		11.24	11.72		158	158		19.6
24.47	0.2279		24		0.2261		11.25	11.88		157	158		19.6
25.68	0.2421		25		0.2375		11.31	12.03		-	157		19.5
26.90	0.2564		26		0.2490		11.50	12.19		157	157		19.5
28.11	0.2700		27		0.2607		11.60	-		-	-		-
29.32	0.2925		28		0.2720		11.73	12.50		157	156		19.4
31.34	0.3143		29		0.2840		11.88	-		-	-		-
33.35	0.3399		30		0.2960		12.21	12.82		156	155		19.3
35.37	0.3685		31		0.3081		12.91	-		-	-		-
36.97	0.3925		32		0.3210		13.09	13.13		155	154		19.2
38.98	0.4144		33		0.3360		-	-		-	-		-
40.99	0.4459		34		0.3475		13.48	13.43		153	153		19.1
43.39	0.4805		36		0.3750		14.02	13.74		152	152		19.0
45.39	0.5121		38		0.4038		14.55	14.04		150	151		18.9
47.39	0.5475		40		0.4330		15.01	14.34		148	149		18.7
49.39	0.5820		42		0.4640		15.42	14.63		147	148		18.6
51.38	0.6114		44		0.4950		15.83	14.92		147	146		18.4
53.37	0.6430		46		0.5270		16.09	15.22		145	145		18.2
55.36	0.6753		48		0.5598		16.13	15.51		143	143		18.0
57.35	0.7091		50		0.5925		15.99	15.78		140	140		17.8
59.33	0.7467		52		0.6235		15.97	16.07		137	137		17.4
61.31	0.7738		54		0.6550		16.21	16.34		134	133		17.1

TABLE B-3 CONTINUED

63.29	0.8046	56	0.6883	16.61	16.60	129	129	16.7
65.27	0.8490	58	0.7222	16.92	16.85	124	125	16.2
67.24	0.8783	60	0.7560	17.10	17.10	120	120	15.7
69.21	0.9137	62	0.7903	17.29	17.33	115	115	15.2
71.18	0.9468	64	0.8252	17.56	17.56	110	109	14.6
73.15	0.9904	66	0.8605	17.84	17.77	102	103	14.0
75.11	1.0235	68	0.8965	18.01	17.98	98	97	13.4
77.08	1.0536	70	0.9330	18.18	18.14	92	91	12.8
79.04	1.1002	71	-	-	18.25	91	88	12.4
80.99	1.1272	72	0.9690	18.40	18.35	89	84	12.1
82.95	1.1679	73	-	-	18.42	79	81	11.8
84.90	1.2160	74	1.0060	18.67	18.50	73	77	11.4
86.85	1.2491	75	-	-	18.57	70	74	11.0
88.80	1.2814	76	1.0440	18.91	18.64	67	70	10.6
90.74	1.3198	77	-	-	18.70	65	66	10.2
92.69	1.3626	78	1.0822	19.00	18.77	61	63	9.9
94.24	1.3837	79	-	-	18.83	57	59	9.5
96.18	1.4243	80	1.1200	18.99	18.88	50	55	9.1
98.11	1.4649	81	-	-	18.93	49	51	8.7
100.04	1.4987	82	1.1580	18.95	18.97	48	47	8.3
102.36	1.5401	83	-	-	19.03	44	43	7.9
104.29	1.5830	84	1.1960	18.99	19.07	40	39	7.5
106.22	1.6123	85	-	-	19.10	30	35	7.1
108.14	1.6454	86	1.2337	19.00	19.13	25	31	6.7
110.06	1.6897	87	-	-	19.15	22	27	6.3
111.98	1.7146	88	1.2720	19.07	19.17	22	22	5.7
114.28	1.7695	89	-	-	19.19	19	18	5.3
116.19	1.8033	90	1.3100	19.16	19.22	15	14	4.9
118.10	1.8492	91	-	-	19.22	9	10	4.5
		92	1.3485	19.15	19.23	3	5	4.0
		93	-	-	19.23	0	1	3.6
		94	1.3870	19.23	19.23	-5	-4	3.1
		95	-	-	19.22	-10	-9	2.6
		96	1.4250	19.25	19.21	-13	-13	2.2
		97	-	-	19.19	-15	-18	1.7
		98	1.4640	19.20	19.18	-21	-22	1.3
		99	-	-	19.16	-	-27	0.8

TABLE B-3 CONCLUDED

			100		1.5025		19.16	19.12		-35	-		-
			102		1.5402		19.07	19.04		-	-		-
			104		1.5785		18.98	18.93		-	-		-
			106		1.6167		18.86	-		-	-		-
			108		1.6540		18.67	-		-	-		-
			110		1.6910		18.43	-		-	-		-
			112		1.7280		18.25	-		-	-		-
			114		1.7640		18.10	-		-	-		-
			116		1.8000		-	-		-	-		-
			118		1.8360		-	-		-	-		-

TABLE B-4 MODEL-PLUG RESPONSE DATA FOR TEST NO.4

EXPERIMENTAL DATA		CALCULATED DATA						
TIME	DISPLACEMENT	TIME	DISPLACEMENT	VELOCITY	VELOCITY	ACCELERATION	ACCELERATION	PRESSURE
t	s_e	t	s_g	v_c	v_g	a_c	a_g	p
(MSEC)	(FT)	(MSEC)	(FT)	(FT/SEC)	(FT/SEC)	(FT/SEC^2)	(FT/SEC^2)	(PSIG)
0	0	0	0	0	0	0	0	0
0.47	0.0037	0.10	-	-	4.60	-	-	-
0.94	0.0066	0.20	-	-	5.90	17160	17160	1753.8
1.42	0.0162	0.30	-	-	6.80	8420	8420	862.3
1.89	0.0066	0.40	-	-	7.48	6420	6460	662.4
2.36	0.0170	0.50	0.0040	-	8.02	5180	5150	528.8
2.83	0.0332	0.60	-	-	8.50	4300	4250	437.0
3.30	0.0442	0.70	-	-	8.88	3660	3625	373.3
3.77	0.0376	0.80	-	-	9.20	3060	3225	332.5
4.24	0.0590	0.90	-	-	9.50	2760	2975	307.0
4.72	0.0649	1.00	0.0086	9.64	9.72	2340	2800	289.1
5.19	0.0641	1.10	-	-	10.00	2360	2670	275.8
5.66	0.0752	1.20	-	-	10.12	2440	2580	266.7
6.13	0.0811	1.30	-	-	10.48	2460	2500	258.5
6.60	0.0855	1.40	-	-	10.70	-	2450	253.5
7.07	0.0980	1.50	0.0138	10.84	10.94	2504	2400	248.3
7.54	0.1098	2.00	0.0192	11.88	12.05	2196	2180	225.9
8.01	0.1246	2.50	0.0258	13.02	13.12	2084	2060	213.6
8.48	0.1319	3.00	0.0323	14.00	14.12	2000	2000	207.5
8.95	0.1489	3.50	0.0398	14.86	15.12	-	1940	201.4
9.42	0.1481	4.00	0.0472	15.90	16.05	1850	1860	193.2
9.89	0.1644	4.50	0.0555	16.72	-	-	-	-
10.36	0.1909	5.00	0.0642	17.52	17.82	1726	1720	178.9
10.83	0.1909	5.50	0.0731	18.00	-	-	-	-
11.30	0.2123	6.00	0.0822	18.60	19.45	1629	1640	170.8
11.77	0.2233	6.50	0.0915	19.06	-	-	-	-
12.24	0.2307	7.00	0.1015	19.76	21.05	1567	1575	164.2
12.71	0.2506	7.50	0.1111	20.58	-	-	-	-
13.18	0.2565	8.00	0.1218	21.34	22.58	1530	1530	159.6
13.64	0.2771	8.50	0.1328	22.52	-	-	-	-
14.11	0.2948	9.00	0.1440	23.70	24.09	1500	1500	156.5

TABLE B-4 CONTINUED

14.58	0.3088	9.50	0.1563	25.14	-	-	-	-
14.95	0.3250	10.00	0.1693	26.46	25.58	1480	1470	163.6
15.52	0.3434	10.50	0.1830	27.58	-	-	-	-
15.99	0.3648	11.00	0.1968	28.42	27.05	1458	1450	151.4
16.46	0.3729	11.50	0.2115	29.30	-	-	-	-
16.93	0.3855	12.00	0.2261	30.22	28.50	1435	1425	148.9
17.39	0.4127	12.50	0.2416	31.04	-	-	-	-
17.86	0.4216	13.00	0.2573	32.02	29.92	1416	1405	146.8
18.33	0.4422	13.50	0.2735	32.86	-	-	-	-
18.80	0.4510	14.00	0.2902	33.76	31.32	1400	1385	144.8
19.27	0.4798	14.50	0.3073	34.24	-	-	-	-
19.73	0.5004	15.00	0.3248	34.70	32.72	1378	1370	143.2
20.20	0.5122	15.50	0.3418	34.90	-	-	-	-
20.67	0.5336	16.00	0.3597	35.14	34.10	1356	1350	141.2
21.14	0.5454	16.50	0.3771	35.66	-	-	-	-
21.60	0.5741	17.00	0.3950	35.84	35.42	1341	1335	139.7
22.07	0.5933	17.50	0.4133	36.12	-	-	-	-
22.54	0.6117	18.00	0.4312	36.44	36.75	1324	1320	138.1
23.00	0.6265	18.50	0.4493	36.98	-	-	-	-
23.47	0.6486	19.00	0.4681	37.96	38.10	1311	1310	137.1
23.94	0.6707	19.50	0.4873	-	-	-	-	-
24.40	0.7002	20.00	0.5071	39.46	39.38	1290	1295	135.6
24.87	0.7105	21.00	0.5475	40.71	40.66	1274	1280	134.1
25.34	0.7245	22.00	0.5888	41.55	41.92	1266	1270	133.0
25.80	0.7510	23.00	0.6308	42.30	43.20	1258	1250	131.0
26.27	0.7864	24.00	0.6732	43.30	44.44	1245	1225	128.5
26.74	0.8048	25.00	0.7168	44.91	45.69	1222	1205	126.4
27.20	0.8247	26.00	0.7623	46.62	46.90	1187	1180	123.9
27.67	0.8358	27.00	0.8108	48.12	48.08	1126	1140	119.8
28.13	0.8704	28.00	0.8593	49.35	49.18	1060	1090	114.7
28.60	0.8984	28.50	-	-	49.69	-	1060	111.6
29.06	0.9124	29.00	0.9089	50.11	50.18	984	1030	108.6
29.53	0.9338	29.50	-	-	50.67	958	990	104.5
30.00	0.9596	30.00	0.9600	51.01	51.15	930	945	99.9
30.46	0.9846	30.50	-	-	51.60	878	885	93.8
30.93	1.0023	30.75	-	-	51.80	-	855	90.7
31.39	1.0384	31.00	1.0110	51.79	52.04	824	810	86.1

TABLE B-4 CONCLUDED

31.86	1.0650		31.25		-		-	52.22		792	760		81.0
32.32	1.0782		31.50		-		-	52.42		696	695		74.4
32.79	1.1003		31.75		-		-	52.60		632	625		67.3
33.25	1.1269		32.00		1.0633		52.46	52.72		552	540		58.6
33.71	1.1622		32.25		-		-	52.86		440	440		48.4
34.18	1.1704		32.50		-		-	52.98		352	330		37.2
34.64	1.2035		32.75		-		-	53.02		200	210		24.9
35.11	1.2278		33.00		1.1162		53.08	53.08		32	80		11.7
35.57	1.2558		33.25		-		-	53.06		-	-		-
36.04	1.2780		33.50		-		-	53.00		-	-		-
36.50	1.3023		34.00		1.1697		53.08	-		-	-		-
			35.00		1.2232		-	-		-	-		-
			36.00		1.2752		-	-		-	-		-

TABLE B-5 MODEL-PLUG RESPONSE DATA FOR TEST NO. 5

EXPERIMENTAL DATA		CALCULATED DATA						
TIME	DISPLACEMENT	TIME	DISPLACEMENT	VELOCITY	VELOCITY	ACCELERATION	ACCELERATION	PRESSURE
t	s_e	t	s_g	v_c	v_g	a_c	a_g	p
(MSEC)	(FT)	(MSEC)	(FT)	(FT/SEC)	(FT/SEC)	(FT/SEC^2)	(FT/SEC^2)	(PSIG)
0	0	0	0	0	0	0	0	0
0.47	0.0015	0.1	-	-	0.95	-	-	-
0.95	0.0052	0.2	-	-	1.41	4670	4670	1392.1
1.42	0.0052	0.3	-	-	1.72	2920	2960	886.0
1.90	0.0059	0.4	-	-	1.95	2200	2200	661.0
2.37	0.0066	0.5	0.0015	-	2.14	1750	1720	518.9
2.84	0.0081	0.6	-	-	2.30	1520	1515	458.2
3.32	0.0132	0.7	-	-	2.42	1410	1395	422.7
3.79	0.0110	0.8	-	-	2.57	1330	1320	400.5
4.26	0.0184	0.9	-	-	2.71	-	1270	385.7
4.74	0.0132	1.0	0.0024	2.70	2.82	-	1230	373.9
5.21	0.0280	1.5	0.0040	3.02	3.37	1062	1055	322.1
5.68	0.0258	2.0	0.0055	3.66	3.85	942	945	289.5
6.15	0.0272	2.5	0.0075	4.10	4.28	866	875	268.8
6.63	0.0316	3.0	0.0098	4.72	4.72	824	820	252.5
7.10	0.0346	3.5	0.0121	5.20	5.10	784	770	237.7
7.57	0.0375	4.0	0.0150	5.64	5.50	734	733	226.8
8.04	0.0383	4.5	0.0179	5.96	5.85	704	700	217.0
8.52	0.0449	5.0	0.0210	6.10	6.18	670	672	208.7
8.99	0.0464	5.5	0.0240	6.36	6.52	648	648	201.6
9.46	0.0515	6.0	0.0272	6.56	6.84	628	625	194.8
9.93	0.0596	6.5	0.0308	6.76	7.14	608	605	188.9
10.40	0.0596	7.0	0.0340	6.86	7.44	584	585	183.0
10.88	0.0648	7.5	0.0375	6.88	7.74	568	570	178.5
11.35	0.0655	8.0	0.0410	7.08	8.00	552	552	173.2
11.82	0.0743	8.5	0.0445	7.28	8.28	542	538	169.0
12.29	0.0802	9.0	0.0482	7.76	8.55	536	525	165.2
12.76	0.0824	9.5	0.0521	8.28	8.82	516	515	162.2
13.23	0.0898	10.0	0.0566	8.82	9.07	502	505	159.3
13.70	0.0964	10.5	0.0610	9.28	9.31	490	495	156.3
14.18	0.1023	11.0	0.0658	9.50	9.56	506	487	154.0

TABLE B-5 CONTINUED

14.65	0.1001	11.5	0.0707	9.86	9.80	502	480	151.9
15.12	0.1089	12.0	0.0755	10.02	10.09	492	472	149.5
15.59	0.1214	12.5	0.0808	10.18	10.30	482	465	147.4
16.06	0.1133	13.0	0.0858	10.28	10.54	460	459	145.7
16.53	0.1273	13.5	0.0910	10.54	10.78	460	453	143.9
17.00	0.1354	14.0	0.0961	10.88	11.00	448	447	142.1
17.47	0.1391	14.5	0.1020	11.16	11.22	448	441	140.3
17.94	0.1457	15.0	0.1075	11.60	11.44	444	437	139.2
18.41	0.1472	15.5	0.1132	11.76	11.68	-	432	137.7
18.88	0.1524	16.0	0.1195	12.04	11.88	426	427	136.2
19.35	0.1641	16.5	0.1254	12.28	-	-	-	-
19.82	0.1774	17.0	0.1315	12.30	12.30	418	419	133.8
20.29	0.1774	17.5	0.1379	12.54	-	-	-	-
20.76	0.1818	18.0	0.1440	12.72	12.70	406	410	131.2
21.23	0.1884	18.5	0.1505	12.96	-	-	-	-
22.17	0.2017	19.0	0.1570	13.22	13.12	404	403	129.1
23.11	0.2171	19.5	0.1638	-	-	-	-	-
24.04	0.2193	20	0.1704	13.58	13.50	400	395	126.7
24.98	0.2363	21	0.1820	13.60	13.92	392	388	124.6
25.92	0.2576	22	0.1974	14.15	14.30	392	383	123.2
26.86	0.2672	23	0.2115	14.80	14.68	378	377	121.4
27.79	0.2878	24	0.2264	14.92	15.08	374	372	119.9
28.73	0.3032	25	0.2415	15.32	15.42	-	368	118.7
29.66	0.3150	26	0.2570	15.67	15.80	367	364	117.5
30.60	0.3378	27	0.2728	16.21	-	-	-	-
32.00	0.3555	28	0.2891	16.81	16.52	360	357	115.5
33.40	0.3864	29	0.3065	17.21	-	-	-	-
34.80	0.4085	30	0.3242	17.76	17.25	360	350	113.4
36.20	0.4401	31	0.3413	18.13	-	-	-	-
37.60	0.4622	32	0.3605	18.43	17.95	353	345	111.9
39.00	0.4961	33	0.3790	18.70	-	-	-	-
40.39	0.5255	34	0.3975	18.79	18.68	344	340	110.4
41.79	0.5505	35	0.4163	19.07	-	-	-	-
43.19	0.5932	36	0.4358	19.39	19.33	338	335	109.0
44.58	0.6234	37	0.4552	19.66	-	-	-	-
45.97	0.6477	38	0.4750	19.98	20.00	329	331	107.8

TABLE B-5 CONCLUDED

47.36	0.6749		39		0.4950		20.24	-		-	-		-
48.76	0.7051		40		0.5158		20.52	20.67		324	325		106.0
50.15	0.7375		41		0.5360		20.87	-		-	-		-
52.00	0.7853		42		0.5571		21.11	21.30		319	320		104.5
53.85	0.8339		43		0.5787		21.49	-		-	-		-
54.77	0.8545		44		0.6000		21.73	21.92		313	315		103.0
56.16	0.8817		45		0.6220		22.07	-		-	-		-
57.55	0.9303		46		0.6441		22.50	22.56		310	307		100.7
58.93	0.9620		47		0.6670		22.85	-		-	-		-
60.31	0.9965		48		0.6900		23.21	23.17		301	300		98.6
61.70	1.0282		49		0.7133		23.50	-		-	-		-
63.08	1.0687		50		0.7370		23.77	23.77		290	290		95.6
64.46	1.1011		51		0.7610		23.94	-		-	-		-
65.84	1.1379		52		0.7850		24.00	24.32		278	280		92.7
67.22	1.1754		53		0.8090		24.20	-		-	-		-
68.14	1.2019		54		0.8330		24.50	24.88		265	267		88.8
68.60	1.2173		55		0.8580		24.82	-		-	-		-
			56		0.8830		25.17	25.39		250	250		83.8
			57		0.9081		25.36	-		-	-		-
			58		0.9338		25.59	25.88		230	232		78.5
			59		0.9594		25.73	-		-	-		-
			60		0.9853		25.82	26.32		203	210		72.0
			61		1.0110		26.10	26.54		-	193		66.9
			62		1.0371		26.34	26.71		169	170		60.1
			63		1.0640		26.74	26.87		133	133		49.2
			64		1.0905		26.98	27.00		81	78		32.9
			65		1.1180		27.05	27.06		2	0		9.8
			66		1.1450		26.98	27.02		-	-		-
			67		1.1720		-	26.85		-	-		-
			68		1.1984		-	-		-	-		-

TABLE B-6 MODEL-PLUG RESPONSE DATA FOR TEST NO.6

EXPERIMENTAL DATA		CALCULATED DATA							
TIME	DISPLACEMENT	TIME	DISPLACEMENT	VELOCITY	VELOCITY	ACCELERATION	ACCELERATION	PRESSURE
t	s_e	t	s_g	v_c	v_g	a_c	a_g	p
(MSEC)	(FT)	(MSEC)	(FT)	(FT/SEC)	(FT/SEC)	(FT/SEC^2)	(FT/SEC^2)	(PSIG)
0	0	0	0	0	0	0	0	0
0.48	0.0059	0.1	-	-	4.7	-	-	-
0.95	0.0022	0.2	-	-	6.4	19400	19400	1982.3
1.42	0.0162	0.3	-	-	7.5	10700	10700	1094.9
1.90	0.0192	0.4	-	-	8.3	8000	8000	819.5
2.37	0.0206	0.5	0.0050	10.20	9.1	6500	6500	666.5
2.85	0.0398	0.6	-	-	9.6	5400	5400	554.3
3.32	0.0361	0.7	-	-	10.1	4500	4850	498.2
3.80	0.0486	0.8	-	-	10.5	4200	4550	467.6
4.27	0.0604	0.9	-	-	10.9	-	4325	444.7
4.74	0.0803	1.0	0.0102	11.42	11.3	-	4150	426.8
5.22	0.0781	1.5	0.0161	12.60	13.2	3680	3660	376.8
5.69	0.1047	2.0	0.0230	14.16	14.9	3420	3440	354.4
6.16	0.1083	2.5	0.0301	15.60	16.5	3300	3320	342.1
6.64	0.1393	3.0	0.0386	17.04	18.2	3220	3240	334.0
7.11	0.1334	3.5	0.0473	18.52	19.8	3180	3175	327.4
7.58	0.1511	4.0	0.0570	20.06	21.3	3100	3125	322.3
8.05	0.1614	4.5	0.0672	21.84	22.9	3060	3075	317.2
8.53	0.1946	5.0	0.0788	23.60	24.4	3040	3025	312.1
9.00	0.2093	5.5	0.0910	25.34	25.9	2960	2990	308.5
9.47	0.2204	6.0	0.1041	26.94	27.4	2900	2945	303.9
9.94	0.2366	6.5	0.1179	28.60	28.8	2880	2910	300.3
10.41	0.2410	7.0	0.1321	30.34	30.2	2820	2870	296.2
10.89	0.2867	7.5	0.1482	32.10	31.7	2800	2850	294.2
11.36	0.2977	8.0	0.1648	33.78	33.0	2780	2810	290.1
11.83	0.3272	8.5	0.1821	35.28	34.4	2760	2800	289.0
12.30	0.3538	9.0	0.2002	36.52	35.8	2800	2760	285.0
12.77	0.3766	9.5	0.2187	37.68	37.2	2760	2740	283.0
13.24	0.3958	10.0	0.2378	39.08	38.6	2740	2710	279.9
13.71	0.4105	10.5	0.1575	40.70	39.9	2700	2690	277.0
14.18	0.3656	11.0	0.2785	42.32	41.3	2660	2670	275.8

TABLE B-6 CONCLUDED

14.65	0.4311		11.5		0.3001		43.76	42.6		2680	2650		273.8
15.12	0.4687		12.0		0.3223		44.98	43.9		2620	2625		271.3
15.59	0.4879		12.5		0.3450		46.32	45.3		2600	2600		268.7
16.06	0.5240		13.0		0.3685		47.52	46.5		2580	2575		266.2
16.53	0.5564		13.5		0.3928		48.94	47.8		2560	2550		263.6
17.00	0.5668		14.0		0.4172		50.20	49.1		2560	2520		260.5
17.47	0.5948		14.5		0.4430		51.42	50.4		2500	2490		257.5
17.94	0.6147		15.0		0.4689		52.74	51.6		2440	2450		253.4
18.41	0.6640		15.5		0.4955		53.70	52.8		2400	2400		248.3
18.88	0.6861		16.0		0.5228		54.80	54.0		2400	2350		243.2
19.35	0.7142		16.5		0.5503		55.74	55.2		2360	2300		238.1
19.82	0.7444		17.0		0.5785		56.82	56.4		2260	2240		232.0
20.29	0.7702		17.5		0.6070		57.80	57.5		2180	2175		225.4
20.76	0.8033		18.0		0.6365		58.28	58.5		2100	2120		219.7
21.22	0.8232		18.5		0.6658		58.46	59.6		2020	2050		212.6
21.69	0.8667		19.0		0.6948		58.88	60.6		1980	2000		207.5
22.16	0.8866		19.5		0.7240		59.96	61.5		1900	1920		199.3
22.63	0.9205		20.0		0.7546		61.20	62.5		1860	1850		192.2
23.10	0.9559		20.5		0.7858		62.34	63.4		1800	1780		185.1
23.56	0.9927		21.0		0.8169		63.34	64.3		1700	1700		176.9
24.03	1.0148		21.5		0.8487		64.24	65.1		1560	1620		168.7
24.50	1.0532		22.0		0.8815		65.20	65.9		1440	1520		155.0
24.96	1.0760		22.5		0.9141		65.98	66.5		1380	1410		147.3
25.43	1.1121		23.0		0.9472		66.58	67.2		1280	1280		134.1
25.90	1.1446		23.5		0.9808		67.08	67.9		1160	1125		118.3
26.37	1.1814		24.0		1.0146		67.70	68.4		940	950		100.4
26.83	1.2131		24.5		1.0481		68.28	68.8		720	720		76.9
27.30	1.2617		25.0		1.0828		69.02	69.1		480	450		49.4
27.76	1.2684		25.5		1.1174		69.50	69.3		0	25		6.1
			26.0		1.1525		69.20	69.1		-	-		-
			26.5		1.1870		68.38	68.5		-	-		-
			27.0		1.2210		-	-		-	-		-
			27.5		1.2541		-	-		-	-		-

TABLE B-7 MODEL-PLUG RESPONSE DATA FOR TEST NO.7

EXPERIMENTAL DATA		CALCULATED DATA						
TIME	DISPLACE-MENT	TIME	DISPLACE-MENT	VELOCITY	VELOCITY	ACCEL-ERATION	ACCEL-ERATION	PRESSURE
t	s_e	t	s_g	v_c	v_g	a_c	a_g	p
(MSEC)	(FT)	(MSEC)	(FT)	(FT/SEC)	(FT/SEC)	(FT/SEC^2)	(FT/SEC^2)	(PSIG)
0	0	0	0	0	0	0	0	0
0.36	0.0032	0.1	-	-	2.45	-	-	-
0.73	0.0024	0.2	-	-	3.06	8040	8040	823.6
1.09	0.0064	0.3	-	-	3.33	2920	2920	301.3
1.45	0.0056	0.4	-	-	3.58	1680	1730	180.0
1.81	0.0072	0.5	0.0020	-	3.65	1140	1140	119.8
2.18	0.0088	0.6	-	-	3.74	710	880	93.3
2.54	0.0112	0.7	-	-	3.82	530	700	74.9
2.90	0.0120	0.8	-	-	3.85	300	300	34.1
3.26	0.0136	0.9	-	-	3.86	-	264	30.4
3.63	0.0128	1.0	0.0040	3.90	3.87	-	240	28.0
3.99	0.0144	1.5	0.0059	3.88	3.92	178	168	20.6
4.35	0.0144	2.0	0.0078	3.90	3.98	112	124	16.1
4.71	0.0192	2.5	0.0098	3.96	4.04	114	116	15.3
5.08	0.0200	3.0	0.0118	4.04	4.09	114	117	15.4
5.44	0.0216	3.5	0.0138	4.10	4.15	124	128	16.6
5.80	0.0248	4.0	0.0159	4.20	4.21	144	143	18.1
6.17	0.0240	4.5	0.0180	4.30	4.29	166	162	20.[illegible]
6.52	0.0272	5.0	0.0202	4.36	4.38	190	184	22.3
6.88	0.0288	5.5	0.0224	4.48	4.48	214	214	25.3
7.25	0.0296	6.0	0.0246	4.64	4.59	244	250	29.0
7.61	0.0311	6.5	0.0270	4.82	4.72	284	290	33.1
7.97	0.0359	7.0	0.0295	5.00	4.87	334	336	37.8
8.33	0.0343	7.5	0.0320	5.14	5.05	390	394	43.7
8.69	0.0399	8.0	0.0346	5.26	5.26	446	453	49.7
9.05	0.0415	8.5	0.0373	5.48	5.50	492	488	53.3
9.41	0.0431	9.0	0.0400	5.78	5.76	522	510	55.5
9.78	0.0439	9.5	0.0430	6.12	6.03	532	522	56.7
10.14	0.0463	10.0	0.0462	6.50	6.30	522	528	57.4
10.50	0.0487	10.5	0.0495	-	6.56	512	529	57.5
10.86	0.0543	11.0	0.0530	7.02	6.80	504	525	57.1

TABLE B-7 CONTINUED

11.22	0.0575	11.5	-	-	7.06	510	516	56.1
11.58	0.0567	12.0	0.0602	7.46	7.31	512	508	55.3
11.94	0.0615	12.5	-	-	7.58	510	498	54.3
12.30	0.0631	13.0	0.0681	7.92	7.82	496	489	53.4
12.66	0.0695	13.5	-	-	8.08	480	480	52.5
13.02	0.0727	14.0	0.0760	8.42	8.30	468	470	51.4
13.38	0.0719	14.5	-	-	8.54	460	460	50.4
13.74	0.0751	15.0	0.0847	8.88	8.76	452	451	49.5
14.10	0.0767	15.5	-	-	9.00	440	442	48.6
14.47	0.0807	16.0	0.0940	9.30	9.20	432	433	47.7
14.83	0.0863	16.5	-	-	9.42	426	425	46.9
15.19	0.0879	17.0	0.1035	9.71	9.63	422	416	45.9
15.55	0.0942	17.5	-	-	9.85	-	408	45.1
15.91	0.0966	18.0	0.1131	10.04	10.04	400	401	44.4
16.99	0.1022	19	0.1237	10.40	10.43	349	388	43.1
18.07	0.1150	20	0.1341	10.81	10.80	376	377	42.0
19.14	0.1270	21	0.1450	11.10	11.19	368	368	41.0
20.22	0.1374	22	0.1565	11.58	11.54	367	364	40.6
21.66	0.1541	23	0.1680	12.00	11.90	360	361	40.3
22.74	0.1653	24	0.1805	12.30	12.28	360	359	40.1
23.81	0.1821	25	0.1930	12.50	12.62	354	357	39.9
24.17	0.1853	26	0.2055	12.70	12.98	352	354	39.6
25.25	0.1973	27	0.2180	13.00	13.32	349	352	39.4
26.32	0.2093	28	0.2315	13.40	13.69	347	350	39.2
27.40	0.2236	29	0.2450	13.81	14.01	344	348	39.0
28.47	0.2380	30	0.2590	14.31	14.37	335	345	38.7
29.54	0.2524	31	0.2733	14.70	14.70	339	343	38.5
30.62	0.2700	32	0.2880	15.09	15.02	332	340	38.2
31.69	0.2867	33	0.3040	15.45	15.38	327	338	38.0
32.76	0.2979	34	0.3191	15.70	15.69	320	335	37.7
33.83	0.3203	35	0.3350	15.95	16.00	314	332	37.4
34.90	0.3323	36	0.3510	16.30	16.31	320	330	37.2
36.68	0.3634	37	0.3678	16.52	16.64	322	327	36.9
38.46	0.3882	38	0.3842	16.72	16.97	322	324	36.5
40.24	0.4217	39	0.4010	-	17.26	317	322	36.3
42.02	0.4521	40	0.4180	17.56	17.60	317	319	36.0

TABLE B-7 CONCLUDED

43.80	0.4880	41	-	-	17.91	318	316	35.7
45.57	0.5216	42	0.4540	18.27	18.24	320	313	35.4
47.35	0.5535	43	-	-	18.55	318	310	35.1
49.12	0.5934	44	0.4917	18.95	18.88	313	307	34.8
50.89	0.6254	45	-	-	19.18	307	304	38.2
52.66	0.6645	46	0.5300	19.19	19.49	300	300	34.1
54.42	0.7037	47	-	-	19.78	295	297	33.8
56.19	0.7396	48	0.5695	19.48	20.08	288	294	33.5
57.95	0.7779	49	-	-	20.36	284	290	33.1
59.71	0.8195	50	0.6070	20.03	20.64	282	287	32.8
61.47	0.8626	51	-	-	20.92	283	283	32.4
63.23	0.9017	52	0.6480	20.80	21.21	281	279	32.0
64.99	0.9417	53	-	-	21.49	275	275	31.6
66.74	0.9872	54	0.6910	21.78	21.76	271	271	31.1
68.50	1.0311	55	-	-	22.02	272	266	30.6
70.25	1.0758	56	0.7355	22.40	22.30	266	261	30.1
72.00	1.1198	57	-	-	22.58	261	256	29.6
73.75	1.1637	58	0.7810	22.90	22.81	249	249	28.9
75.50	1.2116	59	-	-	23.07	237	241	28.1
77.24	1.2588	60	0.8270	23.31	23.30	233	232	27.2
78.99	1.3027	61	-	-	23.52	227	222	26.1
80.73	1.3498	62	0.8742	23.65	23.75	220	212	25.1
		63	-	-	23.98	204	201	24.0
		64	0.9220	24.07	24.17	185	189	22.8
		65	-	-	24.33	173	178	21.7
		66	0.9700	24.42	24.50	161	164	20.2
		67	-	-	24.68	150	149	18.7
		68	1.0198	24.78	24.80	133	134	17.2
		69	-	-	24.93	120	119	15.6
		70	1.0695	25.16	25.04	107	104	14.1
		71	-	-	25.16	-	-	-
		72	1.1200	25.52	25.22	-	-	-
		74	1.1715	25.85	-	-	-	-
		76	1.2240	-	-	-	-	-
		78	1.2760	-	-	-	-	-

TABLE B-8 MODEL-PLUG RESPONSE DATA FOR TEST NO.8

EXPERIMENTAL DATA		CALCULATED DATA						
TIME	DISPLACE-MENT	TIME	DISPLACE-MENT	VELOCITY	VELOCITY	ACCEL-ERATION	ACCEL-ERATION	PRESSURE
t	s_e	t	s_g	v_c	v_g	a_c	a_g	p
(MSEC)	(FT)	(MSEC)	(FT)	(FT/SEC)	(FT/SEC)	(FT/SEC^2)	(FT/SEC^2)	(PSIG)
0	0	0	0	0	0	0	0	0
0.37	0.0024	0.1	-	-	2.25	-	-	-
0.73	0.0048	0.2	-	-	2.57	7050	7050	722.6
1.09	0.0040	0.3	-	-	3.02	2510	2510	259.5
1.46	0.0088	0.4	-	-	3.14	1580	1360	142.2
1.82	0.0064	0.5	0.0018	-	3.22	620	630	67.8
2.19	0.0112	0.6	-	-	3.26	310	310	35.1
2.55	0.0096	0.7	-	-	3.27	130	130	16.8
2.91	0.0112	0.8	-	-	3.27	50	58	9.4
3.28	0.0096	0.9	-	-	3.28	-	57	9.3
3.64	0.0096	1.0	0.0034	3.34	3.28	-	56	9.2
4.01	0.0144	1.5	0.0051	3.26	3.30	70	60	9.6
4.37	0.0176	2.0	0.0067	3.32	3.33	70	70	10.6
4.73	0.0168	2.5	0.0083	3.36	3.37	90	88	12.4
5.10	0.0184	3.0	0.0101	3.46	3.42	110	108	14.5
5.46	0.0208	3.5	0.0118	3.50	3.48	130	124	16.1
5.82	0.0224	4.0	0.0136	3.54	3.55	142	138	17.6
6.19	0.0232	4.5	0.0153	3.64	3.63	154	152	19.0
6.55	0.0232	5.0	0.0172	3.76	3.70	164	165	20.3
6.92	0.0256	5.5	0.0191	3.86	3.79	176	176	21.4
7.28	0.0256	6.0	0.0211	3.90	3.88	190	187	22.6
7.64	0.0264	6.5	0.0230	4.02	3.98	200	197	23.6
8.01	0.0288	7.0	0.0250	4.12	4.08	218	206	24.5
8.37	0.0304	7.5	0.0272	4.22	4.19	228	215	25.4
8.73	0.0344	8.0	0.0293	4.32	4.32	240	223	26.2
9.09	0.0352	8.5	0.0314	4.40	4.43	244	231	27.1
9.46	0.0360	9.0	0.0337	4.52	4.56	242	239	27.9
9.82	0.0384	9.5	0.0360	4.68	4.68	244	246	28.6
10.18	0.0408	10.0	0.0383	4.84	4.80	244	253	29.3
10.55	0.0416	10.5	0.0408	5.06	4.92	254	260	30.0
10.91	0.0440	11.0	0.0434	5.26	5.05	266	266	30.6
11.27	0.0440	11.5	0.0461	5.40	5.19	280	273	31.3

TABLE B-8 CONTINUED

11.63	0.0449	12.0	0.0488	5.46	5.33	282	278	31.9
12.00	0.0521	12.5	0.0516	5.46	5.48	292	284	32.5
12.36	0.0481	13.0	0.0543	5.56	5.61	296	290	33.1
12.72	0.0497	13.5	0.0570	5.78	5.78	298	296	33.7
13.08	0.0521	14.0	0.0600	6.00	5.92	302	301	34.2
13.45	0.0593	14.5	0.0632	6.36	6.07	300	307	34.8
13.81	0.0601	15.0	0.0662	6.52	6.22	310	312	35.3
14.17	0.0641	15.5	0.0698	6.88	6.38	316	318	35.9
14.53	0.0657	16.0	0.0730	7.08	6.54	324	321	36.2
14.90	0.0705	16.5	0.0770	7.14	6.70	330	325	36.7
15.26	0.0729	17.0	0.0803	7.32	6.87	336	328	37.0
15.62	0.0753	17.5	0.0840	7.18	7.04	-	329	37.1
15.98	0.0745	18.0	0.0878	7.32	7.21	324	328	37.0
17.07	0.0777	18.5	0.0912	7.48	-	-	-	-
18.15	0.0969	19.0	0.0950	7.58	7.53	318	319	36.0
19.24	0.0993	19.5	0.0991	-	-	-	-	-
20.32	0.1073	20	0.1028	7.92	7.83	308	310	35.1
21.40	0.1161	21	0.1110	8.30	8.15	302	302	34.3
23.21	0.1313	22	0.1194	8.60	8.44	294	294	33.5
25.01	0.1490	23	0.1282	8.94	8.73	285	288	32.9
26.81	0.1698	24	0.1372	9.32	9.01	282	281	32.2
28.61	0.1914	25	0.1468	9.61	9.29	274	276	31.7
30.41	0.1930	26	0.1567	9.89	9.57	271	271	31.1
32.20	0.2227	27	0.1665	10.15	9.82	269	268	30.8
34.00	0.2459	28	0.1768	10.42	10.10	265	262	30.2
35.79	0.2675	29	0.1875	10.85	10.37	264	259	29.9
37.58	0.2835	30	0.1983	11.27	10.62	261	255	29.5
39.38	0.3059	31	0.2100	11.62	10.88	257	252	29.2
41.16	0.3308	32	0.2219	11.92	11.15	257	250	29.0
43.31	0.3588	33	0.2338	12.00	11.39	252	247	28.7
44.74	0.3836	34	0.2460	12.06	11.65	250	245	28.5
46.52	0.4117	35	0.2580	11.89	11.89	250	243	28.3
48.30	0.4413	36	0.2701	11.96	12.15	246	241	28.1
50.09	0.4669	37	0.2812	12.25	12.39	244	240	28.0
52.22	0.5078	38	0.2942	12.78	12.63	238	238	27.8
53.65	0.5238	39	0.3072	-	12.87	239	237	27.7

TABLE B-8 CONTINUED

57.20	0.5823	40	0.3210	13.43	13.10	242	236	27.6
61.10	0.6439	41	-	-	13.35	242	235	27.5
64.29	0.6984	42	0.3485	14.07	13.60	240	234	27.4
67.82	0.7633	43	-	-	13.83	234	233	27.3
71.35	0.8265	44	0.3772	14.47	14.06	226	231	27.1
75.22	0.8994	45	-	-	14.29	224	230	27.0
78.04	0.9627	46	0.4068	14.79	14.50	226	229	26.9
81.90	1.0444	47	-	-	14.73	225	228	26.8
85.40	1.1149	48	0.4365	15.13	14.97	225	226	26.6
86.10	1.1357	49	-	-	15.18	225	225	26.5
87.15	1.1525	50	0.4667	15.44	15.40	226	224	26.3
88.20	1.1741	51	-	-	15.64	231	222	26.1
		52	0.4985	15.53	15.87	230	221	26.0
		53	-	-	16.10	224	219	25.8
		54	0.5302	15.49	16.32	220	217	25.6
		55	-	-	16.54	215	216	25.5
		56	0.5600	15.56	16.75	214	214	25.3
		57	-	-	16.96	211	212	25.1
		58	0.5908	15.95	17.18	210	210	24.9
		59	-	-	17.38	207	208	24.7
		60	0.6238	16.62	17.59	205	206	24.5
		61	-	-	17.79	205	203	24.2
		62	0.6578	17.20	18.00	201	201	24.0
		63	-	-	18.20	196	198	23.7
		64	0.6927	17.61	18.39	195	196	23.5
		65	-	-	18.59	193	193	23.2
		66	0.7283	18.00	18.78	194	190	22.9
		67	-	-	18.97	189	187	22.6
		68	0.7646	18.43	19.17	185	184	22.3
		69	-	-	19.34	181	181	22.0
		70	0.8018	18.93	19.52	176	177	21.6
		71	-	-	19.70	175	173	21.1
		72	0.8402	19.43	19.87	170	168	20.6
		73	-	-	20.04	163	162	20.0
		74	0.8798	19.90	20.20	157	155	19.3
		75	-	-	20.35	148	148	18.6

TABLE B-8 CONCLUDED

		76	0.9199	20.27	20.50	138	139	17.7
		77	-	-	20.63	125	129	16.7
		78	0.9609	20.55	20.75	114	118	15.5
		79	-	-	20.85	105	107	14.4
		80	1.0023	20.85	20.96	90	94	13.1
		81	-	-	21.05	82	81	11.8
		82	1.0441	21.07	21.10	68	68	10.4
		83	-	-	21.19	57	54	9.0
		84	1.0868	21.14	21.23	44	41	7.7
		85	-	-	21.27	23	25	6.1
		86	1.1293	-	21.28	-	-	-
		87	-	-	21.28	-	-	-
		88	1.1711	-	-	-	-	-

TABLE B-9 MODEL-PLUG RESPONSE DATA FOR TEST NO.9

EXPERIMENTAL DATA		CALCULATED DATA						
TIME	DISPLACEMENT	TIME	DISPLACEMENT	VELOCITY	VELOCITY	ACCELERATION	ACCELERATION	PRESSURE
t	s_e	t	s_g	v_c	v_g	a_c	a_g	p
(MSEC)	(FT)	(MSEC)	(FT)	(FT/SEC)	(FT/SEC)	(FT/SEC^2)	(FT/SEC^2)	(PSIG)
0	0	0	0	0	0	0	0	0
0.36	0.0032	0.1	-	-	0.66	-	-	-
0.72	0.0016	0.2	-	-	1.27	5660	5660	580.8
1.08	0.0056	0.3	-	-	1.81	4320	4070	418.6
1.44	0.0016	0.4	-	-	2.25	2740	2590	267.7
1.80	0.0032	0.5	0.0014	-	2.33	1330	1370	143.2
2.16	0.0048	0.6	-	-	2.38	440	601	64.8
2.53	0.0088	0.7	-	-	2.41	290	301	34.2
2.89	0.0072	0.8	-	-	2.43	200	200	23.9
3.25	0.0072	0.9	-	-	2.45	-	164	20.2
3.61	0.0088	1.0	0.0026	2.52	2.46	-	144	18.2
3.97	0.0080	1.5	0.0038	2.46	2.48	88	85	12.2
4.33	0.0112	2.0	0.0051	2.50	2.50	46	53	8.9
4.69	0.0144	2.5	0.0063	2.54	2.53	46	45	8.1
5.05	0.0136	3.0	0.0076	2.56	2.55	44	43	7.9
5.41	0.0152	3.5	0.0089	2.60	2.57	44	43	7.9
5.77	0.0160	4.0	0.0102	2.60	2.59	46	45	8.1
6.13	0.0168	4.5	0.0115	2.64	2.62	50	49	8.5
6.49	0.0176	5.0	0.0128	2.70	2.64	54	54	9.0
6.85	0.0168	5.5	0.0142	2.72	2.67	60	60	9.6
7.21	0.0168	6.0	0.0156	2.82	2.70	66	66	10.2
7.57	0.0200	6.5	0.0169	2.82	2.74	74	75	11.2
7.93	0.0208	7.0	0.0185	2.82	2.77	88	87	12.4
8.29	0.0232	7.5	0.0198	2.82	2.82	102	101	13.8
8.65	0.0240	8.0	0.0212	2.76	2.88	120	119	15.6
9.01	0.0256	8.5	0.0226	2.88	2.94	138	140	17.8
9.36	0.0248	9.0	0.0240	2.96	3.01	160	161	19.9
9.72	0.0280	9.5	0.0256	3.06	3.10	186	185	22.4
10.08	0.0248	10.0	0.0271	3.18	3.20	210	208	24.7
10.44	0.0248	10.5	0.0287	3.30	3.31	226	228	26.8
10.80	0.0312	11.0	0.0304	3.46	3.43	244	245	28.5
11.16	0.0304	11.5	0.0322	3.56	3.55	260	259	29.9

TABLE B-9 CONTINUED

11.52	0.0328	12.0	0.0340	3.76	3.69	264	263	30.3
11.88	0.0336	12.5	0.0358	3.92	3.83	260	260	30.0
12.24	0.0360	13.0	0.0380	4.12	3.95	248	252	29.2
12.60	0.0352	13.5	0.0400	4.32	4.07	236	246	28.6
12.96	0.0400	14.0	0.0422	4.42	4.19	238	241	28.1
13.32	0.0464	14.5	0.0445	-	4.30	240	236	27.6
13.67	0.0449	15.0	0.0468	4.68	4.43	234	231	27.1
14.03	0.0473	15.5	-	-	4.55	228	227	26.7
14.39	0.0505	16.0	0.0520	4.91	4.65	218	223	26.2
14.75	0.0537	16.5	-	-	4.76	216	220	25.9
15.11	0.0521	17.0	0.0565	5.03	4.87	220	217	25.6
16.18	0.0545	17.5	-	-	4.98	-	214	25.3
17.26	0.0585	18.0	0.0619	5.15	5.09	213	211	25.0
18.33	0.0681	19	0.0670	5.46	5.30	207	206	24.5
19.41	0.0681	20	0.0725	5.63	5.50	202	202	24.1
20.48	0.0761	21	0.0785	5.98	5.70	198	197	23.6
21.91	0.0873	22	0.0843	6.35	5.90	195	193	23.2
22.98	0.0945	23	0.0910	6.67	6.09	192	189	22.8
23.70	0.0961	24	0.0980	6.94	6.28	188	186	22.5
25.84	0.1113	25	0.1050	7.16	6.47	185	182	22.1
27.62	0.1233	26	0.1120	7.30	6.65	182	178	21.7
29.41	0.1434	27	0.1198	7.49	6.83	176	175	21.4
31.19	0.1530	28	0.1271	7.65	7.01	172	173	21.1
32.97	0.1690	29	0.1349	7.74	7.17	-	170	20.8
34.74	0.1778	30	0.1427	7.88	7.34	165	167	20.5
36.88	0.1970	31	0.1507	7.89	-	-	-	-
38.30	0.2090	32	0.1586	7.87	7.66	160	162	20.0
40.07	0.2202	33	0.1664	7.88	-	-	-	-
41.84	0.2395	34	0.1742	7.97	7.97	159	158	19.6
43.97	0.2579	35	0.1823	8.11	-	-	-	-
45.38	0.2731	36	0.1905	8.21	8.29	158	154	19.2
47.15	0.2875	37	0.1988	8.19	-	-	-	-
48.92	0.3059	38	0.2070	8.26	8.61	156	151	18.9
51.04	0.3292	39	0.2150	8.31	-	-	-	-
52.45	0.3389	40	0.2237	8.40	8.92	152	149	18.7
54.21	0.3604	41	0.2320	8.52	-	-	-	-
55.97	0.3828	42	0.2405	8.58	9.21	148	147	18.5

TABLE B-9 CONTINUED

57.73	0.3980	43	0.2492	8.77	-	-	-	-
59.49	0.4181	44	0.2580	8.99	9.51	145	146	18.4
63.00	0.4605	45	0.2671	9.31	-	-	-	-
66.86	0.5086	46	0.2765	9.62	9.79	144	144	18.2
70.01	0.5470	47	0.2865	-	-	-	-	-
73.51	0.5959	48	0.2964	10.01	10.08	143	144	18.2
77.00	0.6463	50	0.3170	10.32	10.36	143	143	18.1
78.04	0.6567	52	0.3378	10.49	10.65	144	143	18.1
79.09	0.6752	54	0.3590	10.56	10.93	144	142	18.0
80.48	0.6968	56	0.3803	10.78	11.23	142	142	18.0
83.96	0.7488	58	0.4021	10.99	11.51	142	141	17.9
87.43	0.7937	60	0.4240	11.27	11.78	140	140	17.8
90.90	0.8369	62	0.4470	11.67	12.07	140	139	17.7
91.94	0.8618	64	0.4705	12.23	12.35	139	138	17.6
92.98	0.8690	66	0.4955	12.78	12.62	137	137	17.5
94.36	0.8930	68	0.5220	13.25	12.89	136	135	17.3
97.82	0.9515	70	0.5490	13.59	13.17	134	134	17.2
101.27	1.0019	72	0.5762	13.63	13.43	132	131	16.9
104.72	1.0612	74	0.6043	13.57	13.69	129	129	16.7
107.81	1.1165	76	0.6306	13.59	13.95	128	127	16.5
108.85	1.1317	78	0.6575	13.66	14.20	124	124	16.1
111.59	1.1829	80	0.6855	13.92	14.45	120	121	15.8
115.02	1.2326	81	-	-	14.57	-	119	15.6
118.44	1.2983	82	0.7134	14.11	14.68	115	117	15.4
118.79	1.3039	83	-	-	14.80	113	115	15.2
119.81	1.3223	84	0.7418	-	14.91	112	113	15.0
120.84	1.3367	85	-	-	15.02	110	112	14.9
121.86	1.3535	86	0.7704	14.52	15.13	108	109	14.6
		87	-	-	15.24	105	108	14.5
		88	-	-	15.34	104	106	14.3
		89	-	-	15.44	105	103	14.0
		90	0.8290	14.98	15.55	104	101	13.8
		91	-	-	15.66	102	99	13.6
		92	-	-	15.75	99	96	13.3
		93	-	-	15.85	96	94	13.1
		94	0.8900	15.52	15.95	99	92	12.9

TABLE B-9 CONCLUDED

			95		-		-	16.04		94	89		12.6
			96		-		-	16.15		86	86		12.3
			97		-		-	16.22		80	84		12.1
			98		0.9531		16.05	16.29		75	81		11.8
			99		-		-	16.37		76	77		11.4
			100		-		-	16.45		75	74		11.0
			101		-		-	16.51		70	70		10.6
			102		1.0188		16.51	16.59		65	66		10.2
			103		-		-	16.65		60	62		9.8
			104		-		-	16.71		57	57		9.3
			105		-		-	16.76		53	52		8.8
			106		1.0855		16.89	16.82		48	47		8.3
			107		-		-	16.86		44	41		7.7
			108		-		-	16.90		36	35		7.1
			109		-		-	16.94		30	29		6.5
			110		1.1540		17.05	16.96		-	22		5.7
			111		-		-	16.98		-	-		-
			114		1.2232		16.18	-		-	-		-
			118		1.2909		-	-		-	-		-

TABLE B-10 MODEL-PLUG RESPONSE DATA FOR TEST NO. 10

EXPERIMENTAL DATA		CALCULATED DATA						
TIME	DISPLACE-MENT	TIME	DISPLACE-MENT	VELOCITY	VELOCITY	ACCEL-ERATION	ACCEL-ERATION	PRESSURE
t	s_e	t	s_g	v_c	v_g	a_c	a_g	p
(MSEC)	(FT)	(MSEC)	(FT)	(FT/SEC)	(FT/SEC)	(FT/SEC^2)	(FT/SEC^2)	(PSIG)
0	0	0	0	0	0	0	0	0
0.36	0.0048	0.1	-	-	2.78	-	-	-
0.72	0.0016	0.2	-	-	3.44	7840	7840	803.2
1.09	0.0048	0.3	-	-	3.51	1690	1690	175.9
1.45	0.0112	0.4	-	-	3.55	340	450	49.4
1.81	0.0112	0.5	0.0018	-	3.57	190	200	23.9
2.17	0.0104	0.6	-	-	3.58	100	110	14.7
2.53	0.0152	0.7	-	-	3.59	50	50	8.6
2.90	0.0112	0.8	-	-	3.59	40	40	7.6
3.26	0.0152	0.9	-	-	3.59	-	34	7.0
3.62	0.0128	1.0	0.0036	3.60	3.60	-	26	6.2
3.98	0.0192	1.5	0.0054	3.60	3.60	22	17	5.2
4.34	0.0176	2.0	0.0072	3.60	3.61	12	15	5.0
4.70	0.0248	2.5	0.0090	3.60	3.62	14	14	4.9
5.06	0.0232	3.0	0.0108	3.60	3.62	14	14	4.9
5.43	0.0232	3.5	0.0126	3.64	3.63	20	15	5.0
5.79	0.0224	4.0	0.0144	3.70	3.64	26	17	5.2
6.15	0.0224	4.5	0.0163	3.76	3.66	26	18	5.3
6.51	0.0272	5.0	0.0182	3.80	3.67	28	20	5.5
6.87	0.0240	5.5	0.0201	3.80	3.68	26	23	5.8
7.23	0.0288	6.0	0.0220	3.80	3.70	26	25	6.1
7.59	0.0320	6.5	0.0239	3.84	3.71	28	28	6.4
7.95	0.0312	7.0	0.0258	3.86	3.72	30	31	6.7
8.32	0.0328	7.5	0.0278	3.86	3.74	36	35	7.1
8.68	0.0336	8.0	0.0297	3.80	3.76	40	38	7.4
9.04	0.0320	8.5	0.0316	3.78	3.78	40	43	7.9
9.40	0.0385	9.0	0.0334	3.80	3.80	44	46	8.2
9.76	0.0417	9.5	0.0354	3.86	3.82	50	51	8.7
10.12	0.0360	10.0	0.0373	3.94	3.85	56	55	9.1
10.48	0.0401	10.5	0.0393	3.96	3.88	60	60	9.6
10.84	0.0417	11.0	0.0413	4.00	3.91	60	66	10.2

TABLE B-10 CONTINUED

11.20	0.0409		11.5		0.0433		4.04	3.94		64	71		10.7
11.56	0.0433		12.0		0.0453		4.06	3.97		74	76		11.3
11.92	0.0417		12.5		0.0474		4.06	4.01		82	82		11.9
12.28	0.0465		13.0		0.0494		4.08	4.06		90	88		12.5
12.65	0.0433		13.5		0.0514		4.20	4.10		94	94		13.1
13.01	0.0433		14.0		0.0535		4.22	4.15		100	100		13.7
13.37	0.0457		14.5		0.0557		4.30	4.20		110	107		14.4
13.73	0.0505		15.0		0.0578		4.38	4.26		116	114		15.1
14.09	0.0521		15.5		0.0600		4.42	4.32		120	122		15.9
14.45	0.0529		16.0		0.0623		4.46	4.38		124	129		16.7
14.81	0.0513		16.5		0.0645		4.40	4.44		130	137		17.5
15.17	0.0617		17.0		0.0667		4.42	4.51		136	144		18.2
15.53	0.0601		17.5		0.0688		4.50	4.58		140	150		18.8
15.89	0.0625		18.0		0.0712		4.62	4.65		144	155		19.3
16.25	0.0665		18.5		0.0735		4.70	4.72		-	161		19.9
18.05	0.0737		19.0		0.0759		4.78	4.80		162	165		20.3
19.84	0.0801		19.5		0.0782		-	-		-	-		-
21.64	0.0897		20		0.0808		4.98	4.97		172	173		21.1
23.44	0.1009		21		0.0859		5.17	5.16		176	175		21.4
25.23	0.1138		22		0.0911		5.39	5.33		170	171		20.9
27.02	0.1194		23		0.0966		5.65	5.50		160	163		20.1
28.82	0.1362		24		0.1024		5.91	5.65		154	155		19.3
30.61	0.1482		25		0.1085		6.15	5.80		146	148		18.6
32.40	0.1546		26		0.1147		6.37	5.95		140	141		17.9
34.19	0.1778		27		0.1212		6.52	6.08		136	136		17.4
36.33	0.1891		28		0.1279		6.71	6.21		131	132		17.0
37.76	0.1995		29		0.1345		6.77	6.35		130	126		16.4
41.33	0.2259		30		0.1416		6.85	6.47		123	122		15.9
44.89	0.2531		31		0.1482		6.91	6.60		117	118		15.5
48.45	0.2796		32		0.1553		6.92	6.70		114	115		15.2
52.01	0.3084		33		0.1622		7.09	6.82		111	112		14.9
55.20	0.3429		34		0.1692		7.17	6.93		110	109		14.6
56.26	0.3517		35		0.1767		7.31	7.04		107	107		14.4
57.33	0.3629		36		0.1839		7.39	7.14		105	106		14.3
59.10	0.3757		37		0.1914		7.45	7.25		103	105		14.2
62.64	0.4102		38		0.1988		7.55	7.35		104	105		14.2

TABLE B-10 CONTINUED

66.17	0.4438	39	0.2065	-	7.45	-	104	14.1
69.71	0.4791	40	0.2141	7.73	7.56	105	104	14.1
73.23	0.5215	42	0.2298	7.84	7.77	104	103	14.0
74.29	0.5287	44	0.2457	7.94	7.98	104	102	13.9
75.34	0.5496	46	0.2614	8.05	8.18	104	101	13.8
76.75	0.5632	48	0.2777	8.16	8.40	103	100	13.7
80.27	0.6048	50	0.2943	8.31	8.60	102	100	13.7
83.78	0.6425	52	0.3108	8.48	8.80	99	99	13.6
87.29	0.6881	54	0.3279	8.72	9.00	98	98	13.5
90.79	0.7242	56	0.3457	9.03	9.19	97	97	13.4
94.29	0.7747	58	0.3640	9.32	9.38	97	97	13.4
95.33	0.7875	60	0.3830	9.63	9.58	97	96	13.3
97.78	0.8059	62	0.4024	9.94	9.77	96	96	13.3
101.27	0.8548	64	0.4228	10.20	9.96	95	95	13.2
104.75	0.9052	66	0.4435	10.38	10.15	94	94	13.1
108.57	0.9581	68	0.4644	10.53	10.34	94	94	13.1
109.62	0.9677	70	0.4854	10.69	10.52	94	93	13.0
110.66	0.9894	72	0.5071	10.91	10.72	93	93	13.0
111.70	0.9990	74	0.5290	11.11	10.90	92	93	13.0
115.17	1.0462	76	0.5517	11.28	11.08	91	92	12.9
118.63	1.1047	78	0.5742	-	11.26	92	92	12.9
122.09	1.1480	80	0.5973	11.43	11.45	92	92	12.9
125.55	1.1992	82	-	-	11.63	90	91	12.8
126.58	1.2072	84	0.6432	11.63	11.81	90	91	12.8
129.00	1.2433	86	-	-	11.98	90	90	12.7
132.44	1.2986	88	0.6900	11.87	12.17	90	90	12.7
132.79	1.3066	90	-	-	12.35	88	89	12.6
133.82	1.3218	92	0.7380	12.20	12.52	86	89	12.6
		94	-	-	12.68	85	88	12.5
		96	0.7872	12.60	12.86	86	88	12.5
		98	-	-	13.03	86	87	12.4
		100	0.8385	13.05	13.20	85	87	12.4
		101	-	-	13.28	-	87	12.4
		102	-	-	13.37	85	86	12.3
		103	-	-	13.45	87	86	12.3
		104	0.8917	13.47	13.54	86	86	12.3

TABLE B-10 CONCLUDED

			105		-		-	13.63		87	85		12.2
			106		-		-	13.71		83	85		12.2
			107		-		-	13.80		80	84		12.1
			108		0.9468		13.85	13.87		79	83		12.1
			109		-		-	13.95		78	81		11.8
			110		-		-	14.03		78	78		11.5
			111		-		-	14.11		75	75		11.2
			112		1.0025		14.16	14.18		72	72		10.8
			113		-		-	14.25		68	68		10.4
			114		-		-	14.32		63	63		9.9
			115		-		-	14.38		57	58		9.4
			116		1.0600		14.46	14.43		52	52		8.8
			117		-		-	14.48		46	45		8.1
			118		-		-	14.53		40	39		7.5
			119		-		-	14.56		30	30		6.6
			120		1.1183		14.63	14.59		22	22		5.7
			121		-		-	14.60		13	13		4.8
			122		-		-	14.62		3	4		3.9
			123		-		-	14.61		-	-		-
			124		1.1780		14.58	14.60		-	-		-
			128		1.2360		-	-		-	-		-
			132		1.2928		-	-		-	-		-

TABLE B-11 MODEL-PLUG RESPONSE DATA FOR TEST NO.11

EXPERIMENTAL DATA		CALCULATED DATA						
TIME	DISPLACEMENT	TIME	DISPLACEMENT	VELOCITY	VELOCITY	ACCELERATION	ACCELERATION	PRESSURE
t	s_e	t	s_g	v_c	v_g	a_c	a_g	p
(MSEC)	(FT)	(MSEC)	(FT)	(FT/SEC)	(FT/SEC)	(FT/SEC^2)	(FT/SEC^2)	(PSIG)
0	0	0	0	0	0	0	0	0
0.36	0.0016	0.1	-	-	1.08	-	-	-
0.73	0.0032	0.2	-	-	2.56	11800	11800	1207.1
1.09	0.0056	0.3	-	-	4.18	8480	8100	829.7
1.45	0.0104	0.4	-	-	4.35	4080	4200	431.9
1.81	0.0144	0.5	0.0024	-	4.43	810	930	98.4
2.18	0.0128	0.6	-	-	4.48	490	500	54.5
2.54	0.0128	0.7	-	-	4.52	350	325	36.7
2.90	0.0136	0.8	-	-	4.55	250	250	29.0
3.27	0.0192	0.9	-	-	4.57	-	212	25.1
3.63	0.0192	1.0	0.0048	4.64	4.58	-	188	22.7
3.99	0.0200	1.5	0.0070	4.58	4.61	102	102	13.9
4.35	0.0224	2.0	0.0093	4.56	4.63	50	59	9.5
4.71	0.0248	2.5	0.0116	4.64	4.66	50	53	8.9
5.08	0.0288	3.0	0.0139	4.70	4.68	54	52	8.8
5.44	0.0304	3.5	0.0163	4.80	4.71	52	53	8.9
5.80	0.0296	4.0	0.0187	4.82	4.74	54	53	8.9
6.16	0.0296	4.5	0.0212	4.84	4.76	54	54	9.0
6.52	0.0304	5.0	0.0235	4.84	4.79	56	55	9.1
6.89	0.0360	5.5	0.0260	4.82	4.82	60	57	9.3
7.25	0.0320	6.0	0.0284	4.88	4.85	60	59	9.5
7.61	0.0344	6.5	0.0308	4.90	4.88	60	61	9.7
7.97	0.0344	7.0	0.0333	4.96	4.91	64	64	10.0
8.33	0.0408	7.5	0.0358	5.00	4.94	70	67	10.3
8.70	0.0400	8.0	0.0383	5.00	4.98	76	72	10.8
9.06	0.0480	8.5	0.0408	5.00	5.02	80	76	11.3
9.42	0.0432	9.0	0.0433	5.04	5.06	80	81	11.8
9.78	0.0432	9.5	0.0458	5.10	5.10	84	85	12.2
10.50	0.0496	10.0	0.0484	5.16	5.14	90	90	12.7
11.59	0.0544	10.5	0.0510	5.20	5.19	96	96	13.3
12.67	0.0616	11.0	0.0536	5.28	5.24	100	102	13.9
13.39	0.0664	11.5	0.0562	5.32	5.29	104	108	14.5

TABLE B-II CONTINUED

14.47	0.0728	12.0	0.0590	5.36	5.34	106	113	15.0
15.19	0.0768	12.5	0.0616	5.42	5.40	-	-	-
16.27	0.0857	13.0	0.0643	5.50	5.45	122	121	15.8
16.99	0.0897	13.5	0.0671	5.70	-	-	-	-
18.79	0.0921	14.0	0.0700	5.90	5.60	127	127	16.5
20.59	0.1065	14.5	0.0730	6.06	-	-	-	-
22.39	0.1265	15.0	0.0761	6.04	5.72	128	129	16.7
24.19	0.1393	15.5	0.0792	-	-	-	-	-
25.62	0.1513	16	0.0820	5.84	5.84	121	125	16.3
26.70	0.1529	17	0.0875	5.65	5.97	120	121	15.8
27.77	0.1681	18	0.0935	5.77	6.08	119	118	15.5
31.35	0.1889	19	0.0992	6.01	6.20	118	116	15.3
34.93	0.2169	20	0.1050	6.08	6.32	118	114	15.1
38.49	0.2474	21	0.1118	6.32	6.44	115	113	15.0
42.06	0.2802	22	0.1176	6.55	6.55	112	112	14.9
45.61	0.3122	23	0.1245	6.68	6.66	111	111	14.8
46.68	0.3242	24	0.1314	7.06	6.77	112	109	14.6
47.74	0.3346	25	0.1383	7.26	6.88	111	108	14.5
49.16	0.3506	26	0.1460	7.48	7.00	108	107	14.4
56.24	0.4179	27	0.1535	7.62	7.10	106	106	14.3
65.06	0.5123	28	0.1612	7.71	7.20	105	106	14.3
68.58	0.5467	29	0.1688	7.88	7.31	106	105	14.2
73.84	0.6124	30	0.1770	8.00	7.42	107	104	14.1
74.89	0.6236	31	0.1850	8.15	7.52	105	103	14.0
75.94	0.6372	32	0.1931	8.15	7.63	103	103	14.0
79.09	0.6788	33	0.2015	8.20	7.73	104	102	13.9
84.33	0.7429	34	0.2095	8.21	7.83	105	101	13.8
89.55	0.8069	35	0.2178	8.25	7.94	106	101	13.8
94.76	0.8717	36	0.2260	8.41	8.05	105	100	13.7
95.80	0.8806	37	0.2345	8.56	8.15	102	100	13.7
99.96	0.9454	38	0.2432	8.69	8.25	100	100	13.7
105.14	1.0134	39	0.2520	-	8.35	-	100	13.7
110.31	1.0943	40	0.2607	8.81	8.45	102	99	13.6
115.46	1.1543	42	0.2784	9.05	8.66	102	98	13.5
120.60	1.2472	44	0.2965	9.30	8.86	100	98	13.5
125.73	1.3216	46	0.3158	9.57	9.06	99	98	13.5

TABLE B-II CONTINUED

126.75	1.3360	48	0.3350	9.75	9.25	99	98	13.5
127.78	1.3552	50	0.3548	9.90	9.45	98	98	13.5
		52	0.3745	10.03	9.65	98	98	13.5
		54	0.3950	10.16	9.84	97	98	13.5
		56	0.4152	10.32	10.03	97	97	13.4
		58	0.4360	10.42	10.23	96	96	13.3
		60	0.4572	10.56	10.42	94	96	13.3
		62	0.4782	10.71	10.60	93	96	13.3
		64	0.4997	10.66	10.78	92	95	13.2
		66	0.5218	10.98	10.98	93	94	13.1
		68	0.5420	11.31	11.15	92	94	13.1
		70	0.5668	11.65	11.34	91	93	13.0
		72	0.5903	12.00	11.52	91	92	12.9
		74	0.6141	10.93	11.70	91	92	12.9
		76	0.6383	11.45	11.88	92	92	12.9
		78	0.6521	-	12.07	91	91	12.8
		80	0.6858	12.06	12.25	90	91	12.8
		82	-	-	12.42	88	91	12.8
		84	0.7341	12.27	12.60	88	91	12.8
		86	-	-	12.77	88	90	12.7
		88	0.7836	12.60	12.95	88	90	12.7
		90	-	-	13.12	88	90	12.7
		92	0.8347	13.01	13.30	88	90	12.7
		94	-	-	13.47	88	89	12.6
		96	0.8875	13.40	13.65	88	89	12.6
		98	-	-	13.82	89	89	12.6
		100	0.9424	13.77	14.00	88	89	12.6
		101	-	-	14.08	-	89	12.6
		102	-	-	14.18	89	88	12.5
		103	-	-	14.27	87	87	12.4
		104	0.9978	14.14	14.35	84	86	12.3
		105	-	-	14.43	83	85	12.2
		106	-	-	14.52	81	83	12.0
		107	-	-	14.60	79	81	11.8
		108	1.0550	14.57	14.67	77	77	11.4
		109	-	-	14.75	72	73	10.9

TABLE B-11 CONCLUDED

			110		-		-	14.83		67	68		10.4
			111		-		-	14.88		61	62		9.8
			112		1.1139		14.99	14.94		54	55		9.1
			113		-		-	15.00		50	47		8.3
			114		-		-	15.04		40	38		7.4
			115		-		-	15.08		30	29		6.5
			116		1.1758		15.17	15.10		20	20		5.5
			117		-		-	15.12		-	-		-
			118		-		-	15.12		-	-		-
			120		1.2372		15.09	-		-	-		-
			124		1.2967		-	-		-	-		-
			128		1.3552		-	-		-	-		-

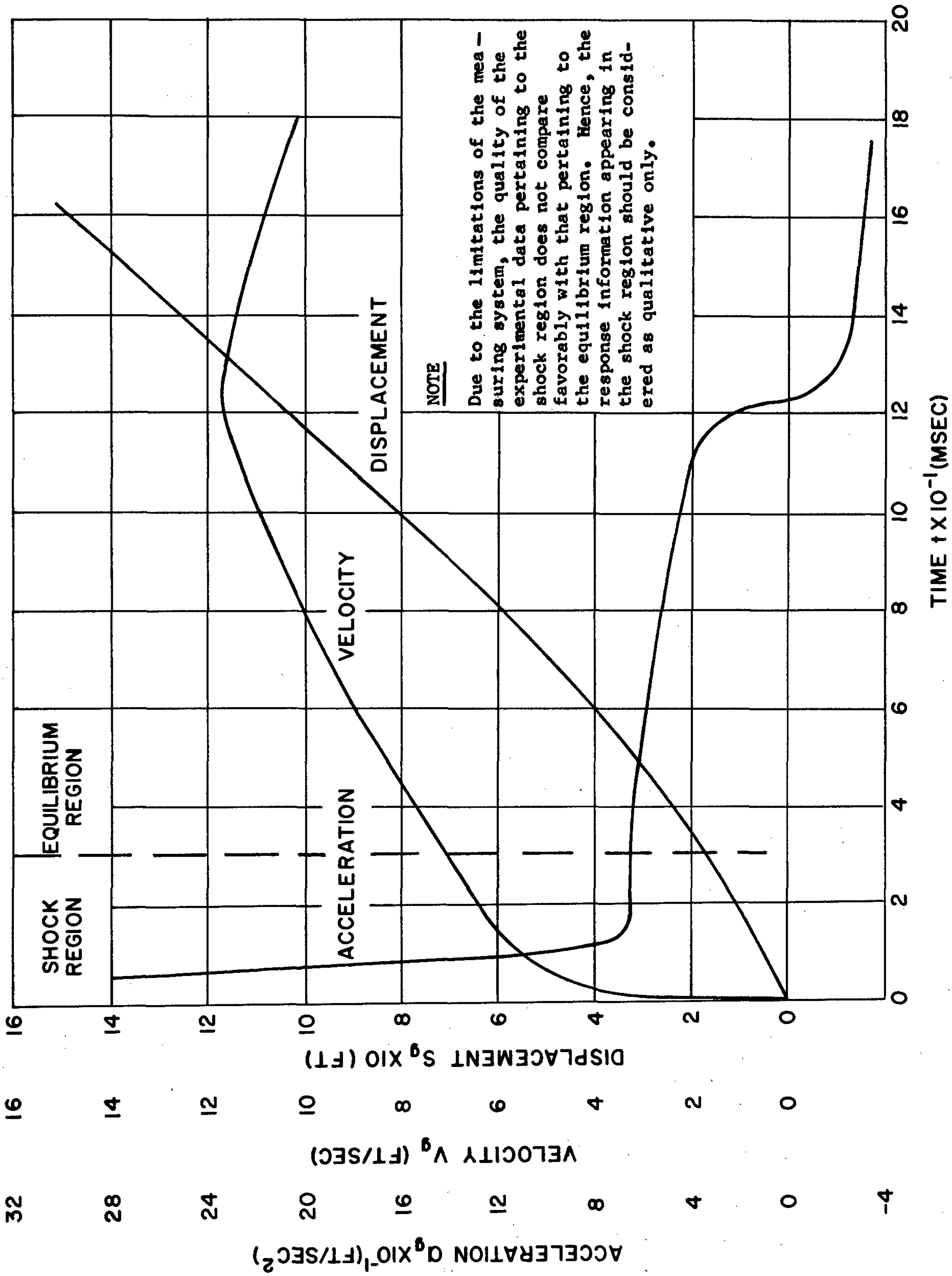

FIG. B-1 VARIATION OF DISPLACEMENT, VELOCITY, AND ACCELERATION WITH TIME FOR TEST NO. I

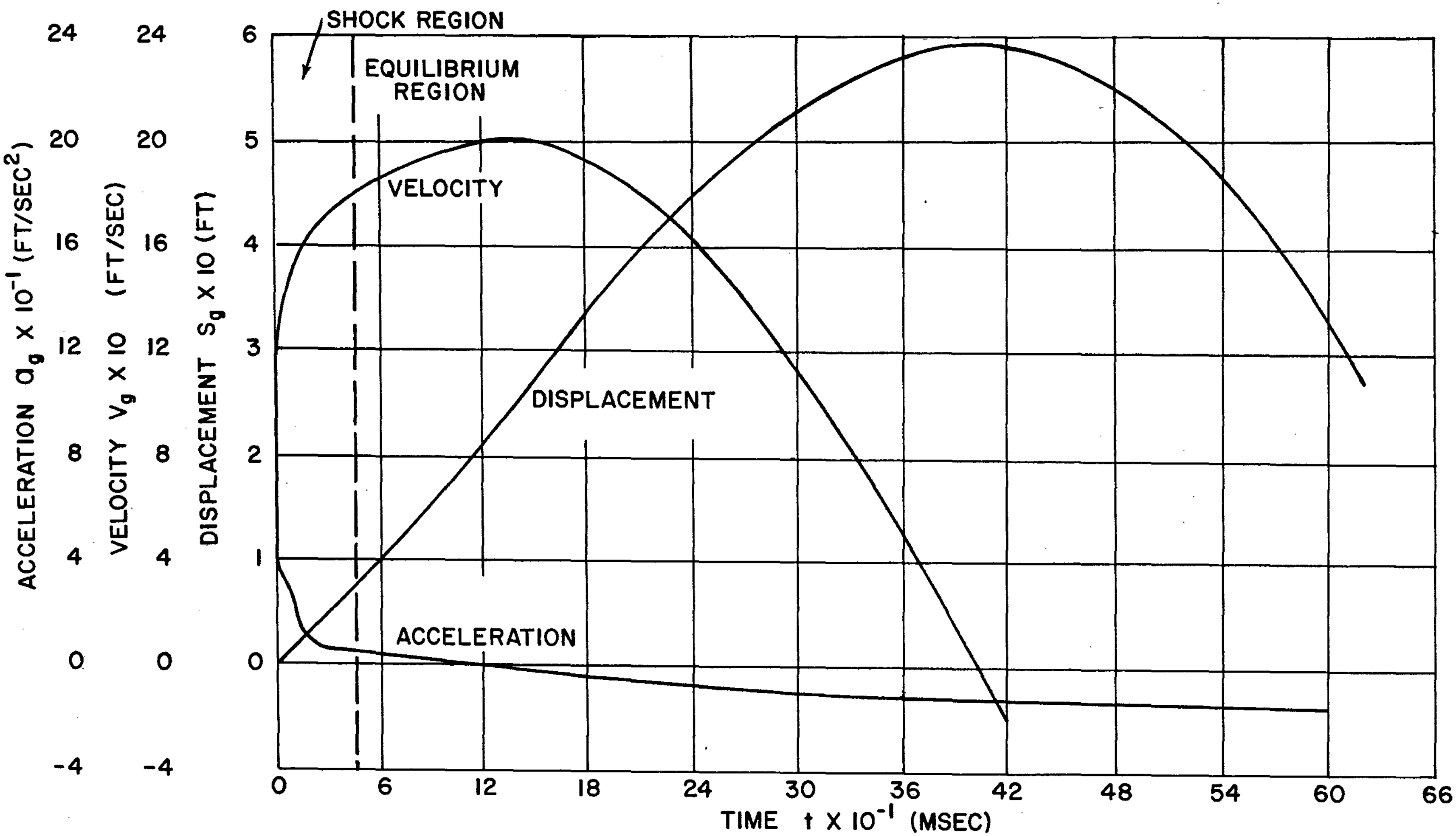

NOTE

Due to the limitations of the measuring system, the quality of the experimental data pertaining to the shock region does not compare favorably with that pertaining to the equilibrium region. Hence, the response information appearing in the shock region should be considered as qualitative only.

FIG. B-2 VARIATION OF DISPLACEMENT, VELOCITY, AND ACCELERATION WITH TIME FOR TEST NO.2

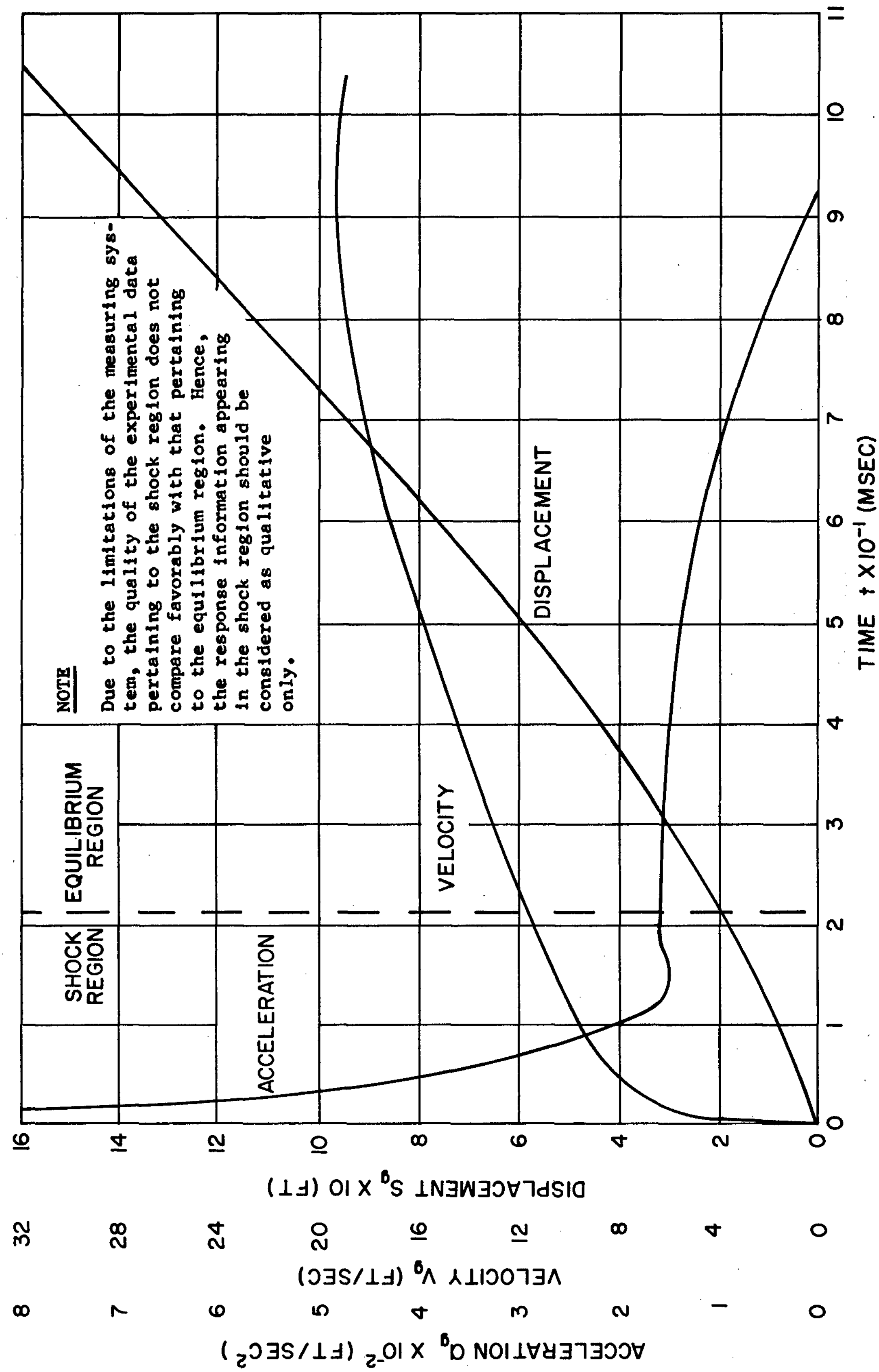

FIG. B-3 VARIATION OF DISPLACEMENT, VELOCITY, AND ACCELERATION WITH TIME FOR TEST NO. 3

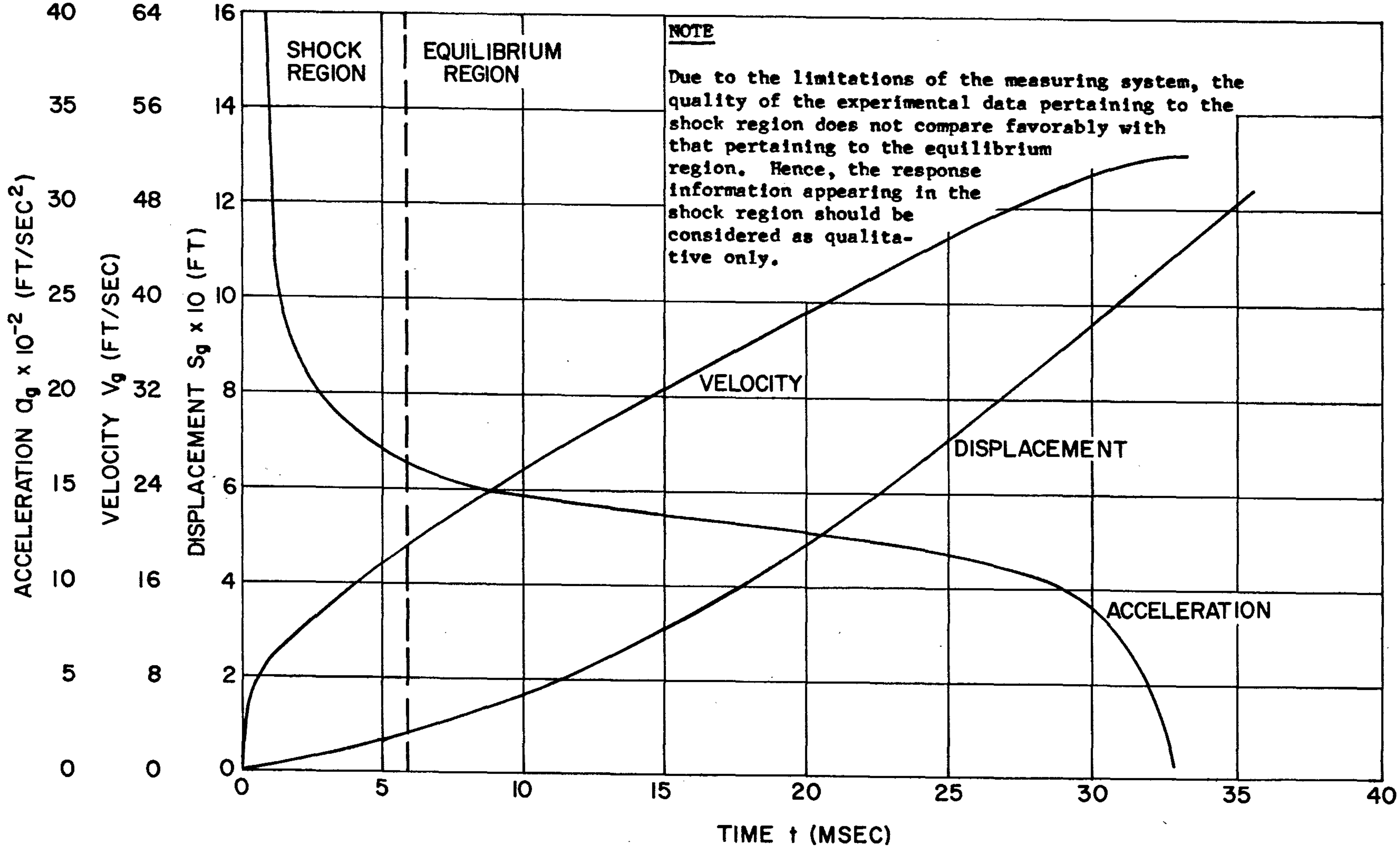

FIG. B-4 VARIATION OF DISPLACEMENT, VELOCITY, AND ACCELERATION WITH TIME FOR TEST NO. 4

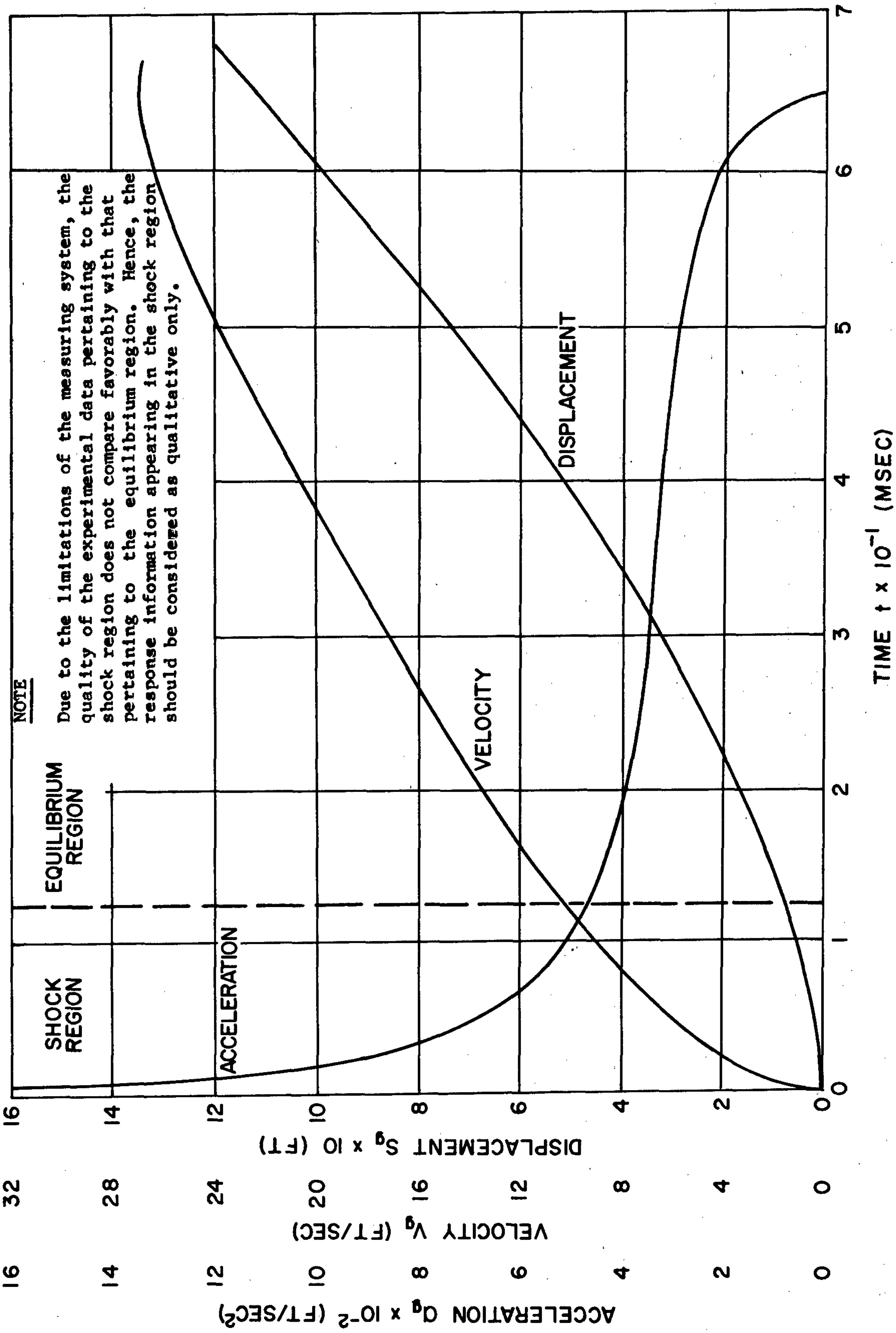

FIG. B-5 VARIATION OF DISPLACEMENT, VELOCITY, AND ACCELERATION WITH TIME FOR TEST NO. 5

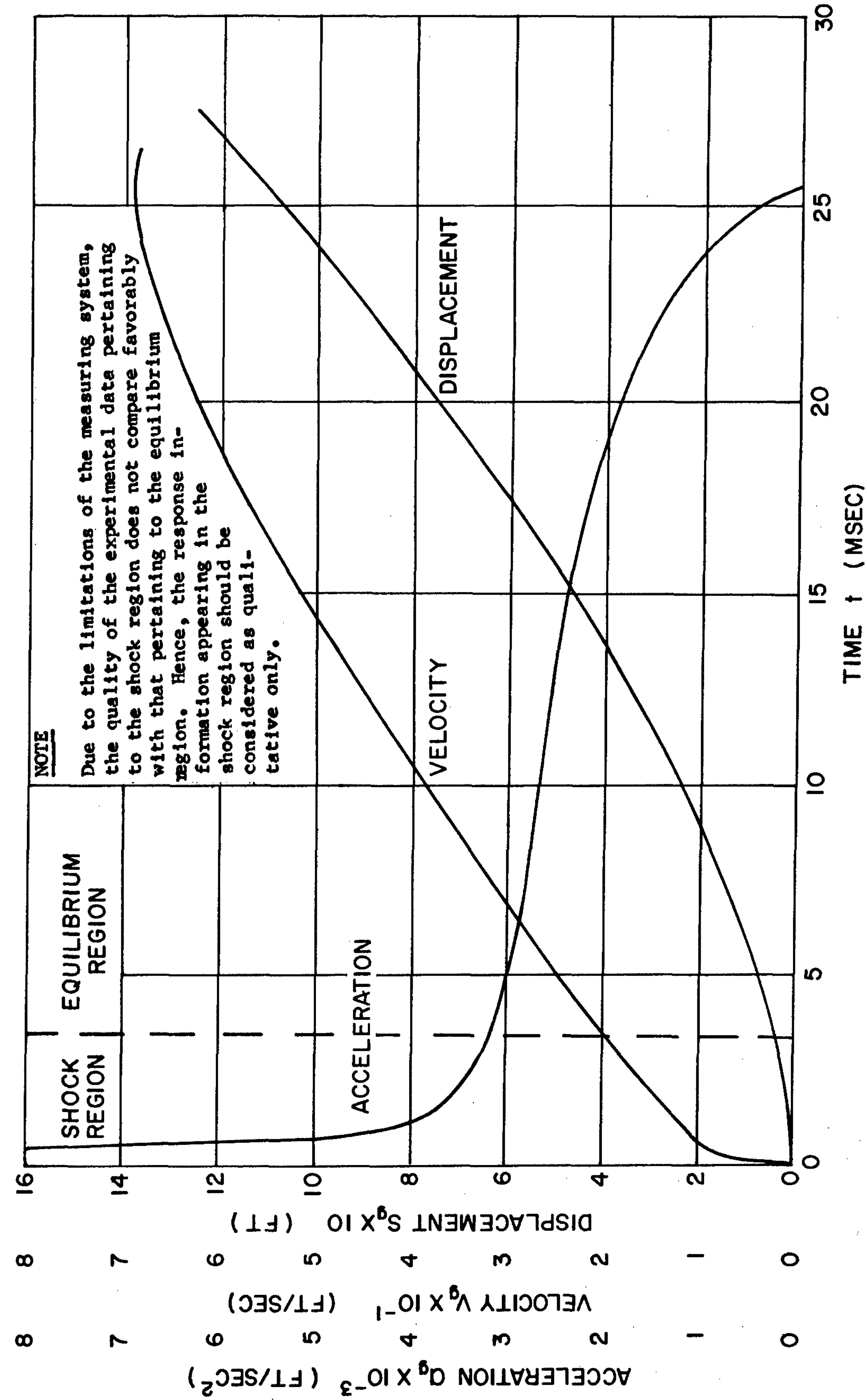

FIG B-6 VARIATION OF DISPLACEMENT, VELOCITY, AND ACCELERATION WITH TIME FOR TEST NO.6

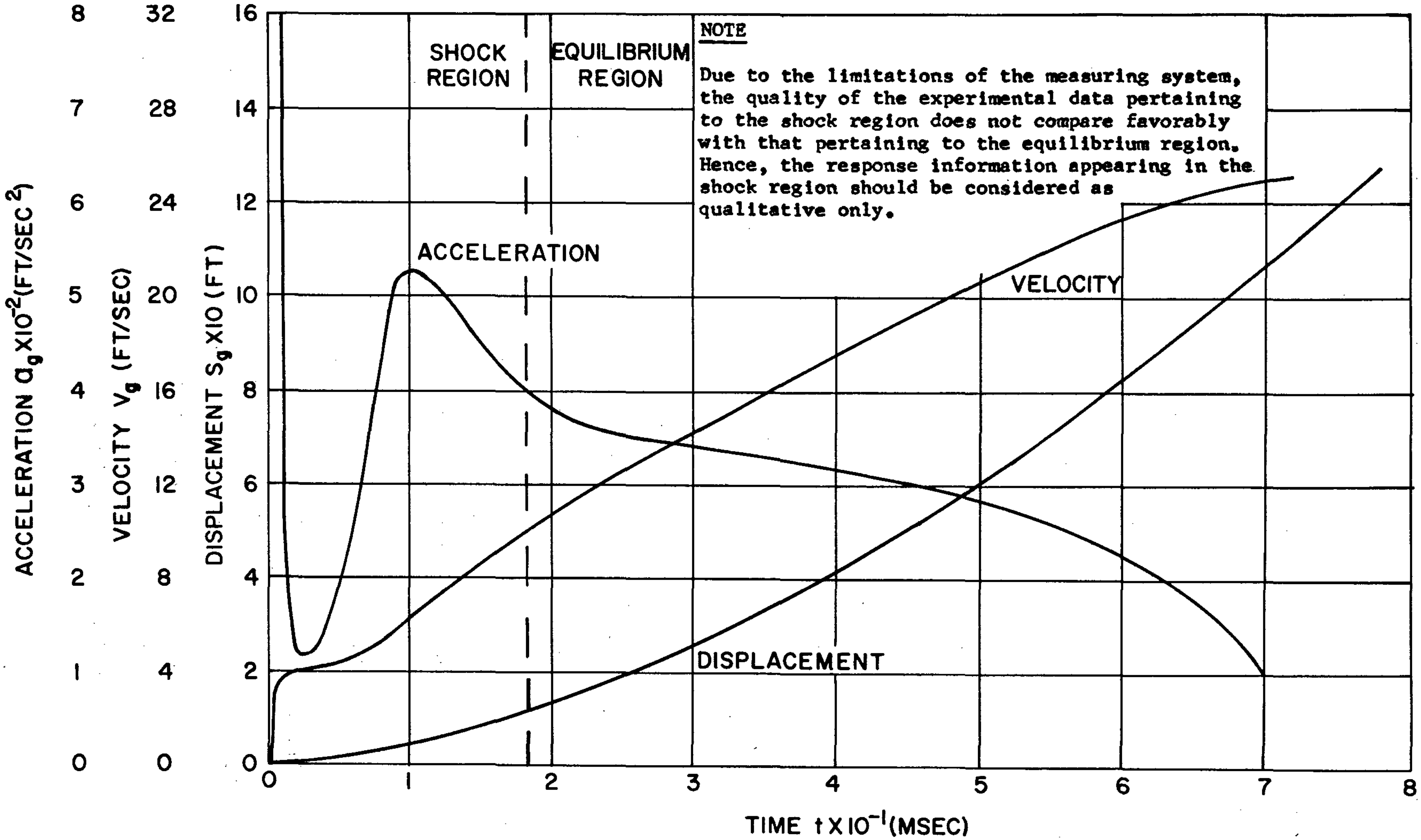

FIG. B-7 VARIATION OF DISPLACEMENT, VELOCITY, AND ACCELERATION WITH TIME FOR TEST NO. 7

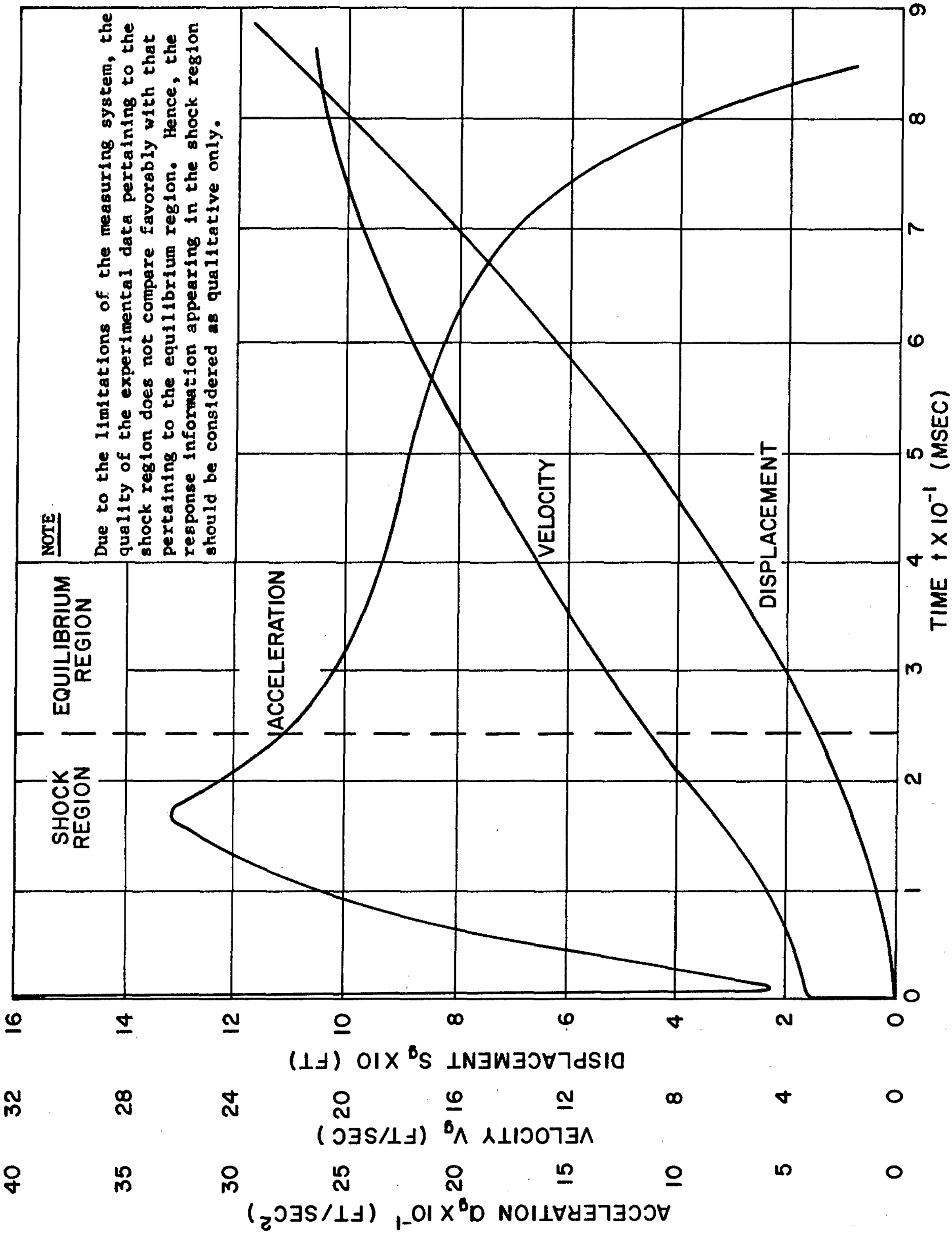

FIG. B-8 VARIATION OF DISPLACEMENT, VELOCITY, AND ACCELERATION WITH TIME FOR TEST NO. 8

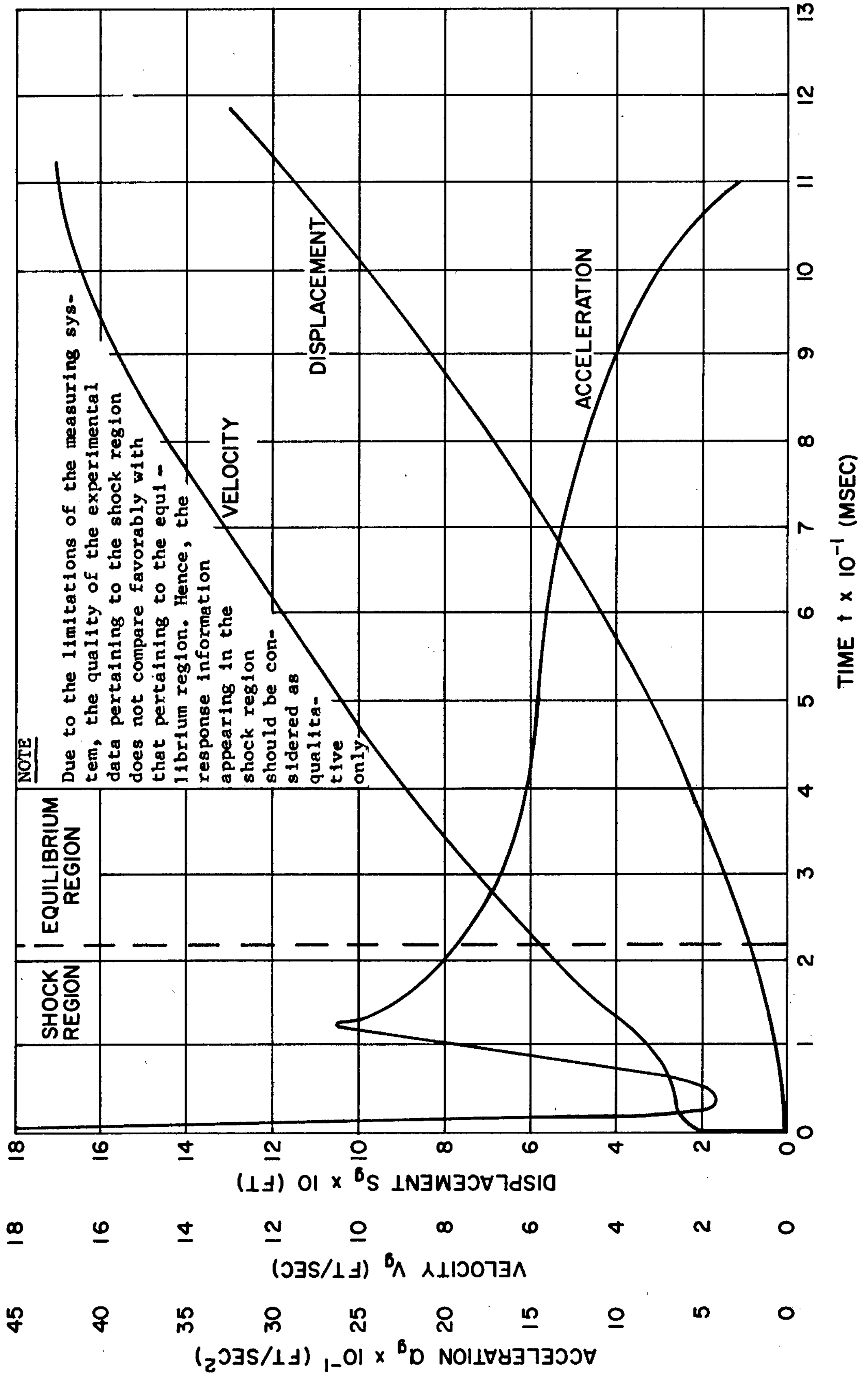

FIG. B-9 VARIATION OF DISPLACEMENT, VELOCITY, AND ACCELERATION WITH TIME FOR TEST NO. 9

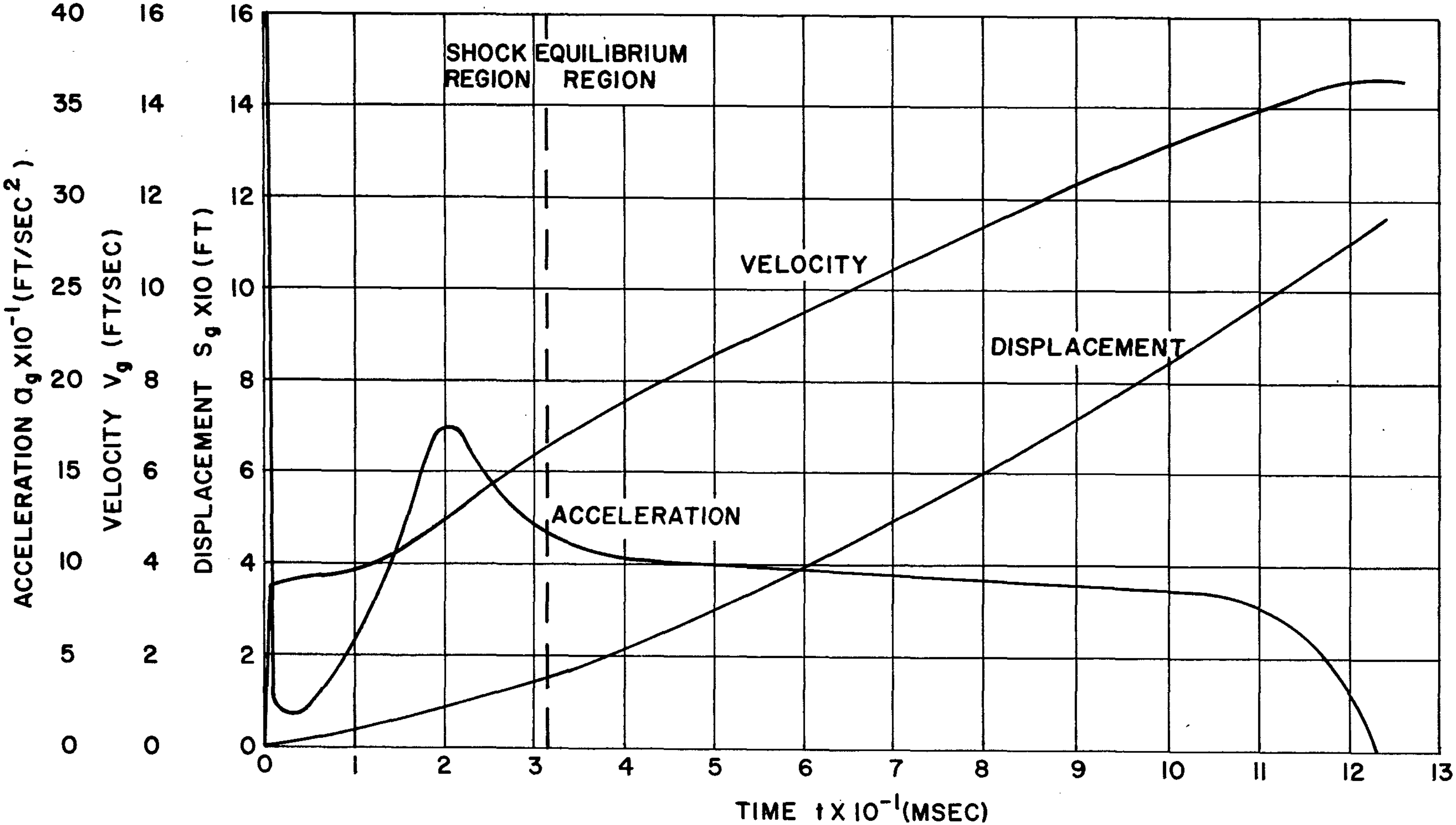

NOTE

Due to the limitations of the measuring system, the quality of the experimental data pertaining to the shock region does not compare favorably with that pertaining to the equilibrium region. Hence, the response information appearing in the shock region should be considered as qualitative only.

FIG. B-10 VARIATION OF DISPLACEMENT, VELOCITY, AND ACCELERATION WITH TIME FOR TEST NO. 10

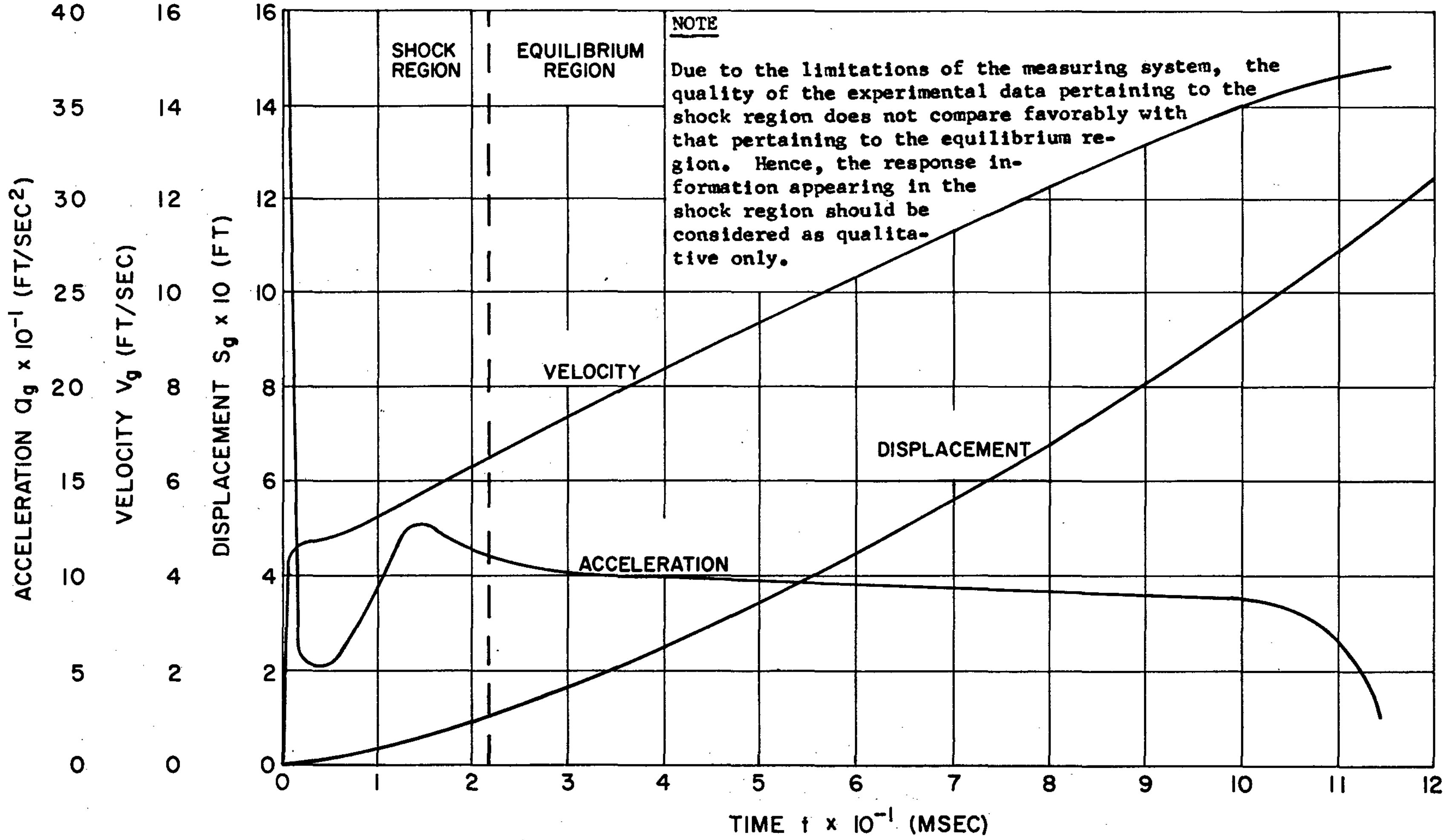

FIG. B-11 VARIATION OF DISPLACEMENT, VELOCITY, AND ACCELERATION WITH TIME FOR TEST NO. 11

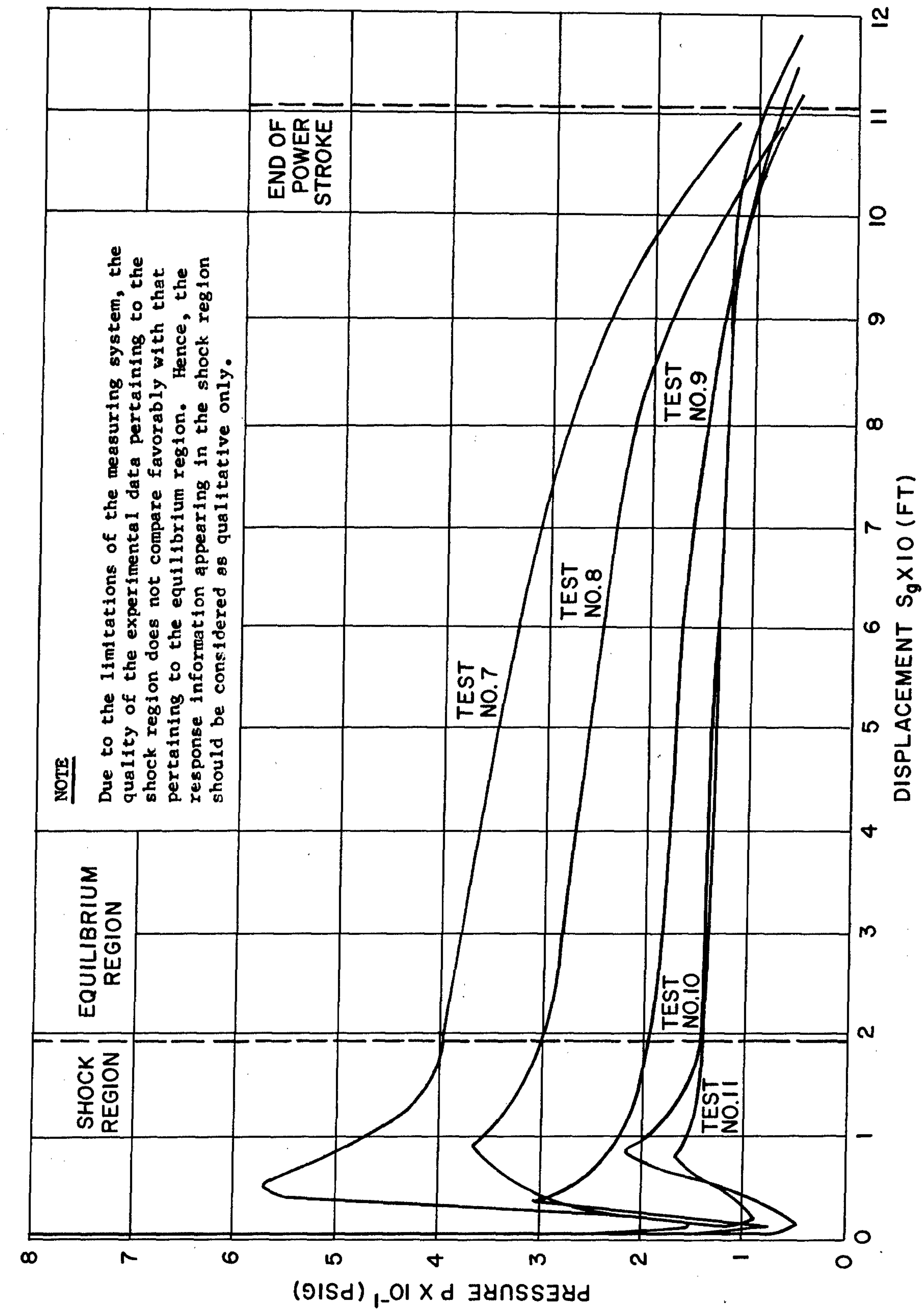

FIG. B-12 VARIATION OF PRESSURE WITH DISPLACEMENT FOR TESTS NO. 7, 8, 9, 10, AND 11

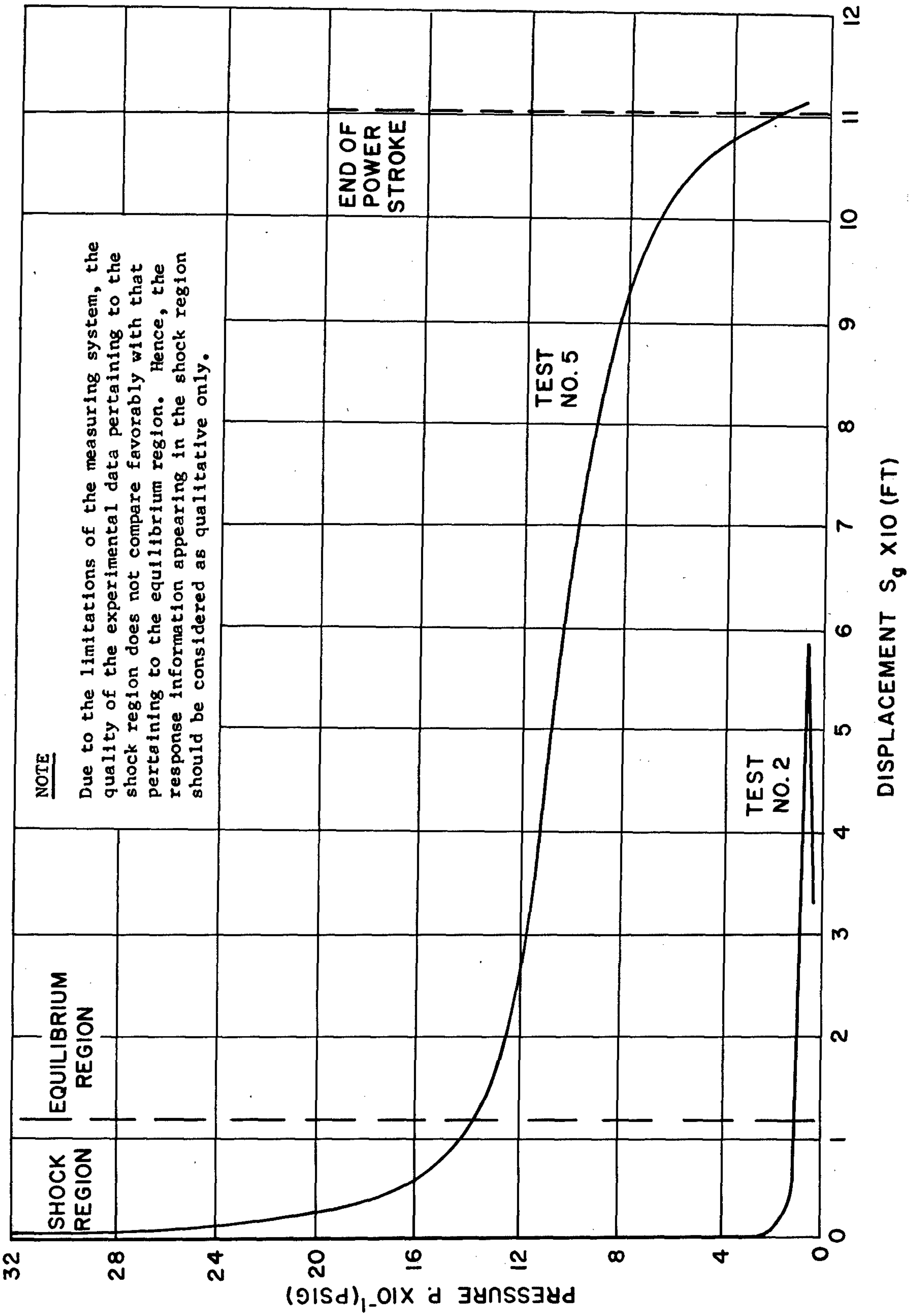

FIG. B-13 VARIATION OF PRESSURE WITH DISPLACEMENT FOR TEST NO. 2 AND 5

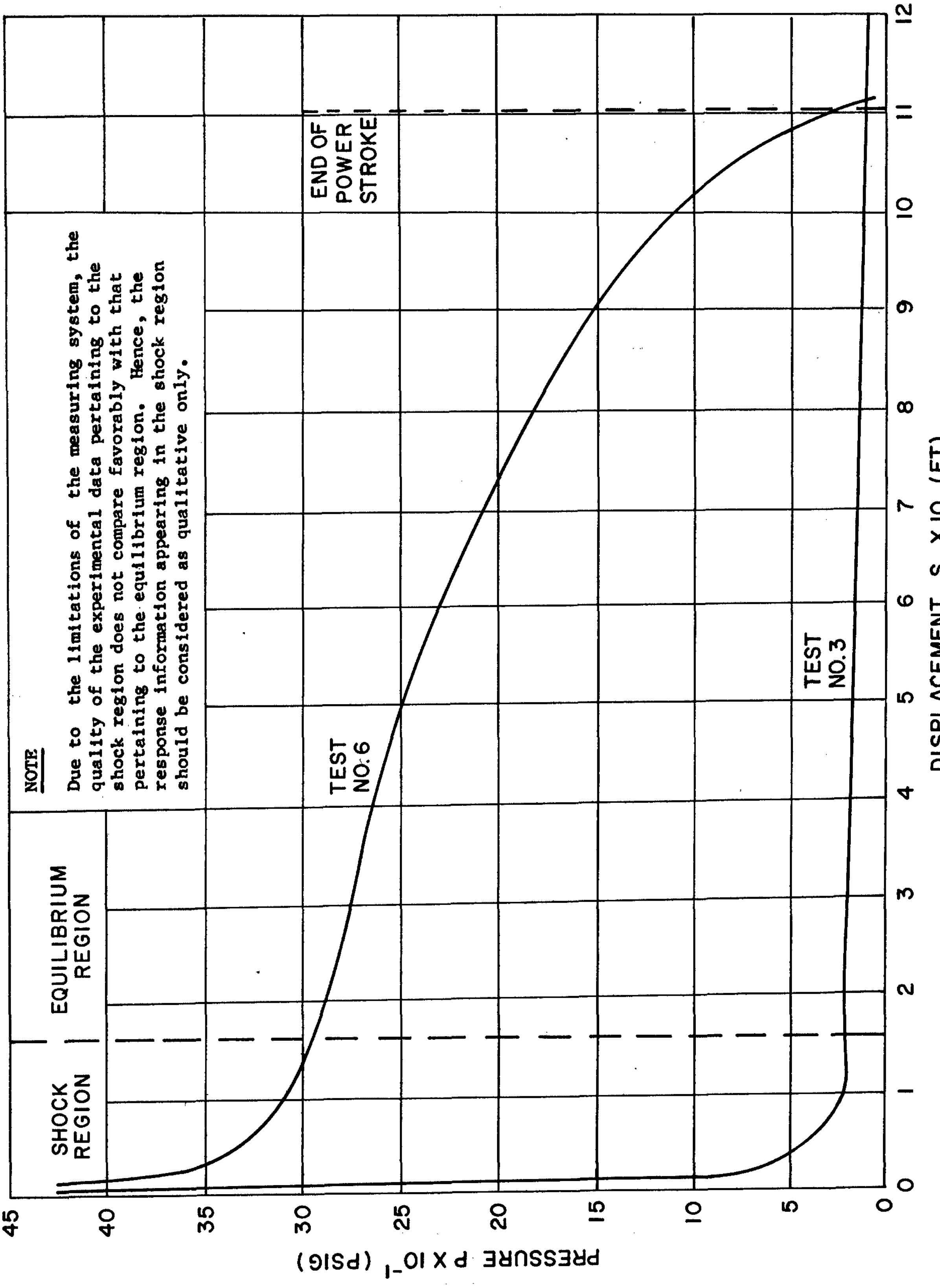

FIG. B-14 VARIATION OF PRESSURE WITH DISPLACEMENT FOR TESTS NO.3 AND 6

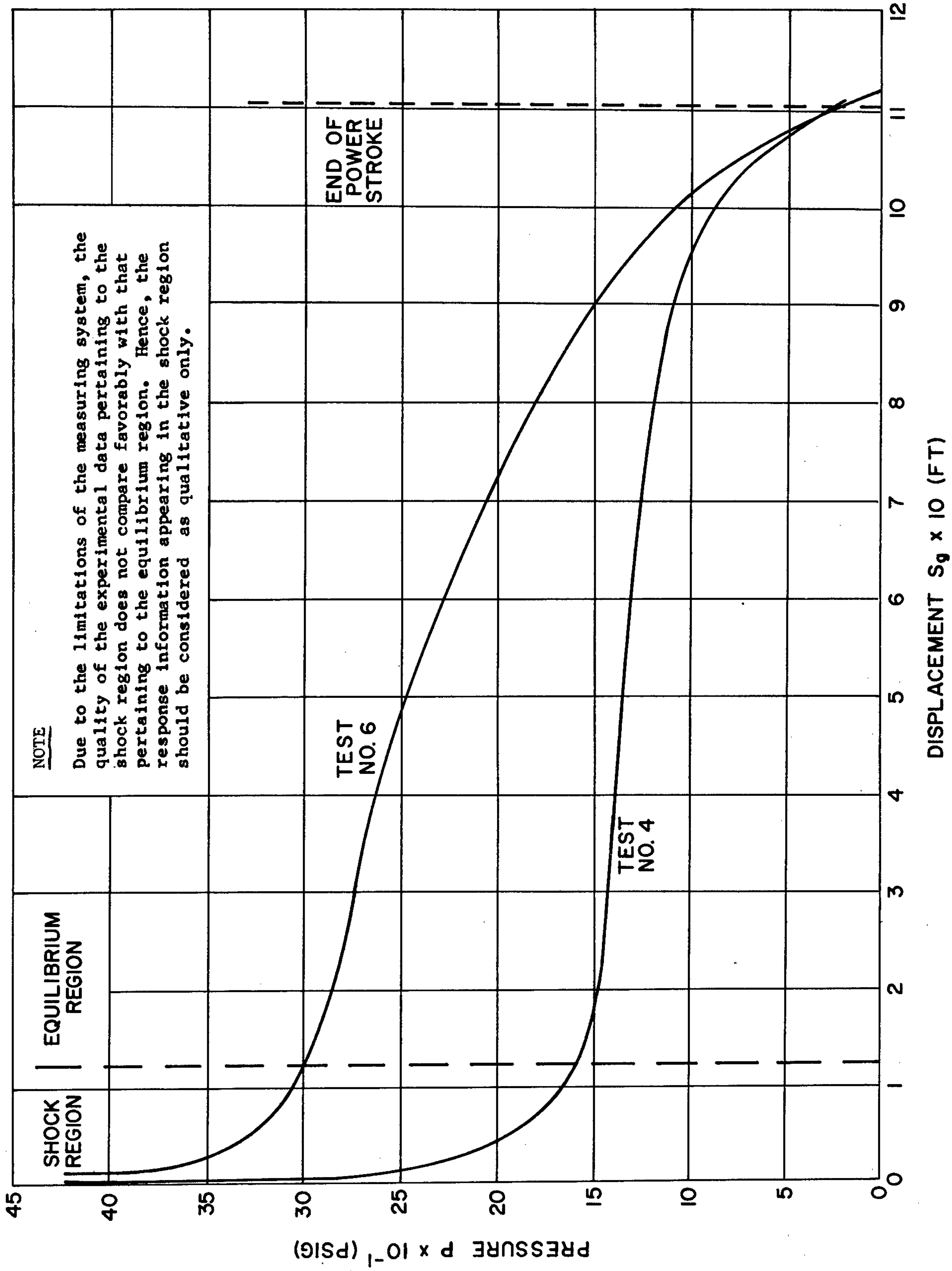

FIG. B-15 VARIATION OF PRESSURE WITH DISPLACEMENT FOR TESTS NO. 4 AND 6

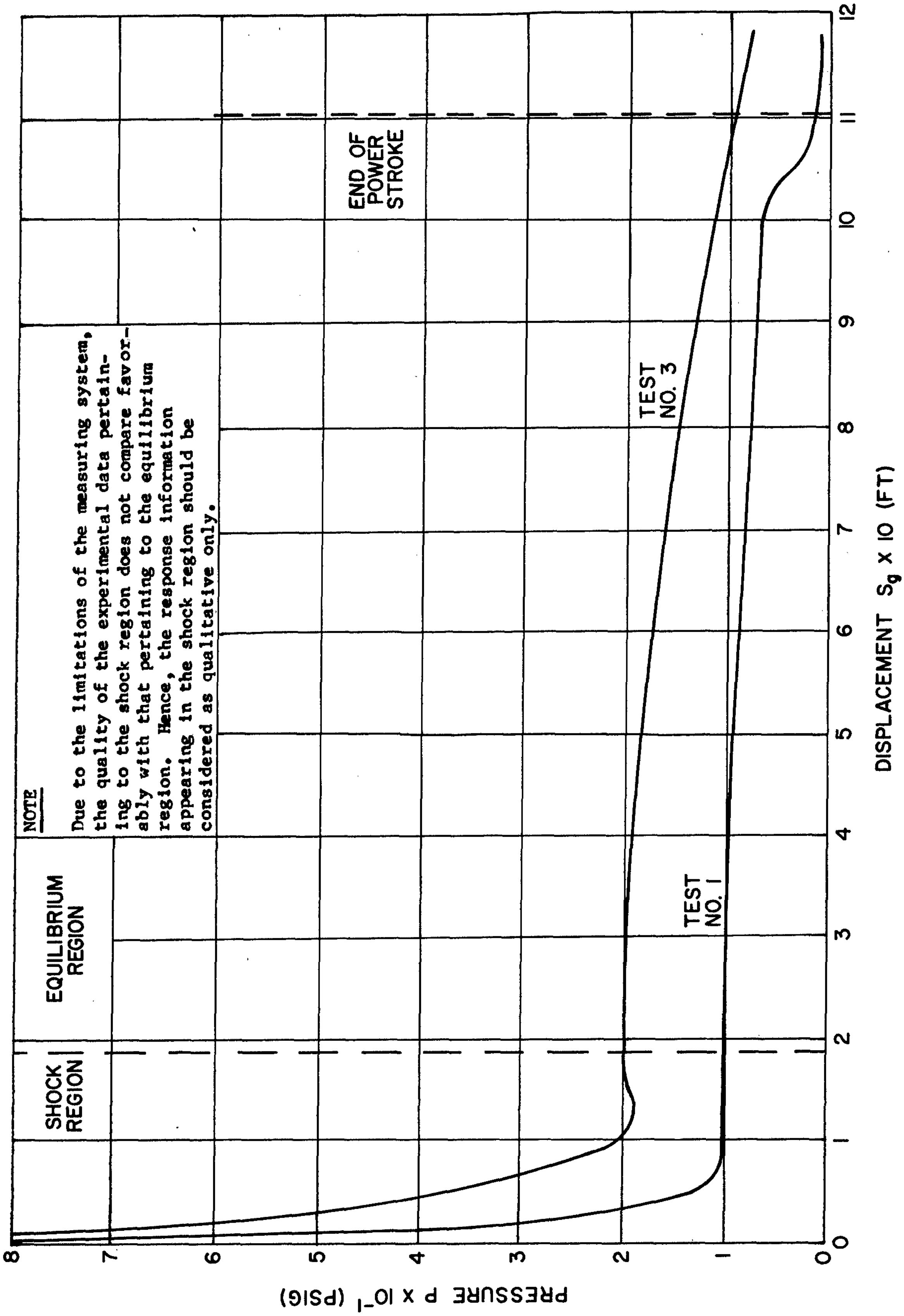

FIG. B-16 VARIATION OF PRESSURE WITH DISPLACEMENT FOR TESTS NO. 1 AND 3

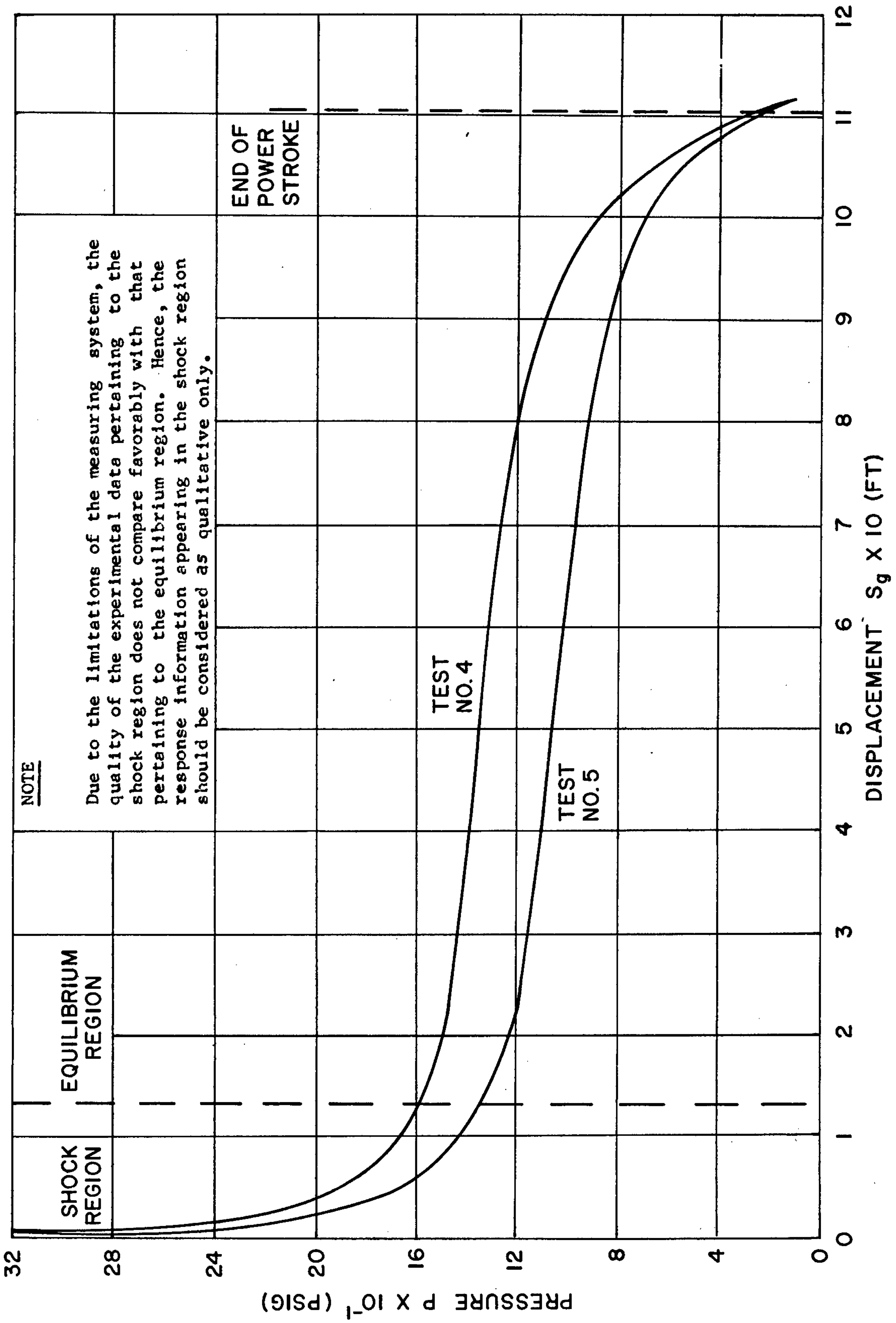

FIG. B-17 VARIATION OF PRESSURE WITH DISPLACEMENT FOR TESTS NO.4 AND 5

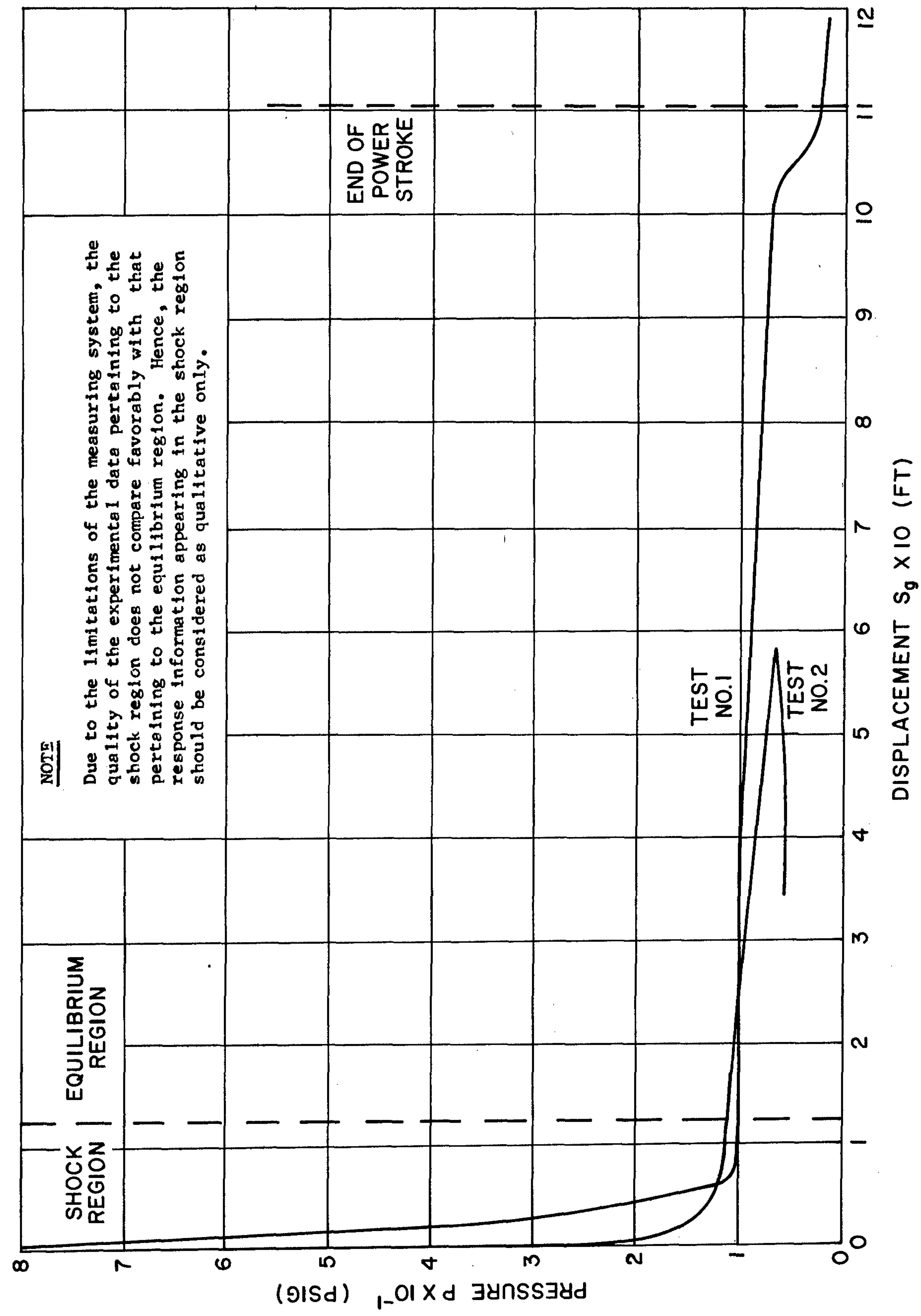

FIG. B-18 VARIATION OF PRESSURE WITH DISPLACEMENT FOR TESTS NO. 1 AND 2

APPENDIX C

Gas-Jet Effect

From the low-pressure tests given in figure B-12, it is observed that a residual pressure of the order of 10 psig continued to act on the model plug after completion of the power stroke. Also from the high-pressure tests given in figure B-15, a residual pressure of the order of 30 psig is observed. It is realized that the pressure on the plug cannot be instantaneously released upon completion of the power stroke. Therefore, the observed residual pressure is the result of the existing chamber gas pressure acting directly on the plug and the momentum change of the high-velocity gas jet formed by the escaping gas. Of course, the chamber gas pressure immediately upon completion of the power stroke is of the order observed, and it will be shown that the gas jet will also produce an effective pressure of the same order.

We study the idealized case of a gas stream acting normal to a fixed plate and being deflected through an angle of 90°. If we assume no losses and the area of the gas stream to be equal to the area of the plate, then the pressure that the plug would feel is

$$p = \frac{\rho v_a^2}{144}$$

where

p .... is pressure, psig

ρ .... is density of gas, slugs/ft^3

v_a ... is exit velocity of gas, ft/sec

For the high-pressure test, if we assume $\rho = 0.0040$ slugs/ft^3 and $v_a = 1{,}000$ ft/sec, then

$$p = 28 \text{ psig}$$

For the low-pressure test, if we assume $\rho = 0.0044$ slugs/ft^3 and $v_a = 600$ ft/sec, then

$$p = 11 \text{ psig}$$

We see that these estimated values of effective pressure explained in terms of the gas jet are of the same order as those observed. The duration of this jet is extremely short because the quantity of gas is insufficient to support the large mass rate-of-flow; and, hence, its effect upon energy partition is quite small.

APPENDIX D

Energy Absorptions

Kinetic Energy of Reactor-Vessel Simulant. When the reactor-vessel simulant is fractured, it is assumed that its total mass is given a velocity equal to the mean particle velocity of the water casing. The simulant, a thin-wall right-circular cylinder with one end closed, was constructed of 1/64-inch brass shim stock. Given a simulant of diameter d in inches, height h in inches, and wall thickness of 1/64-inch and taking the density of brass to be 0.304 lb/in^3, then we can express the total mass of the simulant as

$$m_c = 0.000472\ d(h + \frac{d}{4}),\ \text{slugs}$$

If this mass has a velocity equal to the mean particle velocity v_p, then the kinetic energy of the simulant is

$$KE_c = 0.000236\ d\ (h + \frac{d}{4})\ v_p^{\ 2}\ ,\ \text{ft-lb}$$

Strain Energy of Reactor-Vessel Simulant. To approximate the strain energy of the container (reactor-vessel simulant), it is assumed that the total volume of material is stressed beyond the ultimate strength. An approximation of the strain energy per unit volume for this plastic deformation is taken to be

$$1/2\ (\sigma_{yp} + \sigma_u)\,\epsilon$$

where

σ_{yp} ... is stress at yield point of brass, psi

σ_u .... is ultimate strength of brass, psi

ϵ...... is unit elongation of brass, in/in

If we take the container dimensions given in the previous section and assume for brass

$$\sigma_{yp} = 22{,}000 \text{ psi}$$

$$\sigma_u = 58{,}000 \text{ psi}$$

$$\epsilon = 0.4 \text{ in/in}$$

then, the total energy of the container SE_c is

$$SE_c = 66.7\, d(h + \frac{d}{4}), \text{ ft-lb}$$

<u>Heat Added to Gas</u>. To estimate the amount of heat added to the enclosed gas, we elect to describe the development of the static equilibrium pressure in two steps. The first step accounts for a pressure rise due to adding the explosive product gases to the initial chamber gas. It is necessary to make allowances for this effect because the quantity of product gases is of the same order as the initial chamber gas. We let this process be isothermal and let it occur at ambient temperature. From perfect gas relations

$$p_b = p_a \left(\frac{n_b}{n_a}\right)$$

where

p_b ... is final pressure of isothermal process, psia

p_a ... is atmospheric pressure, psia

n_b ... is number of moles of gas in chamber after detonation at ambient temperature, g-mol

n_a ... is number of moles of gas initially in chamber at atmospheric pressure and ambient temperature, g-mol

The second step is assumed to be the addition of heat at constant volume to this resultant gas mixture. The initial conditions of the gas mixture for this constant volume process are

p_b ... pressure, psia

T_a ... ambient temperature (283°K), °K

w_b ... weight of gas mixture, gm

Heat is added until the gas reaches the experimentally obtained, static equilibrium pressure p_o (psia). Then for a perfect gas

$$Q = w_b c_v T_a \left(\frac{p_o}{p_b} - 1\right)$$

where

Q ... is heat added to gas, cal

c_v .. is specific heat of gas at constant volume, cal/gm °C

<u>Sample Calculations</u>. To illustrate the effectiveness of the several postulated absorptions, sample calculations are given for the conditions found in Test No. 8. To estimate the kinetic energy of the water casing ($1/2\ m_w\ v_p^2$), a mean particle velocity is needed. From reference (d), the particle velocity

at the extremity of the water casing is of the order of 2,600 ft/sec immediately prior to fracture of the reactor-vessel simulant. At the same time, the particle velocity of the water close to the charge is of the order of 3,600 ft/sec. It is reasonable to assume that the entire water casing is moving at a mean velocity of the order of 3,100 ft/sec. With v_p = 3,100 ft/sec and m_w = 0.00602 slug for Test No. 8, an estimate of the kinetic energy of the water casing is 9,370 calories. For estimates of the other postulated absorptions, we take the following values from table 1, table 5, and figure B-12 for Test No. 8.

$$d = 2.0 \text{ in}$$
$$h = 2.5 \text{ in}$$
$$v_p = 3{,}100 \text{ ft/sec}$$
$$n_a = 0.5149 \text{ g-mol}$$
$$n_b = 1.0812 \text{ g-mol}$$
$$w_b = 31.0 \text{ gm}$$
$$T_a = 283^\circ\text{K}$$
$$p_o = 46.0 \text{ psia}$$
$$E_r = 28{,}940 \text{ cal}$$

We also choose the following values,

$$p_a = 14.7 \text{ psia}$$
$$c_v = 0.1718 \text{ cal/gm}^\circ\text{C}$$

Substituting these values into the appropriate equations, we find that the estimates for the kinetic energy of the container, strain energy of the container, heat added to gas, and energy losses are 4,410 calories, 130 calories, 740 calories, and 14,290 calories, respectively.

APPENDIX E

Approximation of Energy Partition and Pressure-Displacement Function

It has been found desirable to correlate the energy partition and pressure-displacement function with the maximum height of plug travel. The following paragraph constitutes a correlation that could possibly be used for future experiments.

Combining equations (5) and (6) found in the section Energy-Partition Analysis, we can write

$$ME = mgH + Fs_f \qquad (10)$$

The usual method given by equations (7) and (1) is then followed to determine energy partition. From equation (2)

$$ME = A \int_{s=0}^{s=s_f} p \; ds \quad , \qquad p = p\,(s)$$

it is possible to approximate the pressure-displacement function if we assume the isentropic expansion of an effective pressure function. This assumed expansion requires that

$$p_e V^k = C \qquad (11)$$

where

p_e ... is effective pressure, psfa

V .... is volume, ft^3

k .... is ratio of specific heats of gas

C .... is constant.

Considering the length of the power stroke and the geometry of the secondary-shield simulant, we can write

$$s = \frac{V - V_o}{A} \tag{12}$$

where

V_0 ... is initial volume of chamber, ft^3

A .... is frontal area of plug, ft^2.

Combining equations (2) and (12), we obtain

$$ME \approx \int_{V = V_o}^{V = V_f} (p_e - p_a)\, dV \quad , \quad p_e = \frac{C}{V^k} \tag{13}$$

where

V_f ... is volume at end of power stroke, ft^3

p_a ... is atmospheric pressure, psfa.

If we perform the indicated integration, equation (13) becomes

$$ME \approx \frac{p_{eo} V_o^{\,k}}{k - 1} \left(V_o^{\,1-k} - V_f^{\,1-k}\right) - p_a \left(V_f - V_o\right) \qquad (14)$$

where p_{eo} is the maximum effective pressure corresponding to V_o, psfa. For given values of ME, V_o, V_f, p_a, and k, equation (14) will yield the maximum effective pressure p_{eo}. It is noted that p_{eo} will closely approximate the static equilibrium pressure. With p_{eo} known, equations (11) and (12) define the pressure-displacement function. Equations (10), (11), (12), and (14) establish a feasible procedure for determining the energy partition and pressure-displacement relations pertaining to future experiments.

To assess the validity of the previously described approach, mechanical energy as obtained from equation (14) was determined for the subject eleven experiments. Shown in figure E-1 are a typical pressure curve and the approximating isentropic curve. Since p_{eo} cannot be obtained from the typical curve, a point p_1, V_1 was chosen from which p_{eo} was calculated by the relation

$$p_{eo} = p_1 \left(\frac{V_1}{V_o}\right)^k$$

where k is taken to be 1.4. The results of this calculation for each test are given in table E-1. With p_{eo} determined, equation (14) was used to calculate mechanical energy for each test. For each test table E-2 presents the mechanical energy obtained from

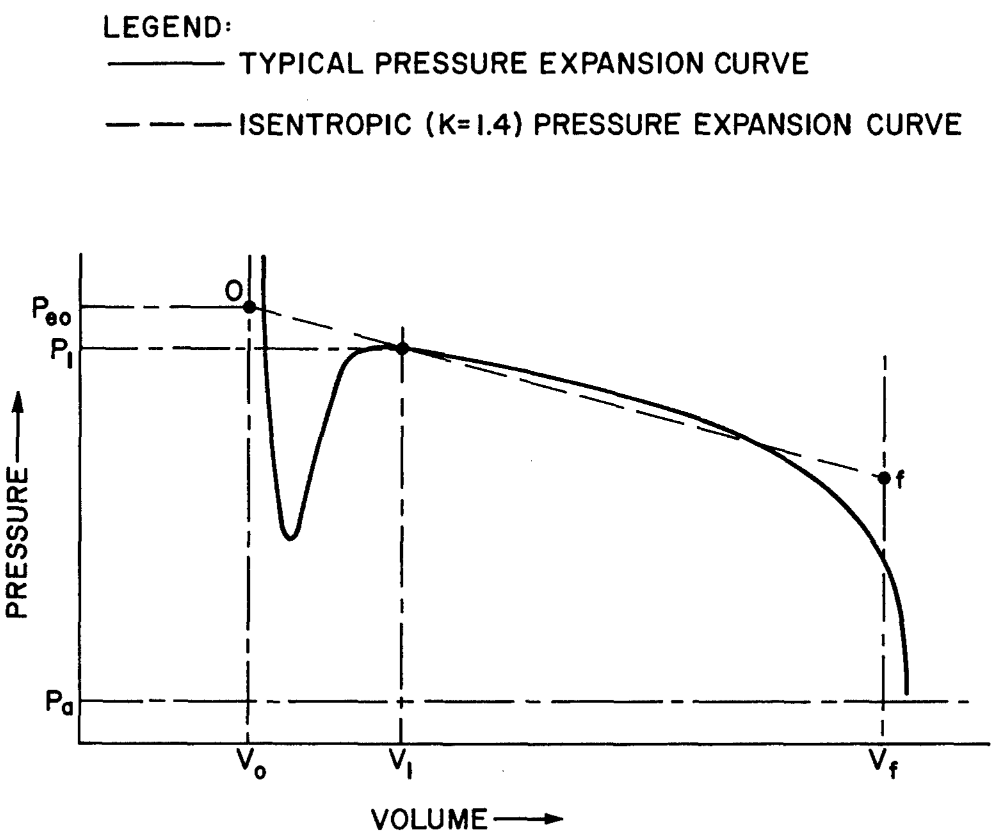

FIG. E-1 APPROXIMATION OF PRESSURE-VOLUME EXPANSION

TEST NUMBER	DISPLACEMENT	PRESSURE	VOLUME	VOLUME	MAX. EFF. PRESSURE	MAX. EFF. PRESSURE
	s_1	p_1	V_1	V_0	p_{eo}	p_{eo}
	(FT)	(PSIA)	(FT^3)	(FT^3)	(PSIA)	(PSIG)
1	0.1984	24.8	0.3754	0.3621	26.1	11.4
2	0.2040	24.9	0.3757	0.3621	26.2	11.5
3	0.2037	34.3	0.3757	0.3621	36.1	21.4
4	0.2261	163.6	0.4392	0.4241	171.8	157.1
5	0.2115	136.1	0.4382	0.4241	142.5	127.8
6	0.2002	299.7	0.4375	0.4241	313.0	298.3
7	0.2055	54.3	0.4362	0.4225	56.8	42.1
8	0.2100	43.9	0.4344	0.4204	46.0	31.3
9	0.2070	33.6	0.4297	0.4159	35.2	20.5
10	0.2065	28.8	0.4256	0.4118	30.2	15.5
11	0.2015	28.6	0.4212	0.4077	29.9	15.2

TABLE E-I MAXIMUM EFFECTIVE PRESSURE

TEST NUMBER	VOLUME	APPROX. MECHANICAL ENERGY		ACTUAL MECHANICAL ENERGY		PERCENT DIFFERENCE
	V_f	W		ME		
	(FT^3)	(FT-LB)		(FT-LB)		(%)
1	0.4359	86.0		103.5		16.9
2	0.4015	53.5		55.3		3.3
3	0.4359	179.3		211.8		15.4
4	0.4979	1452.0		1420.8		2.2
5	0.4979	1177.3		1146.3		2.7
6	0.4979	2773.8		2397.3		15.7
7	0.4963	383.4		349.1		9.8
8	0.4942	265.7		259.6		2.3
9	0.4897	174.3		177.1		1.6
10	0.4856	127.2		141.6		10.2
11	0.4815	122.9		146.7		16.2

TABLE E-2 APPROXIMATE MECHANICAL ENERGY

equation (14) in the column denoted W, the actual mechanical energy denoted ME, and a percentage difference. Even with excessive gas leakage, the average 10 per cent difference represents a good approximation. It may be possible to use this new parameter, maximum effective pressure, as a basis for test comparisons in addition to energy-partition considerations per se. Figure E-2 shows the variation of maximum effective pressure with water-to-air ratio for the various tests. The similarity of these curves to the energy-partition curves shown in figures 9 and 10 is to be noted.

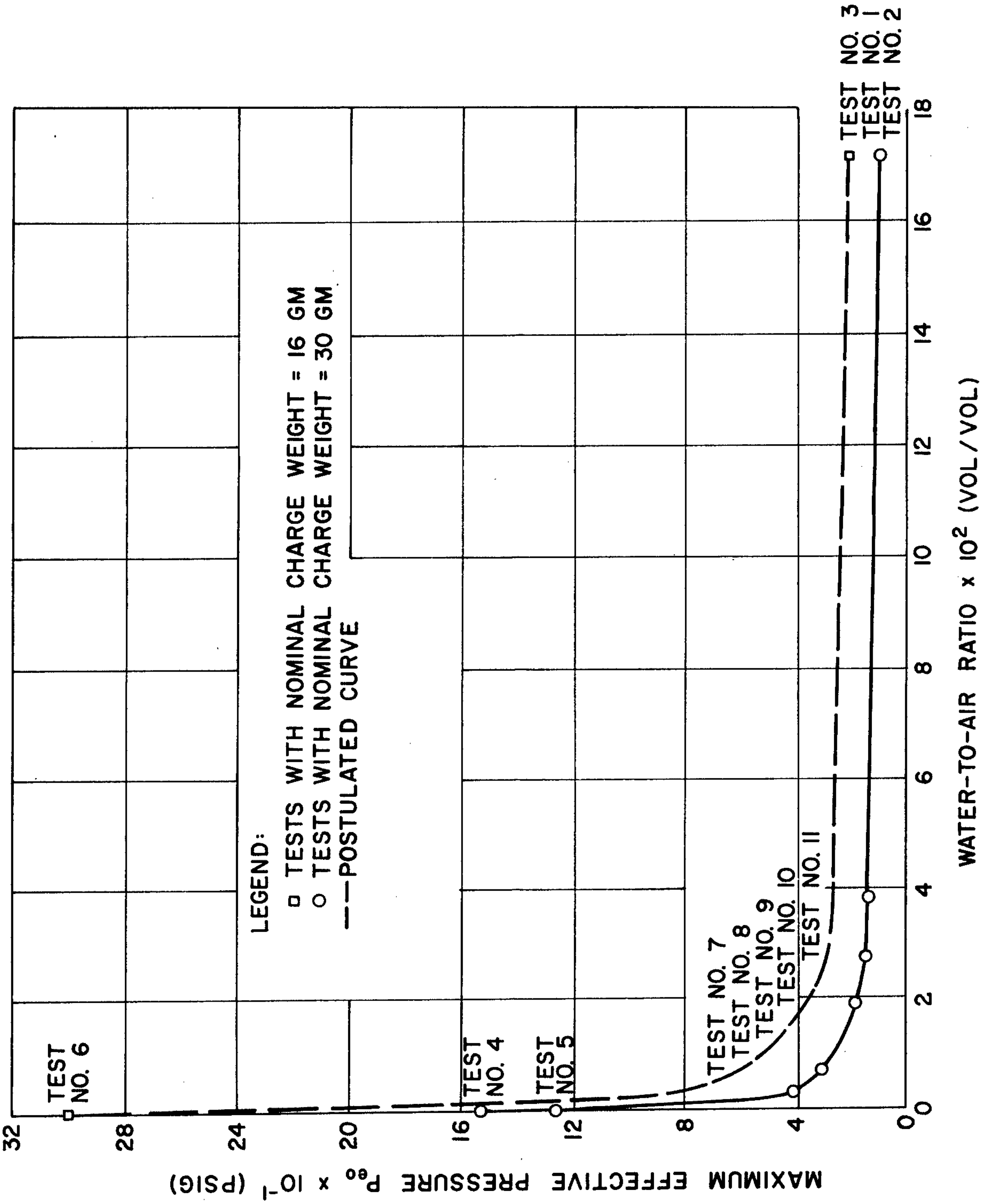

FIG. E-2 VARIATION OF MAXIMUM EFFECTIVE PRESSURE WITH WATER-TO-AIR RATIO

DISTRIBUTION

	Copies
Atomic Energy Commission Washington 25, D. C. Attn: Technical Library	3
Atomic Power Development Associates, Inc. Nuclear and Analytic Division 1911 First Street, Detroit 26, Michigan Attn: Mr. Walter J. McCarthy, Jr. Dr. Alton Klickman	2
Atomics International P.O. Box 309, Canoga Park, California Attn: Mr. A. A. Jarrett Mr. J. W. Flora	2
Babcock and Wilcox Company Atomic Energy Division 161 East 42nd Street New York 17, New York Attn: M. A. Cordovi	1
Ballistic Research Laboratories Aberdeen Proving Ground, Maryland Attn: Mr. Orlando T. Johnson	1
Brookhaven National Laboratory Technical Information Division Upton, Long Island, New York Attn: Research Library	2
University of California Institute of Engineering Research Berkeley 4, California Attn: Dr. Virgil E. Schrock Mr. H. A. Johnson	2
University of California Lawrence Radiation Laboratory Technical Information Division P.O. Box 808, Livermore, California	2
Carnegie Institute of Technology Schenley Park, Pittsburgh 19, Pennsylvania Attn: Dr. Emerson M. Pugh	1
Combustion Engineering, Inc. Reactor Development Division Union Street, Windsor, Connecticut Attn: Francis Bonacci	1

DISTRIBUTION

	Copies
Advisory Committee on Reactor Safeguards Room H-1147, Matomic Building 1717 H Street, N. W., Washington 25, D. C. Attn: Dr. T. J. Thompson Dr. D. Duffey Mr. J. B. Graham Mr. R. F. Fraley	4
Allied Chemical & Dye Corporation General Chemical Division 40 Rector Street, New York 6, N. Y. Attn: Mr. K. R. Osborn, Manager Industrial Development	1
Allied Chemical & Dye Corporation Morristown, New Jersey Attn: Mr. D. A. Rogers, Manager Central Engineering	1
Allis Chalmers Manufacturing Company Nuclear Power Department, Box 512 Milwaukee 1, Wisconsin Attn: Mr. C. B. Graham	1
Argonne National Laboratory 9700 So. Cass Avenue, Argonne, Illinois Attn: Dr. R. C. Vogel	2
Chief, Defense Atomic Support Agency The Pentagon, Washington 25, D. C.	2
Armed Services Technical Information Agency Arlington Hall Station, Arlington 12, Virginia	10
Armour Research Foundation 10 West 35th Street, Chicago 16, Illinois Attn: Dr. T. A. Zaker Dr. N. A. Weil	2
Atomic Energy Commission Army Reactors, Division of Reactor Development Washington 25, D. C.	1
Chicago Operations Office, U. S. Atomic Energy Commission 9800 So. Cass Avenue, Argonne, Illinois Attn: Mr. D. Gardiner	1

DISTRIBUTION

	Copies
Atomic Energy Commission Civilian Reactors, Division of Reactor Development Washington 25, D. C. Attn: Mr. D. H. Stewart	1
Atomic Energy Commission Assistant Director for Reactors Division of Compliance Washington 25, D. C.	1
Director, Division of Research U. S. Atomic Energy Commission Washington 25, D. C.	1
Atomic Energy Commission Hazards Evaluations Branch Division of Licensing and Regulation Washington 25, D. C. Attn: Mr. Edson Case	7
Idaho Operations Office U. S. Atomic Energy Commission P.O. Box 1221, Idaho Falls, Idaho Attn: Mr. J. B. Philipson	1
Atomic Energy Commission Naval Reactors Branch Division of Reactor Development Washington 25, D. C. Attn: Mr. T. Rockwell Mr. R. S. Brodsky	2
Atomic Energy Commission Radiation Branch, Environmental Sciences Division New York Operations Office 376 Hudson Street, New York 14, N. Y. Attn: Mr. James E. McLaughlin	1
Atomic Energy Commission Research and Development Branch Division of Reactor Development Washington 25, D. C. Attn: Mr. S. A. Szawlewicz	2
San Francisco Operations Office U. S. Atomic Energy Commission 2111 Bancroft Way, Berkeley 4, California Attn: Mr. G. H. Helfrich	1

DISTRIBUTION

	Copies
Commanding Officer and Director David Taylor Model Basin Washington 7, D. C.	1
Director of Defense Research and Engineering The Pentagon, Washington 25, D. C.	1
Detroit Edison Company Chemistry Research Department Detroit, Michigan Attn: Mr. Edward Hines	1
Duke University College of Engineering Library Durham, North Carolina	1
Duke University Department of Physics Durham, North Carolina Attn: Dr. H. W. Newson	1
E. I. duPont de Nemours and Company Explosives Department, Atomic Energy Division Wilmington 98, Delaware Attn: Document Custodian	1
Chief of Engineers Department of the Army Washington 25, D. C. Attn: ENGEB	1
Frankford Arsenal Bridge and Tacony Streets Philadelphia 37, Pennsylvania Attn: Librarian	1
General Electric Company Atomic Power Equipment Department 2155 South Street, San Jose, California Attn: Library	1
General Nuclear Engineering Corporation P.O. Box 245, Dunedin, Florida	1
Harvard University School of Public Health 55 Shattuck Street Boston 15, Massachusetts Attn: Dr. Leslie Silvermann	1

DISTRIBUTION

	Copies
Harvard University Cambridge, Massachusetts Attn: Dr. Harvey Brooks Dean of Engineering and Applied Physics	1
Hercules Powder Company Research Department Wilmington, Delaware Attn: Dr. Willard P. Conner, Manager Physical Chemical Division	1
Internuclear Company 7 North Brentwood Boulevard Clayton 5, Missouri	1
Director, Applied Physics Laboratory Johns Hopkins University Baltimore 18, Maryland	1
Johns Hopkins University Operations Research Office 7100 Connecticut Avenue Washington 15, D. C. Attn: Document Control Office	1
Johns Hopkins University Department of Sanitary Engineering and Water Resources Baltimore 18, Maryland Attn: Mr. John C. Geyer	1
Knolls Atomic Power Laboratory P.O. Box 1072, Schenectady, New York Attn: Document Librarian	2
Liberty Mutual Insurance Company 175 Berkeley Street Boston 17, Massachusetts Attn: Dr. C. R. Williams	1
Los Alamos Scientific Laboratory P.O. Box 1663, Los Alamos, New Mexico Attn: Report Librarian	2
Mound Laboratory Monsanto Chemical Company P.O. Box 32, Miamisburg, Ohio	1

DISTRIBUTION

	Copies
National Bureau of Standards Room 301 Northwest Building Washington 25, D. C. Attn: Library	1
National Bureau of Standards Washington 25, D. C. Attn: Dr. C. Muehlhause	1
Chief of Naval Operations, D/N Code 418 Washington 25, D. C.	1
Chief of Naval Research, D/N Bldg. T-3 Washington 25, D. C.	2
Director, U. S. Naval Research Laboratory Washington 25, D. C.	1
Director, Office of Naval Research Branch Office, 1000 Geary Street San Francisco, California	1
Chief, Bureau of Naval Weapons Washington 25, D. C. Attn: Library, DIS 3	2
Chief, Bureau of Naval Weapons Washington 25, D. C. Attn: (RRRE) W. T. August	1
Bureau of Naval Weapons Department of the Navy Code RMMO-13 Washington 25, D. C. Attn: Mr. Edward M. Fisher	1
Commanding Officer U. S. Naval Weapons Evaluation Facility Kirtland AFB, Albuquerque, New Mexico	1
Commander, Naval Weapons Laboratory Dahlgren, Virginia	1
Chief, Bureau of Ships Department of the Navy Washington 25, D. C.	1

DISTRIBUTION

	Copies
Nuclear Development Corporation of America 5 New Street, White Plains, New York Attn: Library	1
Oak Ridge Institute of Nuclear Studies P.O. Box 117, Oak Ridge, Tennessee Attn: Library	1
Oak Ridge National Laboratory P.O. Box X, Oak Ridge, Tennessee Attn: Mr. William Cottrell Mr. Frank Bruce Dr. W. K. Ergen Dr. F. A. Gifford, Jr. Dr. F. C. Maienschein	5
Pacific Missile Range Code 4113, P.O. Box 10 Point Mugu, California Attn: Mr. Harry B. Benefiel	1
U. S. Patent Office Scientific Library Washington 25, D. C.	1
Phillips Petroleum Company Manager, Reactor Projects P.O. Box 1259, Idaho Falls, Idaho Attn: Mr. Warren E. Nyer	1
U. S. Pipe and Foundry Company Steel and Tubes Division Burlington, New Jersey Attn: Dr. A. E. Schuh	1
Commanding Officer Picatinny Arsenal Dover, New Jersey	1
Research Triangle Institute P.O. Box 490, Durham, North Carolina Attn: Dr. Hugh W. Hunter	1
Sandia Corporation Sandia Base, Albuquerque, New Mexico Attn: Library	1

DISTRIBUTION

	Copies
Space Technology Laboratories, Inc. P.O. Box 1085, Los Angeles 45, California Attn: Dr. D. B. Langmuir Mr. Sam Zivi	2
Stanford Research Institute Poulter Laboratory Menlo Park, California Attn: Dr. Donald Davenport Mr. Neilan B. Botsford	2
The Travelers Insurance Companies 700 Main Street, Hartford 15, Connecticut Attn: Mr. Reul C. Stratton, Asst. Director Department of Research	1
Office of Technical Services U. S. Department of Commerce Washington 25, D. C.	4
Technical Information Service Extension U. S. Atomic Energy Commission P.O. Box 62, Oak Ridge, Tennessee	5
Union Carbide Nuclear Company P.O. Box 1223, Paducah, Kentucky Attn: Library	1
Vitro Engineering Division Technical Reports Section 225 Fourth Avenue, New York 3, New York	1
Commanding Officer, Watertown Arsenal Watertown 72, Massachusetts Attn: Technical Information Section	1
Westinghouse Electric Corporation Commercial Atomic Power Activity P.O. Box 355, Pittsburgh 30, Pennsylvania Attn: Document Custodian	1
Atomic Energy Commission Maritime Reactors Branch Division of Reactor Development Washington 25, D. C.	1

DISTRIBUTION

	Copies
Atomic Energy Commission Canoga Park Area Office P. O. Box 591 Canoga Park, California Attn: Mr. C. W. Richards	1
Atomic Energy Commission Idaho Operations Office P. O. Box 2108 Idaho Falls, Idaho Attn: Mr. G. E. Devore Mr. D. William	2
USAEC Technical Representative Toronto, Ontario Canada Attn: Mr. D. Glenn Boyer	1
Brookhaven National Laboratory Upton, New York Attn: Mr. A. W. Castlemann	1
University of Minnesota Department of Chemical Engineering Minneapolis, Minnesota Attn: Prof. H. Isbin	1
Phillips Petroleum Company P. O. Box 1259 Idaho Falls, Idaho Attn: Mr. Frank Schroeder Mr. Glenn O. Bright Mr. T. R. Wilson	7

CATALOGING INFORMATION FOR LIBRARY USE

BIBLIOGRAPHIC INFORMATION

	DESCRIPTORS	CODES		DESCRIPTORS	CODES
SOURCE	NOL technical report	NOLTR	SECURITY CLASSIFICATION AND CODE COUNT	Unclassified	UØ35
REPORT NUMBER	62-155	62Ø155	CIRCULATION LIMITATION		
REPORT DATE	1 June 1960	Ø66Ø	CIRCULATION LIMITATION OR BIBLIOGRAPHIC		
			BIBLIOGRAPHIC (SUPPL., VOL., ETC.)		

SUBJECT ANALYSIS OF REPORT

DESCRIPTORS	CODES	DESCRIPTORS	CODES	DESCRIPTORS	CODES
Reactors	REAC	Model	MODE	Weight	WEIG
Safety	SAFE	Shield	SHIL	Mass	MASZ
Failure	FAIL	Plug	PLUG	Frontal	FRON
Containment	CTAI	Excursion	EXCU	Area	AREA
Power plants	POWE	Loadings	LOAD	Ratio	RATI
Nuclear	NUCL	Simulated	SIMU	Enrico Fermi	ENFR
Energy	ENER	Air	AIRE	Building	BUIL
Partition	PARN	Equations	EQUA	Missile	MISL
Water	WATR	Test	TEST	Damage	DAMA
Cased	CASE	Data	DATA	Hazards	HAZA
Explosions	EXPS	Data analysis	DATP	Explosive	EXPL
Parameters	PARA	Charge	CHAR		

PRNC-NOL-5070/28 (5-62)

Naval Ordnance Laboratory, White Oak, Md.
(NOL technical report 62-155)
ENERGY PARTITION OF WATER-CASED EXPLOSIONS IN AN IDEALIZED MODEL REACTOR VESSEL (U), by James F. Proctor. 1 June 1960. v.p. illus., diagr., tables. Task-285 UNCLASSIFIED

Purpose of energy-partition work being conducted by NOL is to determine model shield-plug response to excursion-type loadings simulated in idealized model reactor vessel.

Scope of this report is limited to energy partitions resulting from water-cased explosions surrounded by air in closed piston-fitted vessel. Analytic equations expressing energy partition in terms of model-plug response have been developed. Description of test apparatus is given, and data obtained from eleven tests are graphically and analytically treated to obtain various plug-response functions and subject energy partition.

1. Reactors - Safety
2. Reactors - Failure
3. Reactors - Containment
4. Plugs, Shield
5. Power plants, Atomic
I. Title
II. Proctor, James F.
III. Project

Abstract card is unclassified.

Naval Ordnance Laboratory, White Oak, Md.
(NOL technical report 62-155)
ENERGY PARTITION OF WATER-CASED EXPLOSIONS IN AN IDEALIZED MODEL REACTOR VESSEL (U), by James F. Proctor. 1 June 1960. v.p. illus., diagr., tables. Task-285 UNCLASSIFIED

Purpose of energy-partition work being conducted by NOL is to determine model shield-plug response to excursion-type loadings simulated in idealized model reactor vessel.

Scope of this report is limited to energy partitions resulting from water-cased explosions surrounded by air in closed piston-fitted vessel. Analytic equations expressing energy partition in terms of model-plug response have been developed. Description of test apparatus is given, and data obtained from eleven tests are graphically and analytically treated to obtain various plug-response functions and subject energy partition.

1. Reactors - Safety
2. Reactors - Failure
3. Reactors - Containment
4. Plugs, Shield
5. Power plants, Atomic
I. Title
II. Proctor, James F.
III. Project

Abstract card is unclassified.

Naval Ordnance Laboratory, White Oak, Md.
(NOL technical report 62-155)
ENERGY PARTITION OF WATER-CASED EXPLOSIONS IN AN IDEALIZED MODEL REACTOR VESSEL (U), by James F. Proctor. 1 June 1960. v.p. illus., diagr., tables. Task-285 UNCLASSIFIED

Purpose of energy-partition work being conducted by NOL is to determine model shield-plug response to excursion-type loadings simulated in idealized model reactor vessel.

Scope of this report is limited to energy partitions resulting from water-cased explosions surrounded by air in closed piston-fitted vessel. Analytic equations expressing energy partition in terms of model-plug response have been developed. Description of test apparatus is given, and data obtained from eleven tests are graphically and analytically treated to obtain various plug-response functions and subject energy partition.

1. Reactors - Safety
2. Reactors - Failure
3. Reactors - Containment
4. Plugs, Shield
5. Power plants, Atomic
I. Title
II. Proctor, James F.
III. Project

Abstract card is unclassified.

Naval Ordnance Laboratory, White Oak, Md.
(NOL technical report 62-155)
ENERGY PARTITION OF WATER-CASED EXPLOSIONS IN AN IDEALIZED MODEL REACTOR VESSEL (U), by James F. Proctor. 1 June 1960. v.p. illus., diagr., tables. Task-285 UNCLASSIFIED

Purpose of energy-partition work being conducted by NOL is to determine model shield-plug response to excursion-type loadings simulated in idealized model reactor vessel.

Scope of this report is limited to energy partitions resulting from water-cased explosions surrounded by air in closed piston-fitted vessel. Analytic equations expressing energy partition in terms of model-plug response have been developed. Description of test apparatus is given, and data obtained from eleven tests are graphically and analytically treated to obtain various plug-response functions and subject energy partition.

1. Reactors - Safety
2. Reactors - Failure
3. Reactors - Containment
4. Plugs, Shield
5. Power plants, Atomic
I. Title
II. Proctor, James F.
III. Project

Abstract card is unclassified.